# OPTIMIZATION OF CENTRAL PATTERN GENERATORS

A THESIS SUBMITTED TO
THE GRADUATE SCHOOL OF NATURAL AND APPLIED SCIENCES
OF
ATILIM UNIVERSITY

BY

ABDALFTAH ELBORI

IN PARTIAL FULFILLMENT OF THE REQUIREMENTS
FOR
THE DEGREE OF DOCTOR OF PHILOSOPHY
IN
MODELING AND DESIGN OF ENGINEERING SYSTEMS

JANUARY 2018

Approval of the Graduate School of Natural and Applied Sciences, Atılım University.

Prof. Dr. Ali Kara
Director

I certify that this thesis satisfies all the requirements as a thesis for the degree of **Doctor of Philosophy in Modeling and Design of Engineering Systems Department, Atılım University**.

Assoc. Prof. Dr. Ender Keskinkılıç
Head of Department

This is to certify that we have read the thesis OPTIMIZATION OF CENTRAL PATTERN GENERATORS submitted by ABDALFTAH ELBORI and that in our opinion it is fully adequate, in scope and quality, as a thesis for the degree of Doctor of Philosophy.

Asst. Prof. Dr. Kutluk Bilge Arıkan
Co-Supervisor

Assoc. Prof. Dr. Mehmet Turan
Supervisor

**Examining Committee Members:**

Asst. Prof. Dr. Ali Emre Turgut
Mechanical Engineering Department, METU

Assoc. Prof. Dr. Mehmet Turan
Mathematics Department, Atılım University

Assoc. Prof. Dr. Senih Gürses
Department of Engineering Science, METU

Assoc. Prof. Dr. Yiğit Yazıcıoğlu
Mechanical Engineering Department, METU

Asst. Prof. Dr. Hakan Tora
Electronics Department, Atılım University

**Date: January 10, 2018**

I declare and guarantee that all data, knowledge and information in this document has been obtained, processed and presented in accordance with academic rules and ethical conduct. Based on these rules and conduct, I have fully cited and referenced all material and results that are not original to this work.

Name, Last Name : ABDALFTAH ELBORI

Signature :

# ABSTRACT


**OPTIMIZATION OF CENTRAL PATTERN GENERATORS**

Elbori, Abdalftah

Ph.D., Department of Modeling and Design of Engineering Systems

Supervisor : Assoc. Prof. Dr. Mehmet Turan

Co-Supervisor : Asst. Prof. Dr. Kutluk Bilge Arıkan

January 2018, 92 pages

Up to this day, it is one of the most difficult tasks to find the humanoid robot that is able to move as dynamic and robust as humans do. Although there are many researches that have investigated bipedal locomotion, at current date, there is no robots with human's capabilities.

In this study, with regard to the optimization of the CPGs for bipedal locomotion in robots, three mathematical structures are discussed. This thesis also investigates how different couplings of the CPGs such as uncoupled, unidirectional, bidirectional, are used to produce rhythmic patterns for one leg with two degrees of freedom. In each case of three types of the CPGs, stability analyzes is done. Bidirectional two CPGs of the third type give us the best performance comparing with all other cases studied here. When the parameters are taken from the stability region, it is seen that significant results are achieved without any sensory feedback.



Keywords: Central Pattern Generators, Stability Analysis, Optimization, Genetic Algortihm

# ÖZ


## MERKEZİ ÖRÜNTÜ ÜRETEÇLERİN OPTİMİZASYONU

Elbori, Abdalftah

Doktora, Mühendislik Sistemlerinin Modellenmesi ve Tasarımı

Tez Yöneticisi : Doç. Dr. Mehmet Turan

Ortak Tez Yöneticisi : Yrd. Doç. Dr. Kutluk Bilge Arıkan

Ocak 2018, 92 sayfa

Günümüzde insanlar gibi dinamik ve sağlam hareket edebilen insan robotunu bulmak en zor görevlerden biridir. İki ayaklı hareketi araştıran birçok araştırma olmasına rağmen, günümüzde insan yetenekleri olan robot bulunmamaktadır.

Bu tezde robotlarda iki ayaklı hareket için Merkezi Örüntü Üreteçlerin (CPG) optimizasyonu ile ilgili olarak, üç matematiksel yapı tartışılmıştır. Ayrıca, bu tezde iki serbestlik dereceli bir bacakta ritmik hareket elde etmek için CPG'lerin, bağlantısız, tek yönlü veya çift yönlü bağlantılı gibi farklı şekillerde eşleşmeleri incelenmiştir. CPG'lerin üç matematiksel yapısı için de kararlılık analizi yapılmıştır. Bu tezde ele alınan farklı yapılardaki farklı eşleştirmeler arasından üçüncü yapıda çift yönlü eşleştirme en iyi sonucu vermiştir. Yapılardaki parametreler kararlılık bölgesinden seçildiği zaman, herhangi bir duyusal geribildirim olmaksızın önemli sonuçların elde edildiği gözlemlenmiştir.



Anahtar Kelimeler: Merkezi Örüntü Üreteçler, Kararlılık Analizi, Optimizasyon, Genetik Algoritma

*To my parents and family*

# ACKNOWLEDGMENTS

In the name of Allah, the Most Gracious and the Most Merciful and Beneficent, all praises to Allah for the strengths and his blessing in completing this thesis.

Special appreciation goes to my supervisor Assoc. Prof. Dr. Mehmet Turan for his guidance, support, and patience. I shall also thank my Co-Supervisor Asst. Prof. Dr. Kutluk Bilge Arıkan who has provided me with support and advice throughout the thesis. Also, my thanks go to Assoc. Prof. Dr. Senih Gürses and Asst. Prof. Dr. Hakan Tora, Assoc. Prof. Dr. Yiğit Yazıcıoğlu and Asst. Prof. Dr. Ali Emre Turgut as the members of examination committee for their careful reading this thesis and valuable comments.

Furthermore, I would like to express my very profound gratitude to my parents and my wife for providing me with unfailing support and endless encouragement throughout my years of study and through the process of researching and writing this thesis. This accomplishment would not have been possible without them. Thank you.

The financial support of the Libyan Higher Education is also acknowledged.

Last but not the least, I thank my friends, I offer my deepest and sincere thanks for their continuous support during my study.

# TABLE OF CONTENTS

# LIST OF TABLES

TABLES

# LIST OF FIGURES

FIGURES

# CHAPTER 1

# INTRODUCTION

Nowadays, locomotion of robot is one of the most widely discussed topics with basic loco-motors at the heart of investigations. Many types of researches have been conducted and focused on bipedal locomotion. Different types of locomotion such as walking, running, jumping, jogging etc. on two or more than two legs have been achieved by using Central Pattern Generators (CPGs).

In biological systems, these locomotions are produced by a central nervous system called Central Pattern Generators (CPGs). The central nervous system of vertebrate and invertebrate animals is located in the spinal cord [1, 2, 3, 4, 5]. Recently, some studies have shown that there are some functions in the human body, for instance breathing and digestion, that can not be controlled consciously, but they are controlled by CPGs [3, 6].

Biologically, CPGs can be defined as inspired networks of nonlinear oscillating neurons that are capable of generating rhythmic patterns without sensory feedback. A neural oscillator comprises a pair of neurons with inhibitive connections between them. Two such neurons suppress one another, which results in two different neurons, flexor and extensor neuron [7, 8, 9]. It should be known that a single CPG is not a small neural network. Rather, it receives inputs from the higher parts of control centers [1, 4].

Various mathematical and physical structures of the robots' legs and limbs have been modeled [10, 11, 12], and the control systems have been copied to reproduce patterns of movement in robots similar to those in certain biological organisms. When the body initiates movement, CPGs commence synchronization and send signals to neurons

simultaneously in a movement cycle [13, 14].

In the literature, various mathematical structures have modeled and mimicked the biological control parameters [2, 3, 10, 15, 16, 17, 18]. Some works related to the CPGs which focus on the lower body will be discussed in this study.

At the beginning of the last century, there were two different explanations for the creation of the rhythmic patterns (RPs), see [19]. The first explanation was that the RPs come from a chain of reflexes in which sensory feedback gives an important role in triggering switches between different parts of a locomotor cycle. The second explanation was that RPs are generated by the neural network without input from the periphery. There is a clear evidence that the RPs are generated centrally, for instance, neural networks do not require any sensory feedback.

One can extract and isolate the spinal cord from the body of the lamprey, and it will produce rhythms that patterns are called fictive locomotion. The fictive locomotion is similar to intact locomotion when activated by chemical or simple electrical stimulation [20, 21, 22]. Similar fictive locomotion has been defined in salamander [23], and many CPGs have been reported in different animals, see [24, 25, 26]. The higher control center or sensory feedback is not needed for producing or generating the rhythms, but it plays a very important role to shape the RPs.

It is fundamental to keep in mind that both the CPGs and the body movements are coordinated. Movement of the tail of the lamprey will induce the CPG activity that is the frequency of the mechanical movements, see [27, 28, 29, 30, 31, 32, 33, 34, 35]. The loco-motor system of a vertebrate animal is organized such that the CPGs play an important role in producing RPs and higher level centers are responsible for modulating these RPs that rely on the environmental conditions.

Various CPG models, including the connectionist models, have been implemented in the robotic systems [36, 37, 38]. The locomotion of the quadruped, hexapod and octopod robots are employed by some different CPG models [6, 39, 40, 41, 42, 43, 44, 45, 46, 47]. There are many models of the CPGs which are used for controlling the bipedal locomotion in human-robot, see [11, 18, 48, 49, 50, 51, 52, 53, 54, 55, 56, 57]. In some of these studies the Van der Pol and the Hopf oscillators are considered.

The CPGs are implemented in two ways; hardware methods and software methods. In hardware implementations, there are two common approaches to implement CPGs. One approach is to construct a system in a Field Programmable Gate Array (FPGA) [57], and the other approach is to use a silicon chip which is able to produce signals [58, 59, 60]. There are some disadvantages in hardware implementations. For example, once a hardware is built, it can not be changed without redesigning the whole structure. For this reason, in this study, only the software implementation is considered to give more freedom to a designer.

In software implementation, there are some different coupled differential equations to represent CPGs in robot control system. These systems of coupled oscillators have synchronized their outputs in order to do constant phase for a given gait pattern. Then, the outputs of these oscillators are used to control the locomotion of the robots [61, 62]. Also, there are some studies discussing how systems of oscillators can be coupled, see for example [61, 62, 63].

This thesis draws attention on and derives support from the studies mentioned above and investigates how the CPGs can best be optimized for bipedal locomotion via an adaptation to the robotic systems that perform a one-leg movement. In particular, this thesis investigates three types of the CPGs. An evolutionary algorithm is used to find the optimum values of the parameters for three types of the CPGs. In each type of the CPGs there are three different cases: (a) uncoupled CPGs, where each CPG works independent from the others to generate RPs to each joint, (b) unidirectional CPGs where only one CPG gives reference to the other one and (c) bidirectional two CPGs where both CPGs give reference to each other. It is predicted that the bidirectional two CPGs will give the best results in all cases by using both stability analysis and the optimization of the CPGs.

## 1.1 Aim and scope of the thesis

- This thesis will present and focus on the CPGs and optimize the CPG for bipedal locomotion. It is aimed to optimize various CPG model structures to generate kinematic motion references for typical periodic limb motions.

- Several cost functions will be employed to be minimized. Resulting change in the behavior of the locomotion will be evaluated.
- Limb kinematics will be simulated with the CPG models. Each joint will involve a CPG. Coupling among CPG units will be assessed during the optimization process. Stability analysis is also utilized to guarantee this switching.
- Stability analysis of the CPG oscillators is required for the purpose of optimization. In addition, CPGs should be able to produce different patterns by changing the input parameter values.

## 1.2 Organization of the thesis

This thesis is organized as follows: In Chapter 2, we explain and derive the mathematical modeling of one leg with two degrees of freedom (DOF) and its kinematic equations with Test Bench. Then, Chapter 3 describes the mathematical model of the CPGs and discusses the three types of the CPGs. Each type of the CPGs has three different cases, uncoupled, unidirectional and bidirectional two CPGs respectively. Stability analysis has been done for all ceases of the CPGs to guarantee this switching. Later, in Chapter 4, the optimization, Genetic algorithm (GA) and hybrid function are explained and used to optimize of the CPGs. In Chapter 5, we compare the outputs of the CPGs with the real data, and also we discuss why some parameters are more effective than others. Finally, Chapter 6 is dedicated to the conclusion and directions for the future studies.

# CHAPTER 2

# TEST BENCH

Economically speaking, the kinematic model is designed to conduct a base analysis. Figures 2.1 and 2.2 show the physical Test Bench and present the two legs with two joints. The model shown in the Figure 2.2 below exists in a laboratory at the Mechatronics Department at Atilim University. However, simulations, genetic algorithms and hybrid function based optimizations describe the function of a single leg system with hip and knee joints in order to reduce the complexity of involving the algorithm during the initial stages. The horizontal beams are crucial here in that they constrain the motion along the vertical axis in order to guide the walking system. Linear bearings help the body to slide via the beams [11].

By looking at the Figure 2.1, we require some tools for the experiment of the Test Bench comprise the legs such as, digital servo actuators, proximity and data acquisition system, real-time control system, force sensors and the offline processing algorithm based on the Genetic algorithm (GA) to find out and optimize a variety of walking gaits. Both MATLAB and Simulink are utilized as the software. Real-Time Windows Target is also utilized to transmit angular references to the servo motors and receive sensor measurements in the real time. Humusoft MF 624 data acquisition board is manipulated in the system. Fast reaction and high torque digital servo actuators are utilized as well.

The Proximity sensor is a Sharp GP2D2 type sensor that has the ability to measure a range of 10 cm to 80 cm. Force sensors are polymer thick film type resistors produced by interlinks Electronics as shown in the Figure 2.1 below. It reveals that resistance decreases while the applied force increases [11]. In the next section, one leg of the

Test Bench is presented.

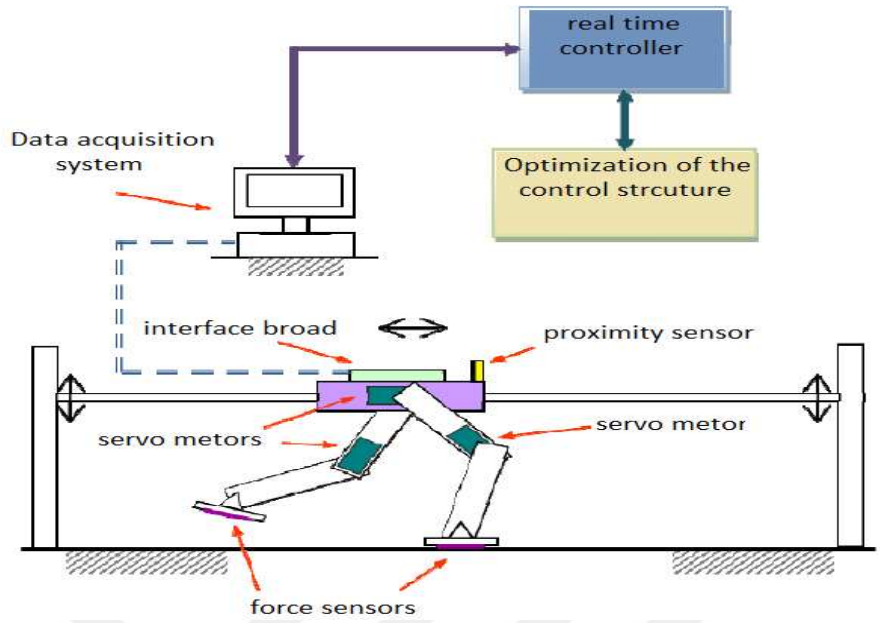


Figure 2.1: Schematics of the physical system [11]

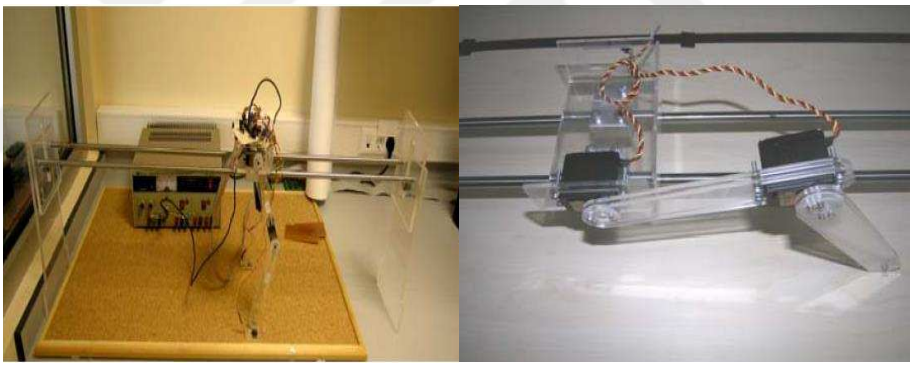

Figure 2.2: The physical system and a closer view of the actuators of one leg of the Test Bench

## 2.1 Kinematic model

The first step in this study is to construct the kinematic model in order to conduct a base analysis. Figure 2.3 presents the leg structure in two cases of motion: swing and stance modes. In Test Bench, $L_1 = 0.145$ and $L_2 = 0.165$ are the lengths from the hip-joint to the knee-joint and from the knee-joint to the end effector, respectively, and $\theta_1$ and $\theta_2$ represent the angular positions of both the hip and the knee. $y_g = 0.25$

stands for the distance between the lower body and the ground.

The coordinates of the lowest part of the hip and knee are denoted by $(x_A, y_A)$ and $(x_f, y_f)$. In fact, there are two cases to consider during motion. The first case is when $y_f = y_g$, that is, the leg touches the ground. This case is known as the stance mode in which case the leg behaves as a re-volute joint. In stance mode, the hip joint angle $\theta_1$ is computed in terms of the knee angle $\theta_2$, which is established by the CPGs. Thus, in this mode the kinematic model has one degree of freedom (DOF). Moreover, only in stance mode will the body move in the $x$-direction. The second case is when $y_f < y_g$, which is the time when the leg does not touch the ground. This mode is known as the swing mode. In this mode, we will have two DOF, and the angles of both the hip and knee are calculated by two different CPGs. In next chapter, we will define how the CPGs will drive the robot, and explain how a single CPG is able to drive a single joint or multiple joints.

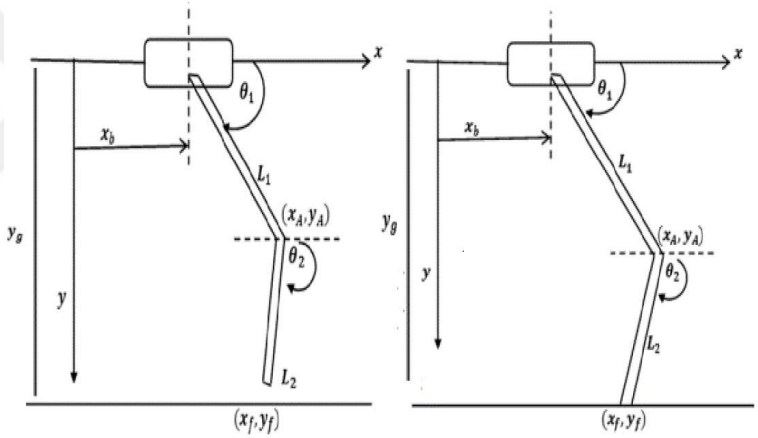


Figure 2.3: Swing and stance modes of the leg during the locomotion

The simple kinematic equations are

$$x_A = x_b + L_1 \cos\theta_1,\ y_A = L_1 \sin\theta_1,\ x_f = x_A + L_2 \cos\theta_2,\ y_f = y_A + L_2 \sin\theta_2,$$

which are considered in the sagittal plane. The lower body is parallel to the ground during the locomotion, as in the Test Bench, where the hip-joint height is fixed. Since the stability during the locomotion is guaranteed, the dynamic equations are not needed (See Figure 2.2).

# CHAPTER 3

# MATHEMATICAL STRUCTURES OF CPGs

The type of oscillator that represents the CPG is one of the most important choices to be made. There are several research groups who adopted CPGs to implement controllers for bipedal locomotion [2, 3, 10, 15, 16, 17, 18]. The scientists have demonstrated that the neurons which exist in the spinal cord of humans, vertebrate and invertebrate animals are able to produce rhythmic patterns without the requirement of any rhythmic input. These neurons are implemented by software methods called CPGs, where the CPG unit is responsible for generating the required angular references for the hip and knee joints. In this part, three different types of mathematical structures of CPGs will be studied and we will call them the first, the second and the third type.

## 3.1 The first type of CPGs

The first type of CPGs are governed by the differential equations [12, 41, 61, 64, 65]:

$$\left.\begin{aligned} \dot{\varphi}_i &= 2\pi v_i + \sum_{i \neq j} r_j w_{ij} \sin(\varphi_j - \varphi_i - \phi_{ij}) \\ \ddot{r}_i &= a_i \left( \frac{a_i}{4}(R_i - r_i) - \dot{r}_i \right) \\ \theta_i &= r_i(1 + \cos(\varphi_i)) \end{aligned}\right\} \tag{3.1}$$

where the state variables $\varphi_i$ and $r_i$ represent the phase and the amplitude, respectively, and $\theta_i$ is the output of oscillator $i$, $v_i$ denotes the angular velocity, the constant $a_i$ determines how fast the amplitude $r_i$ will converge to the limiting amplitude $R_i$, $\phi_{ij}$ is the phase biases and $w_{ij}$ denotes the coupling weight between the oscillator $i$ and $j$. For two CPGs, depending on the value of $w_{ij}$, three different couplings may be considered: uncoupled, unidirectional and bidirectional. The corresponding systems

of differential equations are provided below:

$$\left.\begin{aligned} \dot{\varphi_1} &= 2\pi v_1 \\ \ddot{r_1} &= a_1\left(\frac{a_1}{4}(R_1 - r_1) - \dot{r_1}\right) \\ \dot{\varphi_2} &= 2\pi v_2 \\ \ddot{r_2} &= a_2\left(\frac{a_2}{4}(R_2 - r_2) - \dot{r_2}\right) \end{aligned}\right\} \tag{3.2}$$

$$\left.\begin{aligned} \dot{\varphi_1} &= 2\pi v_1 + r_2 w_{12}\sin(\varphi_2 - \varphi_1 - \phi_{12}) \\ \ddot{r_1} &= a_1\left(\frac{a_1}{4}(R_1 - r_1) - \dot{r_1}\right) \\ \dot{\varphi_2} &= 2\pi v_2 \\ \ddot{r_2} &= a_2\left(\frac{a_2}{4}(R_2 - r_2) - \dot{r_2}\right) \end{aligned}\right\} \tag{3.3}$$

$$\left.\begin{aligned} \dot{\varphi_1} &= 2\pi v_1 + r_2 w_{12}\sin(\varphi_2 - \varphi_1 - \phi_{12}) \\ \ddot{r_1} &= a_1\left(\frac{a_1}{4}(R_1 - r_1) - \dot{r_1}\right) \\ \dot{\varphi_2} &= 2\pi v_2 + r_1 w_{21}\sin(\varphi_1 - \varphi_2 - \phi_{21}) \\ \ddot{r_2} &= a_2\left(\frac{a_2}{4}(R_2 - r_2) - \dot{r_2}\right) \end{aligned}\right\} \tag{3.4}$$

The output of the systems are $\theta_1 = r_1(1 + \cos(\varphi_1))$ and $\theta_2 = r_2(1 + \cos(\varphi_2))$, which represent the angular joints of the hip and the knee, respectively.

System (3.2) is called uncoupled because the two CPGs occurring in the system work independently. On the other hand, in system (3.3), there is a signal transfer from the second CPG to the first one, and that transfer is one way. This is why it is called unidirectional. Finally, in system (3.4), each CPG gives reference to the other CPG. Therefore, it is called bidirectional coupling.

## 3.2 The second type of CPGs

Another set of differential equations that can represent CPGs is

$$\begin{aligned} \dot{x}_i &= \gamma_i\left(\mu_i - r_i^2\right)x_i - \omega y_i + \sum_{j\neq i} E_i x_j \\ \dot{y}_i &= \gamma_i\left(\mu_i - r_i^2\right)y_i + \omega x_i \end{aligned} \tag{3.5}$$

where $\mu_i$ and $\omega$ are the amplitude and frequency, respectively, $\gamma_i$ are some positive constants that determine the speed of convergence, $r_i^2 = x_i^2 + y_i^2$, $E_i$ gives the coupling

weight and its sign decides if these two oscillators are in phase or anti phase. When $E_i = 0$, the corresponding oscillator is called a Hopf oscillator (for more details, see [14, 15, 17, 66, 67, 68, 69, 70]). One of the most advantages of Hopf oscillators lies in the possibility to easily control the amplitude and the frequency of the output independently.

As it was done for the first type of CPGs, we may have three different couplings. The systems of differential equations in case of uncoupled, unidirectional and bidirectional two CPGs are

$$\left.\begin{aligned} \dot{x}_1 &= \gamma_1(\mu_1 - r_1^2)x_1 - \omega y_1 \\ \dot{y}_1 &= \gamma_1(\mu_1 - r_1^2)y_1 + \omega x_1 \\ \dot{x}_2 &= \gamma_2(\mu_2 - r_2^2)x_2 - \omega y_2 \\ \dot{y}_2 &= \gamma_2(\mu_2 - r_2^2)y_2 + \omega x_2 \end{aligned}\right\} \tag{3.6}$$

$$\left.\begin{aligned} \dot{x}_1 &= \gamma_1(\mu_1 - r_1^2)x_1 - \omega y_1 + E x_2 \\ \dot{y}_1 &= \gamma_1(\mu_1 - r_1^2)y_1 + \omega x_1 \\ \dot{x}_2 &= \gamma_2(\mu_2 - r_2^2)x_2 - \omega y_2 \\ \dot{y}_2 &= \gamma_2(\mu_2 - r_2^2)y_2 + \omega x_2 \end{aligned}\right\} \tag{3.7}$$

and

$$\left.\begin{aligned} \dot{x}_1 &= \gamma_1(\mu_1 - r_1^2)x_1 - \omega y_1 + E_1 x_2 \\ \dot{y}_1 &= \gamma_1(\mu_1 - r_1^2)y_1 + \omega x_1 \\ \dot{x}_2 &= \gamma_2(\mu_2 - r_2^2)x_2 - \omega y_2 + E_2 x_1 \\ \dot{y}_2 &= \gamma_2(\mu_2 - r_2^2)y_2 + \omega x_2 \end{aligned}\right\}, \tag{3.8}$$

respectively. The outputs are $x_1 = \theta_1$ and $x_2 = \theta_2$, where $\theta_1$ and $\theta_2$, as defined in the kinematic model, represent the angular positions of the hip and knee, respectively. A disadvantage of this type of CPGs is that it is very difficult to design phase coupling of two CPGs without disturbing the amplitude $\mu$ of both CPGs. More details will be explained later in this chapter when the stability is discussed.

### 3.3 The third type of CPGs

In their papers Marbach and Van den Kieboom (for details, see, [66, 71]) claim that a number of experiments reveal that sinusoidal signals are well suited for locomotion

control:

$$x = A\sin(2\pi f t + \phi),$$

where $A$ is the amplitude, $f$ the frequency and $\phi$ the phase. Differentiating $x$ twice yields the system

$$\tau\dot{x} = v, \quad \tau\dot{v} = -x$$

where $\tau = 1/(2\pi f)$. Here, the amplitude is implicitly defined by the system. In fact, it depends on the initial conditions. Therefore, to force the system to lead to a limit cycle with the desired amplitude, a new term should be included in the system. For example, the new system of differential equations may look like

$$\begin{aligned} \tau\dot{x} &= v \\ \tau\dot{v} &= -\frac{\alpha}{E}\left(x^2 + v^2 - E\right)v - x \end{aligned} \tag{3.9}$$

in which the parameters $\tau$, $\alpha$ and $E$ are positive constants. In (3.9), the term $x^2 + v^2$ stands for the actual energy and the difference $x^2 + v^2 - E$ denotes the energy error of the oscillator. Therefore, the newly added term may be viewed as the normalized energy error multiplied by $\alpha$ and $v$.

To reach the strength of coupling CPGs, we consider a simple coupling strategy given in [15] where each CPG sends a signal proportional to the states variables to every other CPG. More specifically, we consider

$$\left.\begin{aligned} P_{x,i} &= 0 \\ P_{v,i} &= \sum_{i\neq j}\left(\frac{a_{ij}x_j + b_{ij}v_j}{\sqrt{x_j^2 + v_j^2}}\right) \end{aligned}\right\}$$

$a_{ij}$ and $b_{ij}$ are positive constants that determine how oscillator $j$ influences oscillator $i$ and imply a specific phase difference on the limit cycle. The general system for this type of CPGs is given by

$$\left.\begin{aligned} \tau\dot{x}_i &= v_i \\ \tau\dot{v}_i &= -\frac{\alpha}{E_i}\left(x_i^2 + v_i^2 - E_i\right)v_i - x_i + \sum_{j\neq i}\left(\frac{a_{ij}x_j + b_{ij}v_j}{\sqrt{x_j^2 + v_j^2}}\right) \end{aligned}\right\} \tag{3.10}$$

Specific forms of outputs can still occur by changing the numerical values of the parameters [16]. Depending on the values of $a_{ij}$ and $b_{ij}$, the coupling of CPGs may

be called uncoupled, unidirectional and bidirectional. The corresponding systems of differential equations are provided below:

$$\left.\begin{aligned} \tau\dot{x}_1 &= v_1 \\ \tau\dot{v}_1 &= -\frac{\alpha}{E_1}\left(x_1^2 + v_1^2 - E_1\right)v_1 - x_1 \\ \tau\dot{x}_2 &= v_2 \\ \tau\dot{v}_2 &= -\frac{\alpha}{E_2}\left(x_2^2 + v_2^2 - E_2\right)v_2 - x_2 \end{aligned}\right\} \tag{3.11}$$

$$\left.\begin{aligned} \tau\dot{x}_1 &= v_1 \\ \tau\dot{v}_1 &= -\frac{\alpha}{E_1}\left(x_1^2 + v_1^2 - E_1\right)v_1 - x_1 + \frac{a_{12}x_2 + b_{12}v_2}{\sqrt{x_2^2 + v_2^2}} \\ \tau\dot{x}_2 &= v_2 \\ \tau\dot{v}_2 &= -\frac{\alpha}{E_2}\left(x_2^2 + v_2^2 - E_2\right)v_2 - x_2 \end{aligned}\right\} \tag{3.12}$$

and

$$\left.\begin{aligned} \tau\dot{x}_1 &= v_1 \\ \tau\dot{v}_1 &= -\frac{\alpha}{E_1}\left(x_1^2 + v_1^2 - E_1\right)v_1 - x_1 + \frac{a_{12}x_2 + b_{12}v_2}{\sqrt{x_2^2 + v_2^2}} \\ \tau\dot{x}_2 &= v_2 \\ \tau\dot{v}_2 &= -\frac{\alpha}{E_2}\left(x_2^2 + v_2^2 - E_2\right)v_2 - x_2 + \frac{a_{21}x_1 + b_{21}v_1}{\sqrt{x_1^2 + v_1^2}} \end{aligned}\right\} \tag{3.13}$$

In any case, the outputs are $x_1 = \theta_1$ and $x_2 = \theta_2$, where $\theta_1$ and $\theta_2$, as defined in the kinematic model, represent the angular positions of the hip and knee, respectively.

## 3.4 Stability analysis

In this part, the stability analysis for each type of coupling given in the previous section will be discussed.

### 3.4.1 CPGs of the first type

#### 3.4.1.1 Uncoupled two CPGs of the first type

Consider (3.2) where the first and the second CPGs are independent to each other. One can easily show that $r_1$ and $r_2$ converge to $R_1$ and $R_2$, respectively. To see that,

it is enough to show $r_1$ converges asymptotically to $R_1$ when $t \to \infty$. The differential equation

$$\ddot{r_1} = a_1(\frac{a_1}{4}(R_1 - r_1) - \dot{r_1})$$

has a general solution

$$r_1(t) = (c_1 + c_2 t)e^{-a_1 t/2} + R_1.$$

Since $a_1$ is positive, it is clear that $r_1$ asymptotically converge to $R_1$ as $t \to \infty$ no matter what the initial conditions are.

#### 3.4.1.2 Unidirectional two CPGs of the first type

Consider (3.3) and let $\phi = \varphi_2 - \varphi_1$ denotes the phase difference. The time evolution of the phase difference is determined by

$$\dot{\phi} = \dot{\varphi_2} - \dot{\varphi_1} = 2\pi(\nu_2 - \nu_1) - r_2 w_{12} \sin(\phi - \phi_{12}) := f(\phi).$$

If the oscillators synchronize, then they will do so at the fixed points $\phi_\infty$ for which $\dot{\phi} = 0$. Now, if $f(\phi_\infty) = 0$, then

$$\phi_\infty = \arcsin\left(\frac{2\pi(\nu_2 - \nu_1)}{R_2 w_{12}}\right) + \phi_{12}.$$

Note that there is no fixed-point if

$$\left|\frac{2\pi(\nu_2 - \nu_1)}{R_2 w_{12}}\right| > 1.$$

That is, when the difference of intrinsic frequencies is too large compared to the coupling weight $w_{12}$ multiplied by the $R_2$ amplitude of the oscillator 2, the oscillators do not synchronize and are said to drift. If

$$\left|\frac{2\pi(\nu_2 - \nu_1)}{R_2 w_{12}}\right| = 1,$$

then there is a single fixed point $\phi_\infty = \frac{\pi}{2} + \phi_{12}$ when $\nu_2 > \nu_1$, and $\phi_\infty = -\frac{\pi}{2} + \phi_{12}$ when $\nu_2 < \nu_1$. In this case, the two oscillators will synchronize. Finally, if

$$\left|\frac{2\pi(\nu_2 - \nu_1)}{R_2 w_{12}}\right| < 1,$$

then there are two fixed points; one of them is stable and the other one is unstable. The stability of the fixed point is determined by the sign of

$$\frac{\partial f(\phi_\infty)}{\partial \phi} = -R_2 w_{12} \cos(\phi_\infty - \phi_{12})$$

The fixed point is stable if this quantity is negative, and unstable if it is positive. If the initial phase difference is the unstable fixed point, the two oscillators will remain synchronized with that phase difference.

#### 3.4.1.3 Bidirectional two CPGs of the first type

Consider (3.4) and let $\phi_{12} = -\phi_{21}$. In this case, we have

$$\dot{\phi} = f(\phi) = \dot{\varphi_2} - \dot{\varphi_1} = 2\pi(\nu_2 - \nu_1) - (R_1 w_{21} + R_2 w_{12}) \sin(\phi - \phi_{12}).$$

and $f(\phi_\infty) = 0$ results in

$$\phi_\infty = \arcsin(\frac{2\pi(\nu_2 - \nu_1)}{R_1 w_{21} + R_2 w_{12}}) + \phi_{12}.$$

There is no fixed-point if

$$\left|\frac{2\pi(\nu_2 - \nu_1)}{R_1 w_{21} + R_2 w_{12}}\right| > 1.$$

In this case, the oscillators do not synchronize and are said to drift. If

$$\left|\frac{2\pi(\nu_2 - \nu_1)}{R_1 w_{21} + R_2 w_{12}}\right| = 1,$$

then there is a single fixed point $\phi_\infty = \frac{\pi}{2} + \phi_{12}$ when $\nu_2 > \nu_1$, and $\phi_\infty = -\frac{\pi}{2} + \phi_{12}$ when $\nu_2 < \nu_1$. The two oscillators will synchronize with that phase difference. Finally, if

$$\left|\frac{2\pi(\nu_2 - \nu_1)}{R_1 w_{21} + R_2 w_{12}}\right| < 1,$$

then there are two fixed points; one of them is stable and the other one is unstable. The stability of the fixed point is determined by the sign of

$$\frac{\partial f(\phi_\infty)}{\partial \phi} = -(R_1 w_{21} + R_2 w_{12}) \cos(\phi_\infty - \phi_{12})$$

The fixed point is stable if this quantity is negative, and unstable if this quantity is positive. As such, when the initial phase difference is the unstable fixed point, the two oscillators will remain synchronized with that phase difference. To sum up this type of CPGs, the outputs of uncoupled, unidirectional and bidirectional two CPGs are always oscillate. In next chapter, we will optimize this type of CPGs in order to produce rhythmic motions for one leg by using GA and Hybrid function to move along *x*-direction.

### 3.4.2 CPGs of the second type

The Hopf oscillators make up the CPGs network. The CPGs possess the limit cycle property that controls the frequency and the amplitude of the neural structure. Actually, it is possible to adjust the frequency and amplitude through the parameter $\mu$ and $\omega$. Let us consider the first case.

#### 3.4.2.1 Uncoupled two CPGs of the second type

Since the two CPGs are uncoupled it is enough to investigate only one of them. Consider

$$\begin{aligned} \dot{x} &= \gamma(\mu - r^2)x - \omega y \\ \dot{y} &= \gamma(\mu - r^2)y + \omega x \end{aligned} \tag{3.14}$$

It is clear that there is only one equilibrium point which is the origin. Let $x = r\cos\phi$ and $y = r\sin\phi$. Then, (3.14) is written in the phase space as

$$\begin{aligned} \dot{r} &= \gamma(\mu - r^2)r, \\ \dot{\phi} &= \omega. \end{aligned}$$

The sign of $\phi$ determines the direction in which a trajectory is rotating. Depending on the sign of $\mu$, we shall have two cases:

- If $\mu \leqslant 0$, then $\dot{r} < 0$ for all $r$, and hence, $r(t) \to 0$ as $t \to \infty$.

- If $\mu > 0$, then $\dot{r} < 0$ for $r \in (\sqrt{\mu}, \infty)$ and $\dot{r} > 0$ for $r \in (0, \sqrt{\mu})$. This means that origin is unstable and there is a stable orbit when $r = \sqrt{\mu}$. (See [72, 73, 74] for more details.) In this case, a supercritical Hopf bifurcation occurs at $\mu = 0$, as in the Figure 3.3.

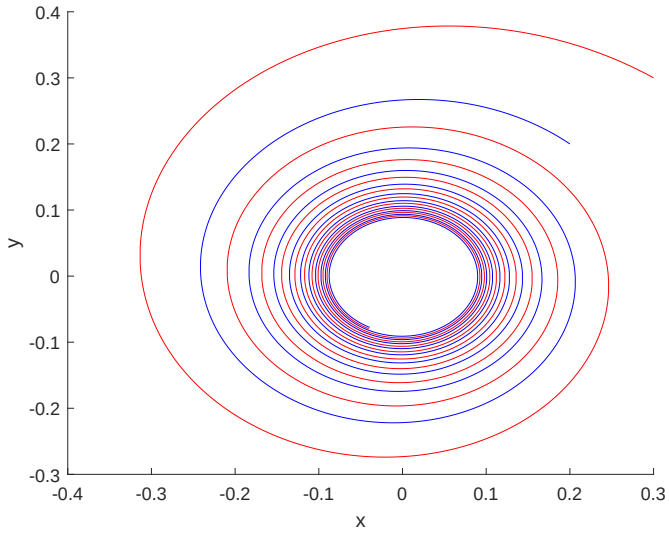


Figure 3.1: Two solutions of (3.14) for $\mu = 0, \omega = \gamma = 1$. Red curve corresponds to the initial condition $x_1(0) = y_1(0) = 0.3$, and the blue one corresponds to the initial condition $x_1(0) = y_1(0) = 0.2$.

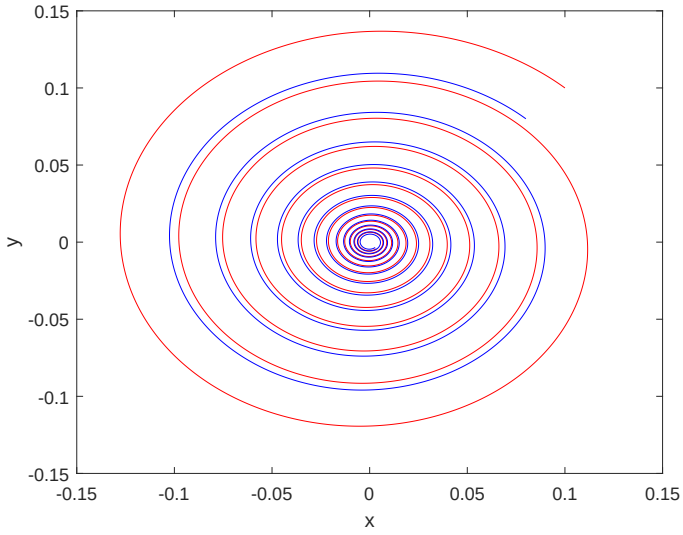


Figure 3.2: Two solutions of (3.14) for $\mu = -0.2, \omega = \gamma = 0.2$. Red curve corresponds to the initial condition $x_1(0) = y_1(0) = 0.08$, and the blue one corresponds to the initial condition $x_1(0) = y_1(0) = 0.1$.

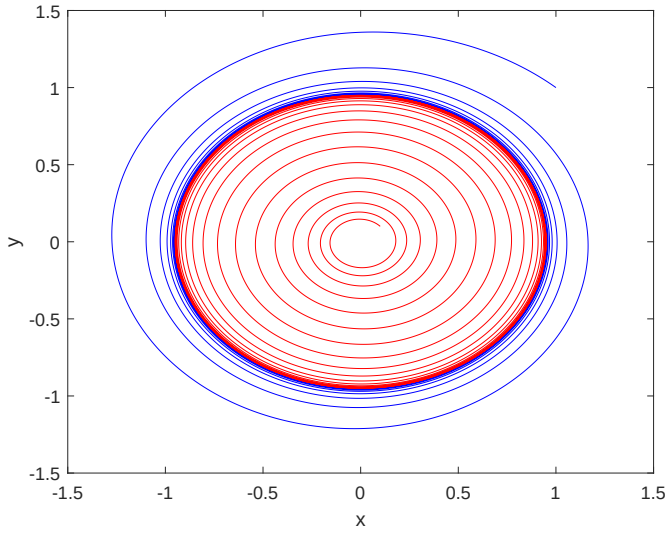


Figure 3.3: Existence of a limit cycle for (3.14) with $m = 0.9$. Here, $\omega = 2$, and $\gamma = 0.1$. Red curve corresponds to the initial condition $x_1(0) = y_1(0) = 1$, and the blue one corresponds to the initial condition $x_1(0) = y_1(0) = 0.1$.

#### 3.4.2.2 Unidirectional two CPGs of the second type

Consider the system (3.7). Again, there is only one equilibrium point which is the origin. The linearized system about the fixed point has the Jacobian matrix

$$J(0,0,0,0) = \begin{bmatrix} \gamma_1\mu_1 & -\omega & 0 & 0 \\ \omega & \gamma_1\mu_1 & 0 & 0 \\ E & 0 & \gamma_2\mu_2 & -\omega \\ 0 & 0 & \omega & \gamma_2\mu_2 \end{bmatrix}$$

which has the characteristic equation $\left[(\lambda - \gamma_1\mu_1)^2 + \omega^2\right]\left[(\lambda - \gamma_2\mu_2)^2 + \omega^2\right] = 0$ whose eigenvalues are $\lambda_{1,2} = \gamma_1\mu_1 \pm i\omega$ and $\lambda_{3,4} = \gamma_2\mu_2 \pm i\omega$.

If $\mu_1 = \mu_2 = 0$, then the eigenvalues demonstrate multiplicity, which means that the fixed point is unstable. If both $\mu_1$ and $\mu_2$ are negative, then the fixed point is asymptotically stable. If at least one of $\mu_1, \mu_2$ is positive, then the fixed point is unstable.

#### 3.4.2.3 Bidirectional two CPGs of the second type

Consider 3.8. As before, origin is the only equilibrium point and the linearized system about that point has the Jacobian matrix

$$J(0,0,0,0) = \begin{bmatrix} \gamma_1\mu_1 & -\omega & E_2 & 0 \\ \omega & \gamma_1\mu_1 & 0 & 0 \\ E_1 & 0 & \gamma_2\mu_2 & -\omega \\ 0 & 0 & \omega & \gamma_2\mu_2 \end{bmatrix}$$

which has the characteristic equation

$$[(\lambda - \gamma_1\mu_1)^2 + \omega^2][(\lambda - \gamma_2\mu_2)^2 + \omega^2] - E_1E_2\gamma_1\gamma_2\mu_1\mu_2 = 0.$$

Assuming

$$\gamma_1 = \gamma_2 = \gamma,\ \mu_1 = \mu_2 = \mu,\ E_1 = E_2 = E$$

and setting

$$E\mu\gamma = \Omega,$$

we get

$$((\lambda - \gamma\mu)^2 + \omega^2)^2 - \Omega^2 = 0$$

whose solutions are

$$\lambda_{1,2} = \gamma\mu \pm i\sqrt{\Omega + \omega^2} \quad \text{and} \quad \lambda_{3,4} = \gamma\mu \pm \sqrt{\Omega - \omega^2}$$

- If $\mu = 0$, then $\Omega = 0$ and the eigenvalues show multiplicity, meaning that the fixed point is unstable.
- If $\mu < 0$ and $\Omega + \omega^2 > 0$, the fixed point is asymptotically stable.
- If $\mu > 0$, the solution is unstable.

The other cases will not be considered here, but during the optimization they will be taken into account.

### 3.4.3 CPGs of the third type

#### 3.4.3.1 Uncoupled two CPGs of the third type

As stated before, it is sufficient to analyze only one CPG in this case. Consider (3.9). Clearly, origin is the only fixed point and the Jacobian matrix of the linearized system at the fixed point is

$$J(0,0) = \begin{bmatrix} 0 & \frac{1}{\tau} \\ -\frac{1}{\tau} & \frac{\alpha}{\tau} \end{bmatrix}$$

whose eigenvalues are

$$\lambda_{1,2} = \frac{1}{\tau}\left(\alpha \pm \sqrt{\alpha^2 - 4}\right).$$

Since $\alpha/\tau > 0$, the fixed point is locally unstable. To make further analysis, let $x = r\cos\phi$, $v = r\sin\phi$. Then, (3.9) becomes

$$\dot{r} = \tfrac{\alpha}{\tau E}(E - r^2) r \sin^2\phi$$
$$\dot{\phi} = -\tfrac{1}{\tau} - \tfrac{\alpha}{\tau E}(r^2 - E)\cos\phi\sin\phi$$

It is now obvious that all solutions with $r(0) > 0$ tend to $\sqrt{E}$ as $t \to \infty$. Translating this into the $xy$-plane, it means that $x^2 + v^2$ increases as long as $x^2 + v^2 < E$, and it decreases when $x^2 + v^2 > E$. Thus, there is a stable limit cycle with radius $\sqrt{E}$ and an unstable equilibrium point at the origin. In Figure 3.4, two solutions corresponding to different values of the parameters for the first CPG are shown. The limit cycle for one CPG can be observed in that figure.

#### 3.4.3.2 Unidirectional two CPGs of the third type

The system (3.12) does not have any fixed point. Since the only candidate is the origin, but there the second equation is not defined. To check whether there is a periodic solution, we subject (3.12) to the change of variables $x_1 = r_1\cos\phi_1$, $v_1 = r_1\sin\phi_1$, $x_2 = r_2\cos\phi_2$ and $v_2 = r_2\sin\phi_2$. Then, we obtain

$$\dot{r}_1 = -\tfrac{\alpha}{\tau E_1}\left(r_1^2 - E_1\right) r_1 \sin^2\phi_1 + \tfrac{1}{\tau}\left(a_{12}\cos\phi_2 + b_{12}\sin\phi_2\right)\sin\phi_1$$
$$\dot{\phi}_1 = -\tfrac{1}{\tau} - \tfrac{\alpha}{\tau E_1}\left(r_1^2 - E_1\right)\cos\phi_1\sin\phi_1 + \tfrac{1}{\tau r_1^2}\left(a_{12}\cos\phi_2 + b_{12}\sin\phi_2\right)$$
$$\dot{r}_2 = -\tfrac{\alpha}{\tau E_2}\left(r_2^2 - E_2\right) r_2 \sin^2\phi_2$$
$$\dot{\phi}_2 = -\tfrac{1}{\tau} - \tfrac{\alpha}{\tau E_2}\left(r_2^2 - E_2\right)\cos\phi_2\sin\phi_2.$$

Clearly, $r_2 = \sqrt{E_2}$ is the periodic solution for the second CPG. The limit cycle for the first CPG can be observed in Figure 3.5. Therefore, as in the case of uncoupled two CPGs, this system has a limit cycle.

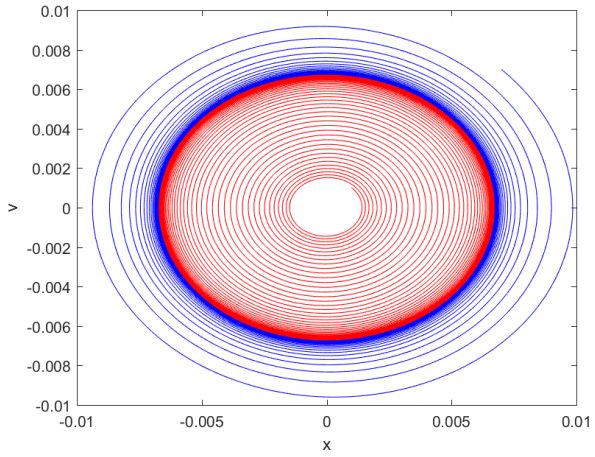


Figure 3.4: Existence of a stable limit cycle of (3.9) when $\tau = 0.009$, $\alpha = 0.03$ and $E_1 = 0.000045$. Red curve corresponds to the initial condition $x_1(0) = v_1(0) = 0.001$, and the blue one corresponds to the initial condition $x_1(0) = v_1(0) = 0.007$.

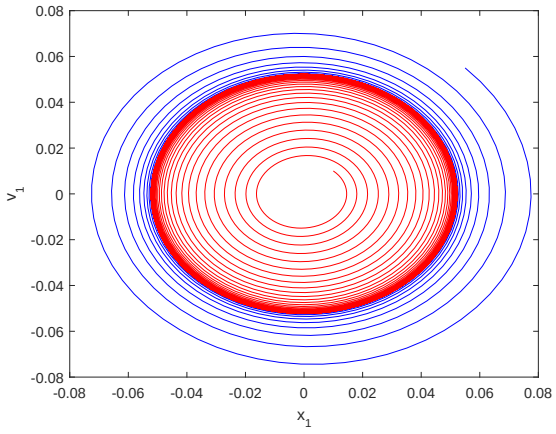


Figure 3.5: Two trajectories of the first CPG in the case of unidirectional two CPGs with $\tau = .01$, $\alpha_1 = .0001$, $\alpha_2 = .001$, $a_{12} = b_{12} = .001$ and $E_1 = E_2 = .00001$. Red curve corresponds to the initial condition $x_1(0) = x_2(0) = v_1(0) = v_2(0) = .01$, and the blue one corresponds to the initial condition $x_1(0) = x_2(0) = v_1(0) = v_2(0) = .05$.

#### 3.4.3.3 Bidirectional two CPGs of the third type

Consider (3.13). For an equilibrium point, note that the first and the third equations give $v_1 = v_2 = 0$ which leads to $-x_1 \pm a_{12} = 0$ and $-x_2 \pm a_{21} = 0$. Since $x_1$ and $x_2$ should have the same signs, the equilibrium points are $(a_{12}, 0, a_{21}, 0)$ and $(-a_{12}, 0, -a_{21}, 0)$ and the points $(a_{12}, 0, -a_{21}, 0)$ and $(-a_{12}, 0, a_{21}, 0)$ are not equilibrium points. The Jacobian matrix at any fixed point is

$$J(\pm a_{12}, 0, \pm a_{21}, 0) = \begin{bmatrix} 0 & \frac{1}{\tau} & 0 & 0 \\ -\frac{1}{\tau} & \frac{\alpha}{\tau E_1}(E_1 - a_{12}^2) & 0 & \pm\frac{b_{12}}{\tau a_{21}} \\ 0 & 0 & 0 & \frac{1}{\tau} \\ 0 & \pm\frac{b_{21}}{\tau a_{12}} & -\frac{1}{\tau} & \frac{\alpha}{\tau E_2}(E_2 - a_{21}^2) \end{bmatrix}$$

Therefore, the eigenvalues for both equilibrium points are the roots of the characteristic equation

$$\left(\lambda^2 + \frac{\alpha(a_{12}^2 - E_1)}{\tau E_1}\lambda + \frac{1}{\tau^2}\right)\left(\lambda^2 + \frac{\alpha(a_{21}^2 - E_2)}{\tau E_2}\lambda + \frac{1}{\tau^2}\right) - \frac{b_{12}b_{21}}{\tau^2 a_{12}a_{21}}\lambda^2 = 0. \tag{3.15}$$

It is difficult to solve this equation manually or to find the eigenvalues analytically. To extract some information from this equation in some particular cases, we let

$$\beta_1 = \frac{\alpha(a_{12}^2 - E_1)}{\tau E_1}, \quad \beta_2 = \frac{\alpha(a_{21}^2 - E_2)}{\tau E_2},$$

and set

$$\mu = \frac{b_{12}b_{21}}{a_{12}a_{21}}.$$

Then the characteristic equation becomes

$$\left(\lambda^2 + \beta_1\lambda + \frac{1}{\tau^2}\right)\left(\lambda^2 + \beta_2\lambda + \frac{1}{\tau^2}\right) - \mu\lambda^2 = 0, \tag{3.16}$$

whose roots are

$$\lambda_{1,2} = \frac{1}{\tau}\left(\frac{1}{4}(-\tau\beta_1 - \tau\beta_2 + D) \pm \frac{\sqrt{2}}{4}\sqrt{\tau^2\beta_1^2 - \tau\beta_1 D + \tau^2\beta_2^2 - \tau\beta_2 D + 2\mu - 8}\right)$$

and

$$\lambda_{3,4} = \frac{1}{\tau}\left(\frac{1}{4}(-\tau\beta_1 - \tau\beta_2 - D) \pm \frac{\sqrt{2}}{4}\sqrt{\tau^2\beta_1^2 + \tau\beta_1 D + \tau^2\beta_2^2 + \tau\beta_2 D + 2\mu - 8}\right),$$

where

$$D = \sqrt{\tau^2\beta_1^2 - \tau\beta_1\beta_2 + \tau^2\beta_2^2 + 4\mu}$$

Still, the analysis cannot be done manually. Thus, either one has to trust the simulation results only, which is not scientifically strong because of the errors that may occur during the computation, or one can consider special cases as we do here.

**Case 1**: $\beta_1 = \beta_2 = \beta$. In that case, the eigenvalues are

$$\lambda_{1,2} = \frac{\left(-\tau\beta + \sqrt{\mu} \pm \sqrt{\tau^2\beta - 2\tau\beta\sqrt{\mu} + \mu - 4}\right)}{2\tau},$$

and

$$\lambda_{3,4} = \frac{\left(-\tau\beta - \sqrt{\mu} \pm \sqrt{\tau^2\beta + 2\tau\beta\sqrt{\mu} + \mu - 4}\right)}{2\tau}.$$

- When $\mu < 0$, as the Figure 3.6 supports;
  - If $\beta < 0$, then there are complex eigenvalues with positive real part. Hence, the fixed points an unstable source.
  - If $\beta = 0$, then the eigenvalues are purely imaginary, and the system will oscillate around the steady state. The fixed points are stable.
  - If $\beta > 0$, the real parts of all eigenvalues are negative. So, the fixed points are asymptotically stable.
- When $\mu = 0$, as the Figure 3.7 supports;
  - If $\beta < 0$, then the eigenvalues are repeated and their real parts are positive. So, the fixed points are unstable.
  - If $\beta = 0$, then the eigenvalues are repeated purely imaginary complex numbers. Thus, the fixed points are unstable.
  - If $\beta > 0$, then the real parts of eigenvalues are negative. For $\tau_1 \neq \tau_2$, the fixed points are asymptotically stable and for $\tau_1 = \tau_2$, the eigenvalues are repeated which means that the fixed points are unstable.
- When $\mu > 0$, as the Figure 3.8 supports;
  - If $\beta < 0$, then the eigenvalues have positive real parts. So, the fixed points are an unstable.
  - If $\beta > 0$, the fixed points are stable for small values of $\mu$ and unstable for large values of $\mu$.

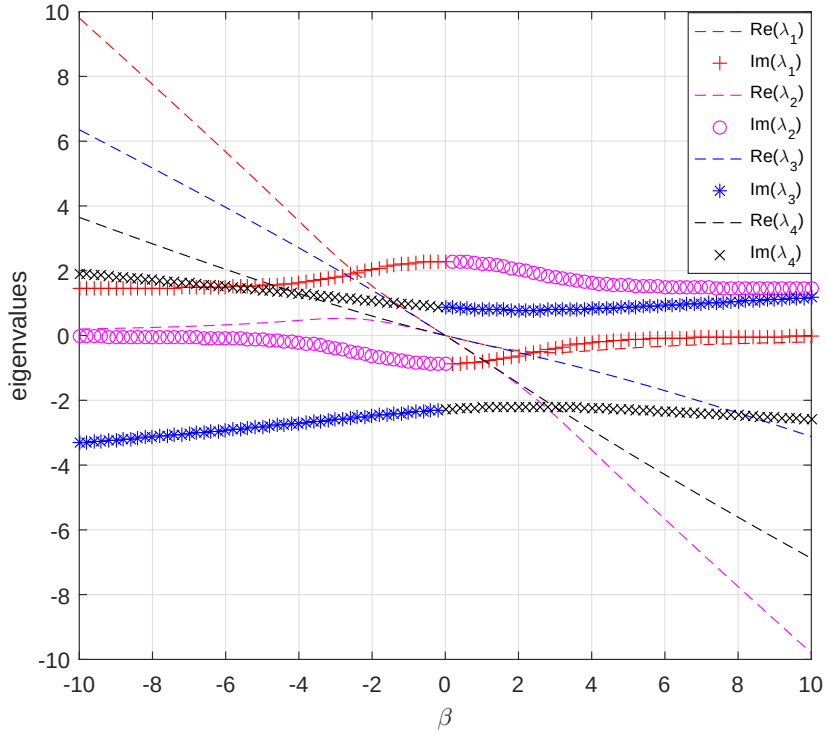


Figure 3.6: The eigenvalues against $\beta$, when $\mu < 0$.

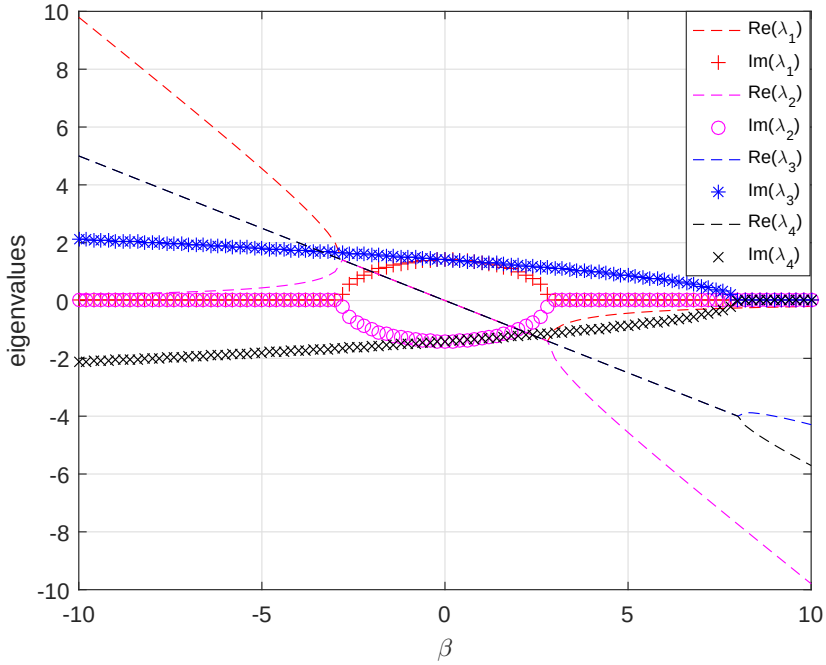


Figure 3.7: The eigenvalues against $\beta$, when $\mu = 0$.

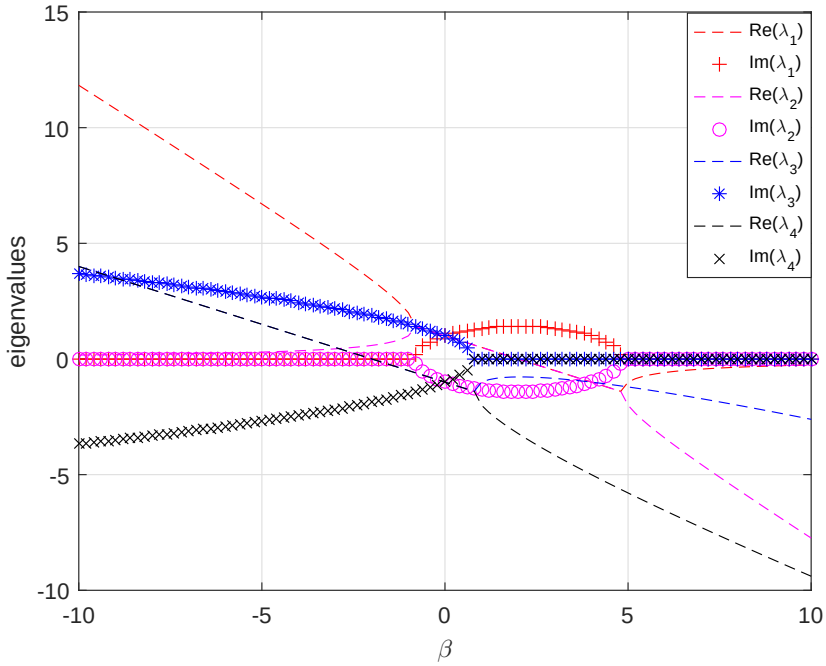


Figure 3.8: The eigenvalues against $\beta$, when $\mu > 0$.

**Case 2**: $\beta_1 \neq \beta_2$.

- When $\mu < 0$, with the help of the Figures 3.9, 3.10, 3.11 and 3.12, one has
  - If $\beta_1 > 0, \beta_2 > 0$, then the fixed points are stable.
  - If $\beta_1 < 0, \beta_2 > 0$, then the fixed points are stable for $\mu$ close to zero, otherwise the fixed points are unstable.
  - If $\beta_1 > 0, \beta_2 < 0$, then the fixed points are unstable.
  - If $\beta_1 < 0, \beta_2 < 0$, then the fixed points are unstable.
  - If $\beta_1 = 0$, then the fixed points are asymptotically stable for $\beta_2 > 0$ and they are unstable for $\beta_2 < 0$.
  - If $\beta_2 = 0$, then the fixed points are asymptotically stable for $\beta_1 > 0$ and they are unstable for $\beta_1 < 0$.
- When $\mu = 0$, with the help of the Figures 3.13, 3.14, 3.15 and 3.16, one has
  - If $\beta_1 > 0, \beta_2 > 0$, then the fixed points are asymptotically stable.
  - If $\beta_1 < 0, \beta_2 > 0$, then the fixed points are unstable.

- If $\beta_1 < 0, \beta_2 < 0$, then the fixed points are unstable.
- If $\beta_1 > 0, \beta_2 < 0$, then the fixed points are stable.
- If $\beta_1 = 0$, then the fixed points are asymptotically stable for $\beta_2 > 0$, while they are unstable for $\beta_2 < 0$.
- If $\beta_2 = 0$, then the fixed points are asymptotically stable for $\beta_1 > 0$, while they are unstable for $\beta_1 < 0$.

- When $\mu > 0$, with the help of the Figures 3.17, 3.18, 3.19 and 3.20, one has
  - If $\beta_1 > 0, \beta_2 > 0$, then the fixed points are stable for $\mu$ close to zero, otherwise the fixed points are unstable.
  - If $\beta_1 < 0, \beta_2 > 0$, then the fixed points are unstable.
  - If $\beta_1 > 0, \beta_2 < 0$, then the fixed points are unstable.
  - If $\beta_1 < 0, \beta_2 < 0$, then the fixed points are unstable.
  - If $\beta_1 = 0$, then the fixed points are stable for $\beta_2 > 0$, or $\beta_2 < 0$ when $\mu$ close to zero, otherwise the fixed points are unstable.
  - If $\beta_2 = 0$, then the fixed points are unstable for $\beta_1 > 0$, and $\beta_1 < 0$.

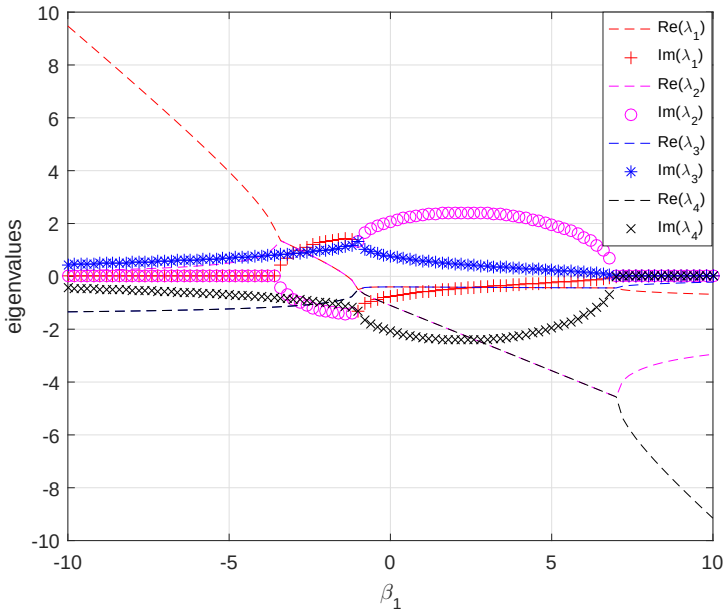


Figure 3.9: The eigenvalues against $\beta_1$, when $\mu < 0$ and $\beta_2 > 0$.

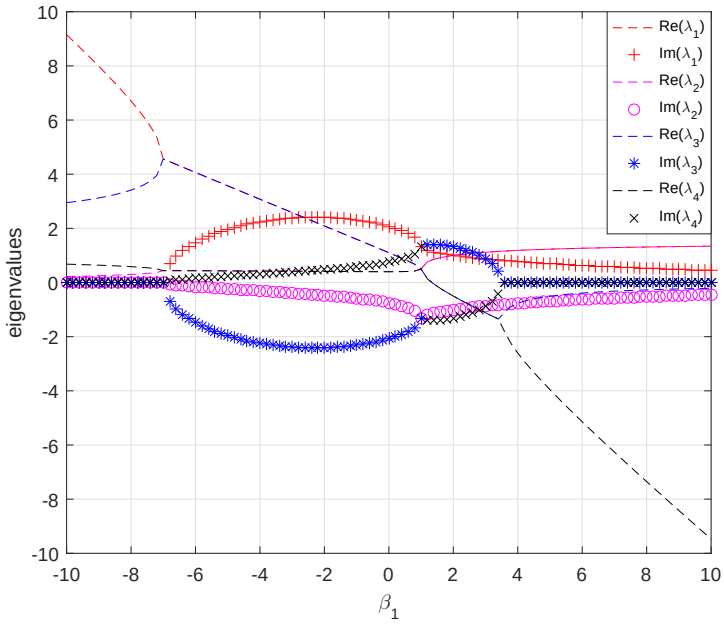


Figure 3.10: The eigenvalues against $\beta_1$, when $\mu < 0$ and $\beta_2 < 0$.

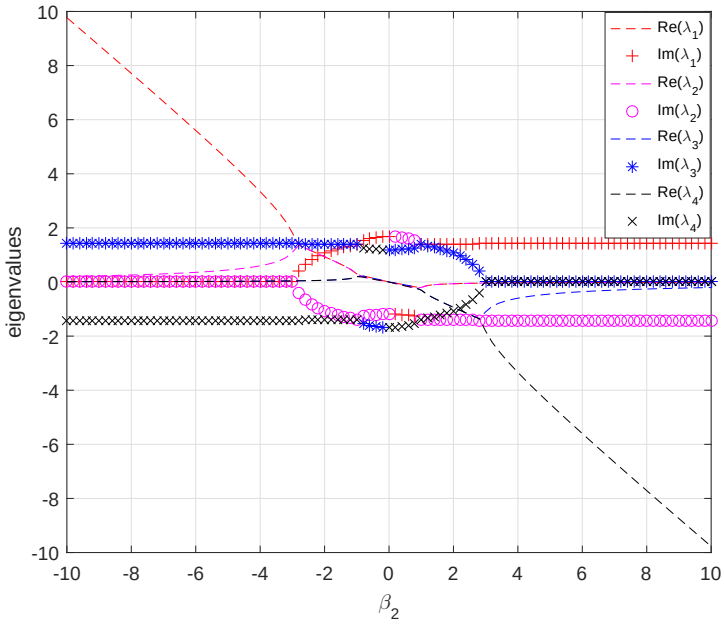


Figure 3.11: The eigenvalues against $\beta_2$, when $\mu < 0$ and $\beta_1 = 0$.

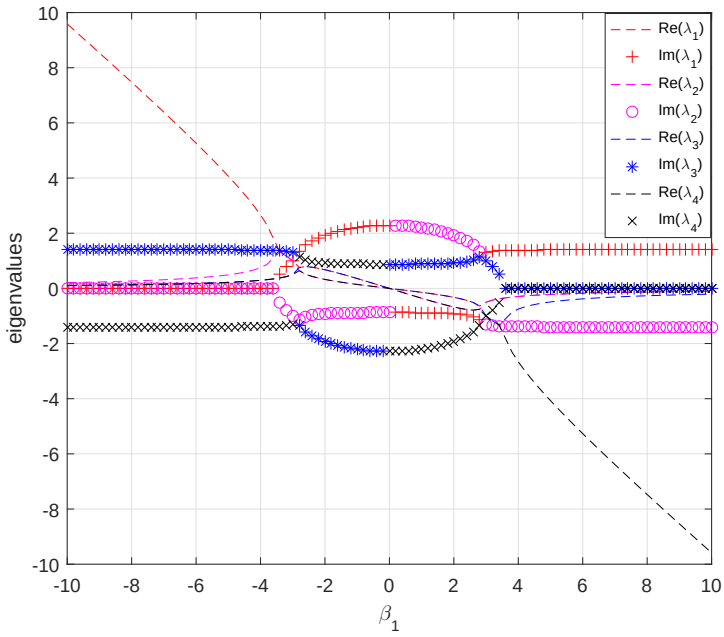


Figure 3.12: The eigenvalues against $\beta_1$, when $\mu < 0$ and $\beta_2 = 0$.

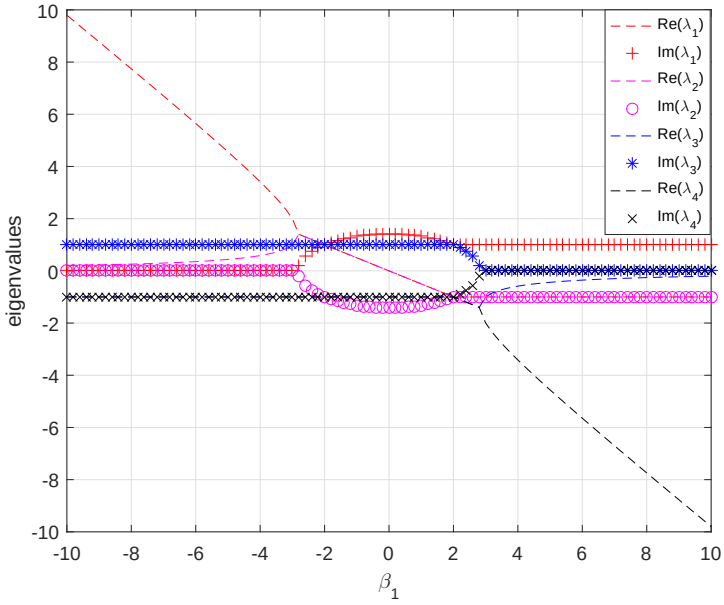


Figure 3.13: The eigenvalues against $\beta_1$, when $\mu = 0$ and $\beta_2 > 0$.

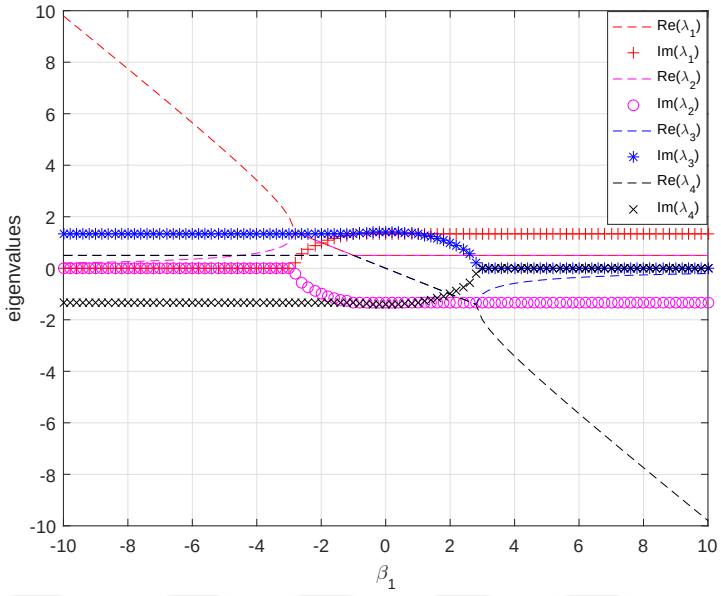


Figure 3.14: The eigenvalues against $\beta_1$, when $\mu = 0$ and $\beta_2 < 0$.

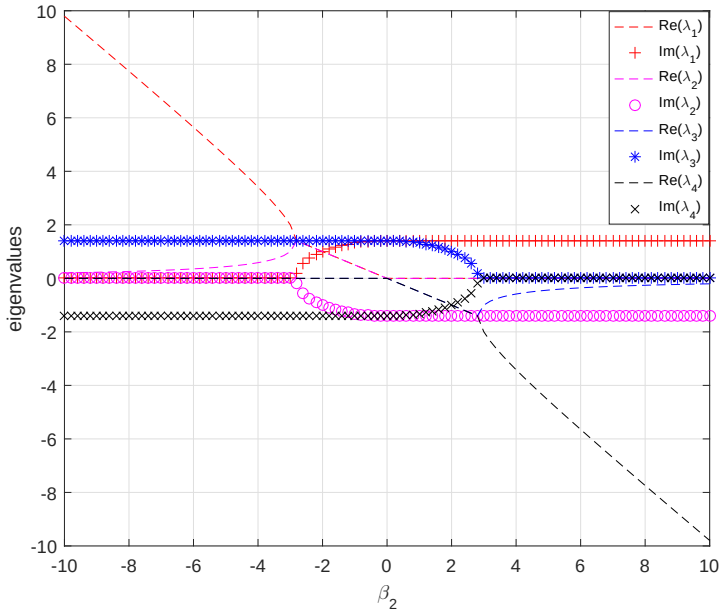


Figure 3.15: The eigenvalues against $\beta_2$, when $\mu = 0$ and $\beta_1 = 0$.

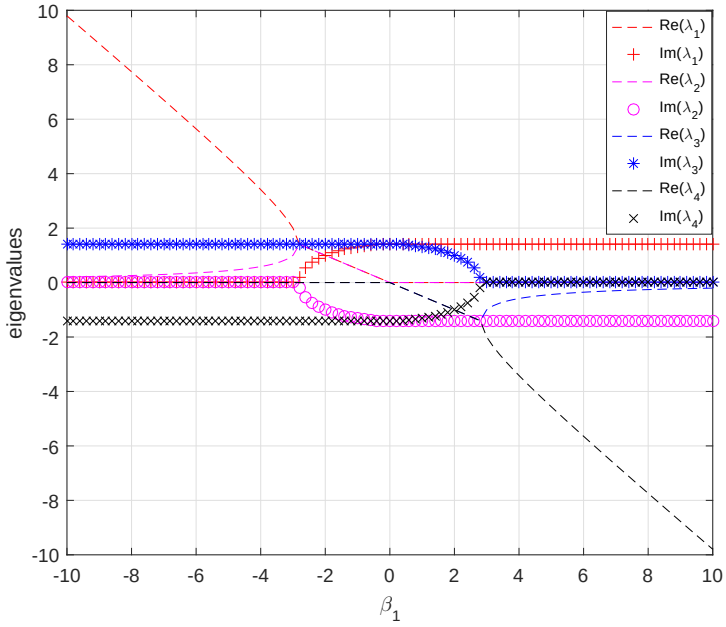


Figure 3.16: The eigenvalues against $\beta_1$, when $\mu = 0$ and $\beta_2 = 0$.

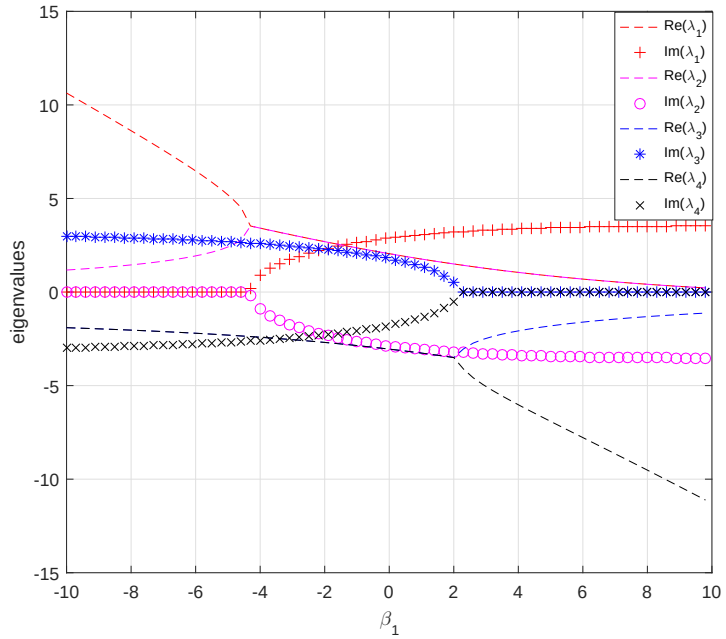


Figure 3.17: The eigenvalues against $\beta_1$, when $\mu > 0$ and $\beta_2 > 0$.

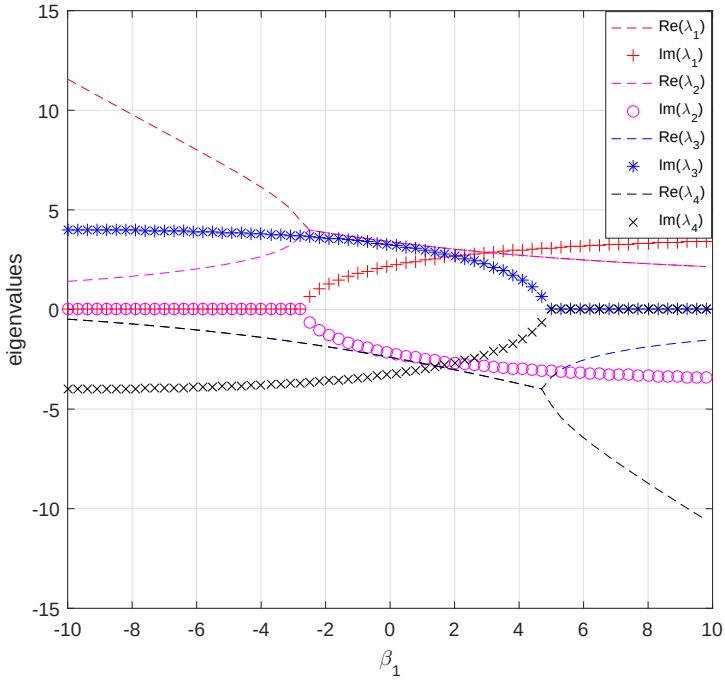


Figure 3.18: The eigenvalues against $\beta_1$, when $\mu > 0$ and $\beta_2 < 0$.

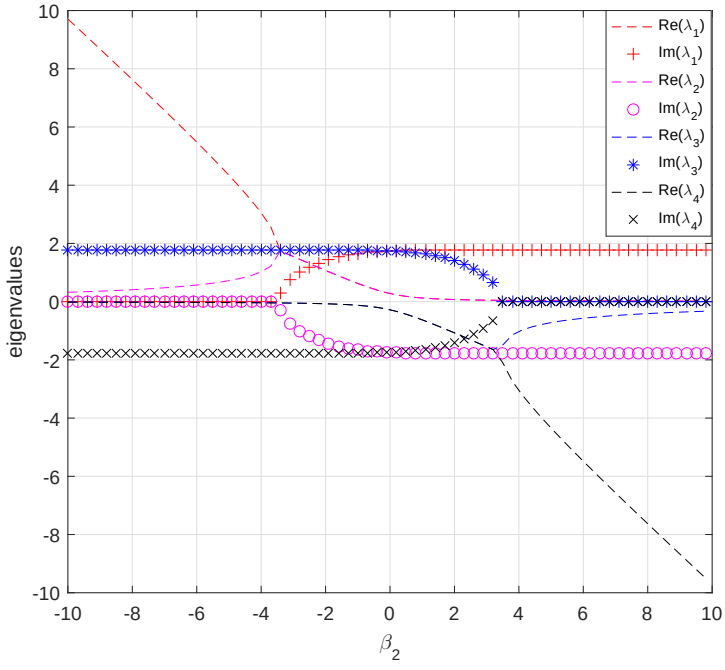


Figure 3.19: The eigenvalues against $\beta_2$, when $\mu > 0$ and $\beta_1 = 0$.

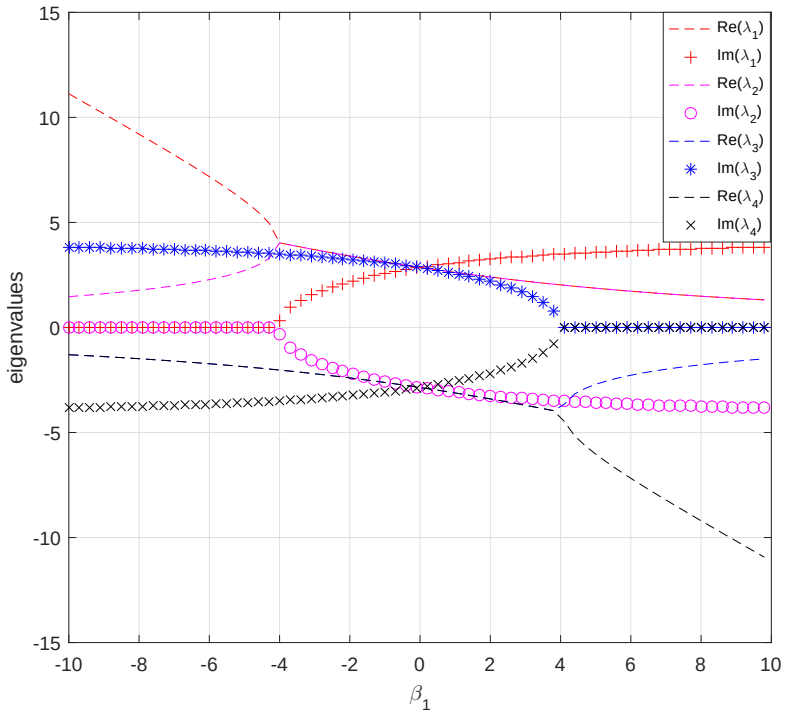


Figure 3.20: The eigenvalues against $\beta_1$, when $\mu > 0$ and $\beta_2 = 0$.

# CHAPTER 4

# OPTIMIZATION OF CPGS

One of the most important steps is to optimize the CPGs and find the optimal parameter sets for each CPG in order to produce RPs for one leg with two DOFs. This can be done, for example, to maximize the displacement or to minimize energy. It should be kept in mind that there are different solvers. Also, there are different algortihms; for instance, the Genetic Algorithm (GA), Global Search (GS), MultiStart (MS), fminsearch (FM) and Pattern Search (PS), also called the direct search, to look for the optimum parameter values. One can select one of the suitable algorithms or combine some of them to make a so-called hybrid function. For any optimization, a problem has the cost function with or without some constraints, where both the objective and constraint functions can be continuous or discontinuous. Algorithmic customization is supported by both the GA and pattern search solvers. It is possible to create a custom genetic algorithm variant by modifying an initial population and fitness scaling options or by defining parent selection, crossover fraction and mutation rate [75].

## 4.1 Genetic algorithm and hybrid function

One of the important questions is how to choose an optimizer. The optimizer is based on problem characteristics and on the type of the solution desired. Solver characteristics contain some information that can help to decide which solver is likely to be the most suitable. To optimize two CPGs in different cases, we start with the GA for three types of couplings since it can randomly select the initial population [76, 77]. Although the GA finds a local minimum, it is very commonly used, since it is not complicated and easy to use. For some problems the GA can fail to converge.

The GA can also be used for multiple objective functions that are subject to a set of constraints. Additionally and most importantly, the multiple objective genetic algorithm solver function is used to solve both smooth and non-smooth problems with or without lower and upper bounds of linear constraints and they do not require the function to be differentiable or continuous.

The most important two parameters of the GA are crossover fraction (C) and mutation rate (M). When the crossover rate is zero ($C = 0$), offspring are the exact copies of their parents and when it is 100% ($C = 1$), all offspring are made by the crossover. When there is a crossover probability ($0 < C < 1$), offspring are made from parts of the chromosomes of the parents. This technique of a crossover is made in the hope that new chromosomes will be better. Nevertheless, we recommend leaving some parts of the population to survive to the next generation. The mutation probability is how often the parts of chromosomes mutate. When $M = 0$, offspring are taken after crossover without any change. If the mutation is performed, part of the chromosome is changed. If $M = 1$, the entire chromosome is changed. Mutation occurs to prevent the GA from falling into a local extreme; however, it should not occur very often because the GA will in fact change to a random search.

Normally, a higher population size produces good results for differential equations. However, a very large population size may not give good results. No general rule can be guaranteed to achieve the global optimum solution by fixing the population size. Therefore, a comprehensive testing is required to fix the population size for each problem. A further increase or decrease of the population size leads to an increase or decrease in the accuracy of the solution. This effect is observed in a population size of 100 chromosomes. The use of a large population improves the solution accuracy (for more details see [78]). We will take the population size to be between 45 and 200.

We will also use a hybrid function during the optimization in order to improve the value of the fitness function. In this thesis, we always start with GA and, in some cases, after it terminates, we run either Pattern Search (PS) or fminsearch (FM). The hybrid function uses the final point from the GA as its initial point [79, 80]. With regard to the stability, the leg is either able or unable to move when the different types couplings are considered.

## 4.2 Walking one leg with 2 DOFs

Main point of this thesis is to optimize two CPGs in different cases, including uncoupled, unidirectional and bidirectional two CPGs in order to generate motion for one leg to move. The model is discussed Chapter 2 and different types of mathematical structures of CPGs are presented in Chapter 3. Each type of CPG will be optimized by using the GA. It is important to mention here that each CPG produces angular patterns as outputs for each joint.

In order to obtain gait generation, it is necessary to compute the optimal parameter sets for each CPG. In other words, it is necessary to understand how the angular position of the hip and knee would change in time in order to produce motion. The parameter sets in the cases of the uncoupled, unidirectional and bidirectional two CPGs for three types of the CPGs are as follows:

- CPGs of the first type:
  - Uncoupled two CPGs: $\{a_1, v_1, R_1, a_2, v_2, R_2\}$.
  - Unidirectional two CPGs: $\{a_1, v_1, R_1, w_{12}, \phi_{12}, a_2, v_2, R_2\}$.
  - Bidirectional two CPGs: $\{a_1, v_1, R_1, w_{12}, \phi_{12}, a_2, v_2, R_2, w_{21}, \phi_{21}\}$.
- CPGs of the second type:
  - Uncoupled two CPGs: $\{\mu_1, a_1, b_1, \omega_1, \mu_2, a_2, b_2, \omega_2\}$
  - Unidirectional two CPGs: $\{\mu_1, a_1, b_1, \omega_1, E, \mu_2, a_2, b_2, \omega_2\}$
  - Bidirectional two CPGs: $\{\mu_1, a_1, b_1, \omega_1, E_1, \mu_2, a_2, b_2, \omega_2, E_2\}$
- CPGs of the third type:
  - Uncoupled two CPGs: $\{\alpha_1, \tau_1, E_1, \alpha_2, \tau_2, E_2\}$.
  - Unidirectional two CPGs: $\{\alpha_1, \tau_1, E_1, a_{12}, b_{12}, \alpha_2, \tau_2, E_2\}$.
  - Bidirectional two CPGs: $\{\alpha_1, \tau_1, E_1, a_{12}, b_{12}, \alpha_2, \tau_2, E_2, a_{21}, b_{21}\}$.

Each type of CPGs has more than five parameters. As mentioned in [81], GA will not be very efficient. For that reason, we shall impose some conditions on parameters to obtain better results.

The cost function that will be used is

$$J = -C_1 \sum_{k=1}^{n} x_b(k) + C_2 \sum_{k=1}^{n} \left( \frac{\theta_1^2(k) + \theta_2^2(k)}{N} \right), \tag{4.1}$$

where $C_1 + C_2 = 1$ and $n$ is the number of elements of the position vector that is simulated with the objective of establishing patterns in order to maximize the displacement or velocity, and $N$ is the length of time. The first term in (4.1) stands for the displacement and the second one is energy related. When $C_2 = 0$, the energy consumption is ignored; hence, the displacement is maximized. On the other hand, when $C_1 = 0$, the energy consumption is minimized ignoring the displacement. It is obvious that for $C_1 = 0$, the minimum displacement is obtained when there is no locomotion. Therefore, throughout this study, it is assumed that $C_1 \neq 0$. Moreover, the requirement $C_1 + C_2 = 1$ is used just to balance the energy consumption and total displacement. The values of $C_1$ and $C_2$ are varied to clarify the relationship between the velocity and the energy constraints during CPG optimization. The ultimate goal here is to minimize the energy while altering the position (for more details on biological locomotion, see [82, 83]).

The two constraints revealed here are $0 \leq \theta_1, \theta_2 \leq \pi$ due to physical reasons. We take the length of the upper link (hip to knee) in the leg as 0.145 m and the lower link (knee to foot) as 0.165 m according to the Test Bench. The height of the sliding body from the ground is taken as $0.25 \pm 0.01$ m. Some figures below show some gaits as a result of the evolutionary optimization technique.

## 4.3 Optimization of the first type of CPGs

### 4.3.1 Uncoupled two CPGs of the first type

Different results of optimizing uncoupled two CPGs are summarized in Tables 4.1 and 4.2 when the parameters of CPGs are constrained and the initial conditions are not fixed. The initial conditions are also determined by optimizing them. By optimizing uncoupled two CPGs when the parameters of CPGs are not constrained, the CPGs are also able to generate RPs for one leg with two DOFs. However, there will be a large variance between steps, and as a result, it is difficult to implement it physically.

Table 4.1: Uncoupled two CPGs of the first type when $C_1C_2 \neq 0$, IC is not fixed

| Solver | Parameter values | $J$ | $x_b$ |
|---|---|---|---|
| GA | 6.2674 1.3937 0.6640 0.1111 1.3961 2.9890 | −1859.7 | 3.8048 |
| GA | 7.2739 1.3950 0.6877 0.1046 1.3973 2.9928 | −1993.5 | 4.0253 |
| GA and PS | 21.4785 2.0180 0.7195 0.1099 2.0208 3.0549 | −3110.9 | 6.0427 |
| GA and FM | 8.6053 1.4939 0.7208 0.1069 1.4912 3.2999 | −2254.7 | 4.4876 |

Table 4.2: Uncoupled two CPGs of the first type when $C_2 = 0$, IC is not fixed

| Solver | Parameter values | $J$ | $x_b$ |
|---|---|---|---|
| GA | 8.6071 1.4938 0.7218 0.1077 1.4912 3.3034 | −2266.4 | 4.4839 |
| GA | 22.4988 2.0174 0.7236 0.1096 2.0210 3.0527 | −3130.1 | 6.0856 |
| GA and PS | 33.7496 2.0175 0.7236 0.1093 2.0210 3.0543 | −3138.8 | 6.0872 |
| GA and FM | 33.7510 2.0174 0.7234 0.1094 2.0209 3.0520 | −3141.7 | 6.0934 |

### 4.3.2 Unidirectional two CPGs of the first type

The results of the optimization in this case are given in Tables 4.3 and 4.4. Comparing Tables 4.1, 4.2, 4.3 and 4.4, we see that the results of the unidirectional case are much better than the uncoupled case.

Table 4.3: Unidirectional two CPGs of the first type when $C_1C_2 \neq 0$, IC is not fixed

| Solver | Parameter values | $J$ | $x_b$ |
|---|---|---|---|
| GA | 12.4504 9.2728 0.8901 5.7888 4.5130 1.2253 6.9333 7.1551 | −4801.4 | 9.3577 |
| GA | 13.0343 57.1958 0.8314 5.9874 4.7665 1.2378 8.0715 36.5990 | −8754.9 | 17.4629 |
| GA and PS | 20.6705 57.1948 0.7905 6.5840 4.7665 1.2382 8.3161 37.6267 | −8940.7 | 18.1305 |
| GA and FM | 14.8514 57.2735 0.8923 11.2956 14.2857 1.3228 14.8913 39.5832 | −21187 | 44.0914 |

Table 4.4: Unidirectional two CPGs of the first type when $C_2 = 0$, IC is not fixed

| Solver | Parameter values | $J$ | $x_b$ |
|---|---|---|---|
| GA | 13.6221 10.9868 0.8620 9.4963<br>12.5940 1.2120 8.6787 10.4065 | −17732 | 38.0833 |
| GA | 18.7442 16.0011 0.9070 16.6791<br>17.6464 1.2234 9.0500 10.4742 | −27015 | 56.3742 |
| GA and PS | 17.8890 16.0022 0.9072 16.7160<br>17.6465 1.2236 9.0535 10.4777 | −27090 | 56.5362 |
| GA and FM | 17.1386 15.9985 0.9075 16.2074<br>17.6467 1.2293 9.0548 10.561 | −28260 | 58.8559 |

### 4.3.3 Bidirectional two CPGs of the first type

The results are given in Tables 4.5 and 4.6. We note that the rhythmic patterns in this case are much better than the other two cases. The results, when the parameters of the CPGs are not constrained, are summarized in Table 4.7, and the results when the parameters of the CPGs are constrained are summarized in Tables 4.8 and 4.9. Also, Figures 4.1, 4.2, 4.3, 4.4, 4.5, 4.6 and 4.7 present one leg animation, the outputs of the CPGs and displacement against time for the uncoupled two CPGs.

Table 4.5: Bidirectional two CPGs of the first type when $C_1C_2 \neq 0$, IC is not fixed

| Solver | Parameter values | $J$ | $x_b$ | E |
|---|---|---|---|---|
| GA | 12.0277 11.2523 0.8263 5.5271 6.0924 6.4723<br>10.0342 1.2105 4.4558 5.5903 | −15247 | 31.5239 | 2.7564 |
| GA | 12.2638 13.1812 0.8607 5.6775 6.2364 6.5007<br>11.6507 1.2551 6.3547 5.6226 | −22913 | 47.7194 | 3.0519 |
| GA and PS | 12.2638 13.1818 0.8601 5.6811 6.2388 6.4978<br>11.6542 1.2563 6.3548 5.6348 | −22827 | 47.6528 | 3.0603 |
| GA and FM | 12.2689 13.2206 0.8670 5.6917 6.2263 6.5196<br>11.6373 1.2564 6.3573 5.6350 | −23101 | 47.7814 | 3.0533 |

Table 4.6: Bidirectional two CPGs of the first type when $C_2 = 0$, IC is not fixed

| Solver | Parameter values | $J$ | $x_b$ | E |
|---|---|---|---|---|
| GA | 8.4231 15.5376 0.7865 9.5072 5.3567 6.9389<br>16.1480 1.1995 4.1472 3.1645 | −24920 | 50.8137 | 2.6918 |
| GA | 8.1883 16.6302 0.9950 9.6418 5.5169 6.8858<br>17.1167 1.2343 4.5534 3.2144 | −33210 | 68.1002 | 3.0328 |
| GA and PS | 8.1882 16.6302 0.9951 9.6422 5.5169 6.8854<br>17.1167 1.2343 4.5536 3.2145 | −33211 | 67.9497 | 3.0332 |
| GA and FM | 8.3143 16.6291 0.9887 9.5097 5.5162 6.9143<br>17.1168 1.2343 4.5682 3.2114 | −33250 | 67.8962 | 3.0344 |

Table 4.7: Optimization of two CPGs in the unbounded region when $C_1C_2 \neq 0$

| Case | Solver | Parameter values | $J$ | $x_b$ | $E$ |
|---|---|---|---|---|---|
| Unc | GA and FM | 30.7363 28.5866 0.8628 20.3314 14.2796 1.2202 | −23849 | 47.8770 | 3.0341 |
| Unc | GA and PS | 30.6689 28.5866 0.8629 20.3406 14.2796 1.2202 | −11924 | 47.8777 | 3.0343 |
| Unid | GA and FM | 17.5270 40.6125 1.0038 27.1307 33.3437 1.2270 51.1525 50.1892 | −57859 | 116.9131 | 3.0240 |
| Unid | GA and PS | 17.2865 40.4284 0.9287 28.0195 33.3458 1.2273 52.0449 50.3126 | −28213 | 112.8684 | 2.9301 |
| Bid | GA and FM | 61.4180 34.8193 0.8691 8.8225 1.0938 61.9136 34.4234 1.3595 12.1180 6.7896 | −68743 | 138.4982 | 3.6014 |
| Bid | GA and PS | 62.4355 34.8369 0.8565 8.9123 1.1130 61.9463 34.4603 1.3678 12.1621 6.8044 | −34536 | 139.0181 | 3.6486 |

Table 4.8: Optimization of two CPGs in the bounded region when $C_1C_2 \neq 0$

| Type | Solver | Parameter values | $J$ | $x_b$ | E |
|---|---|---|---|---|---|
| Unc | GA and PS | 18.6883 1.9928 0.7746 46.4124 1.9604 1.5327 | −1326 | 4.9613 | 4.1004 |
| Unid | GA and PS | 50.0000 1.9850 0.7804 13.1020 1.9230 1.5356 2.0000 −0.3699 | −1707.4 | 6.4220 | 4.2509 |
| Bid | GA and PS | 61.4180 34.8193 0.8691 8.8225 1.0938 61.9136 34.4234 1.3595 12.1180 6.7896 | −1623 | 6.2665 | 4.2799 |

Table 4.9: Optimization of two CPGs in the bounded region when $C_2 = 0$

| Type | Solver | Parameter values | $J$ | $x_b$ | $E$ |
|---|---|---|---|---|---|
| Unc | GA and FM | 35.3887 1.9955 0.7564 26.4992 1.9606 1.5707 | −2731.2 | 4.9856 | 4.2406 |
| Unid | GA and FM | 20.2328 1.9347 0.7369 25.6692 −1.9619 1.5424 −0.3227 3.2986 | −3022.7 | 5.5084 | 4.1719 |
| Bid | GA and FM | 9.5946 1.9499 0.8009 1.2422 5.5546 48.1560 1.9717 1.2744 1.9235 | −3137.6 | 6.1787 | 2.9796 |

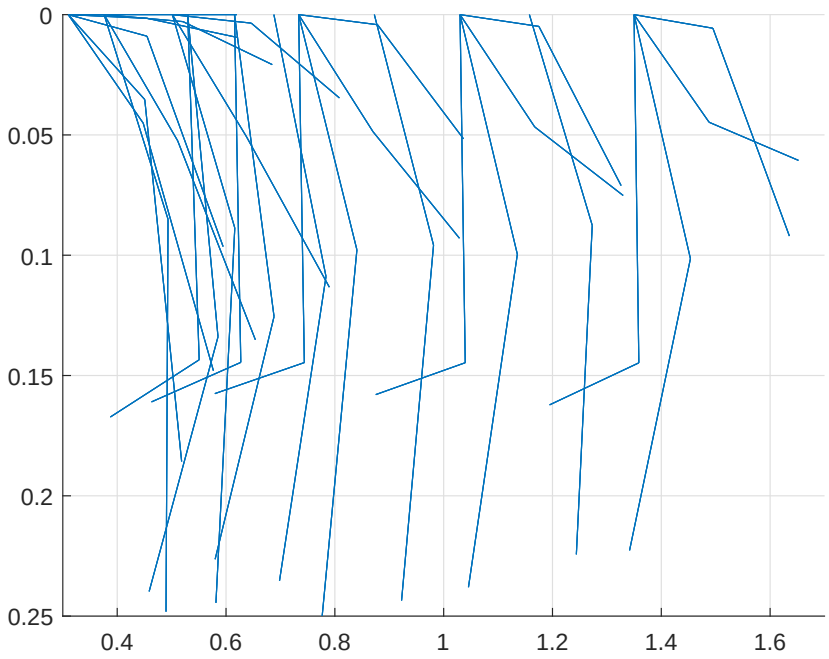


Figure 4.1: One leg animation for uncoupled two CPGs of the first type corresponding to the values $a_1 = 18.6883$, $\nu_1 = 1.9928$, $R_1 = 0.7746$, $a_2 = 46.4124$, $\nu_2 = 1.9604$ and $R_2 = 1.5327$.

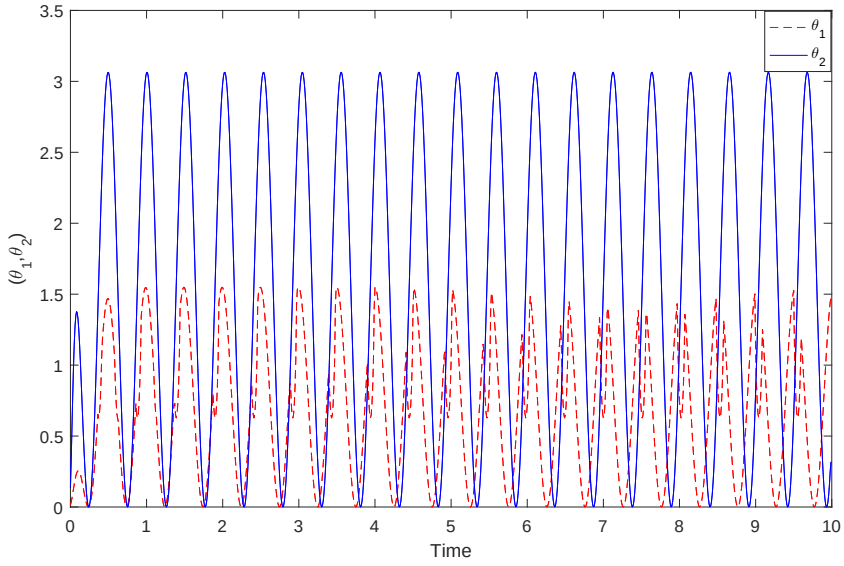


Figure 4.2: Outputs of uncoupled two CPGs corresponding to the same values in Figure 4.1.

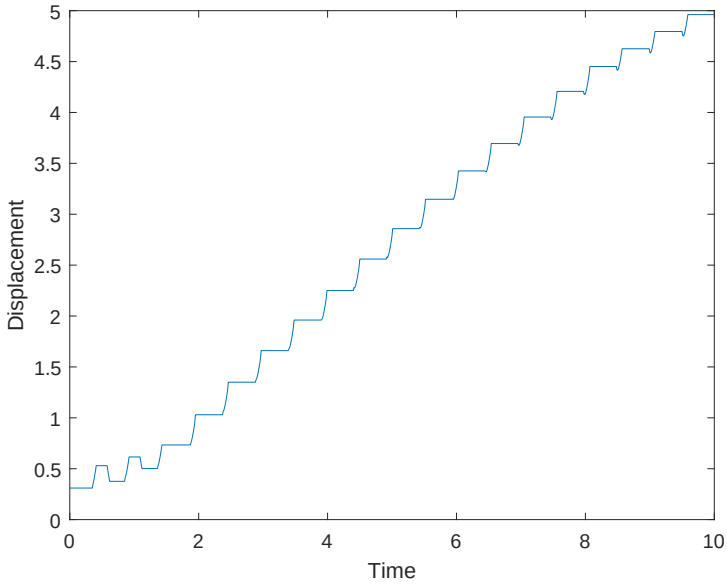


Figure 4.3: Displacement of one leg by uncoupled two CPGs corresponding to the same values in Figure 4.1.

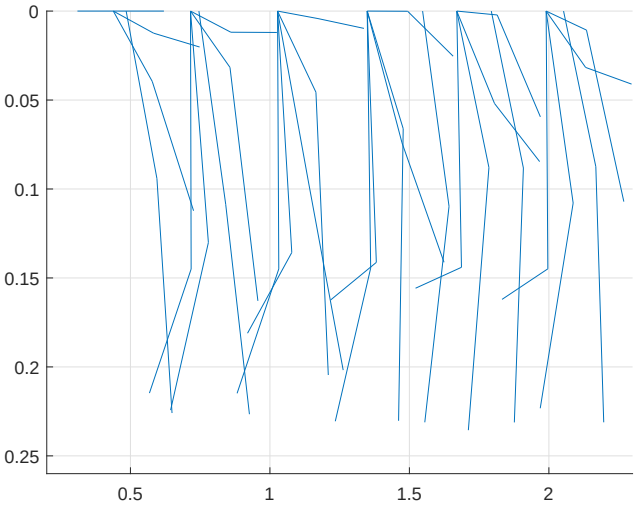


Figure 4.4: One leg animation for unidirectional two CPGs corresponding to the values $a_1 = 50$, $\nu_1 = 1.9850$, $R_1 = 0.7804$, $a_2 = 13.1020$, $\nu_2 = 1.9230$, $R_2 = 1.5356$, $w_{12} = 2$ and $\phi_{12} = -0.3699$.

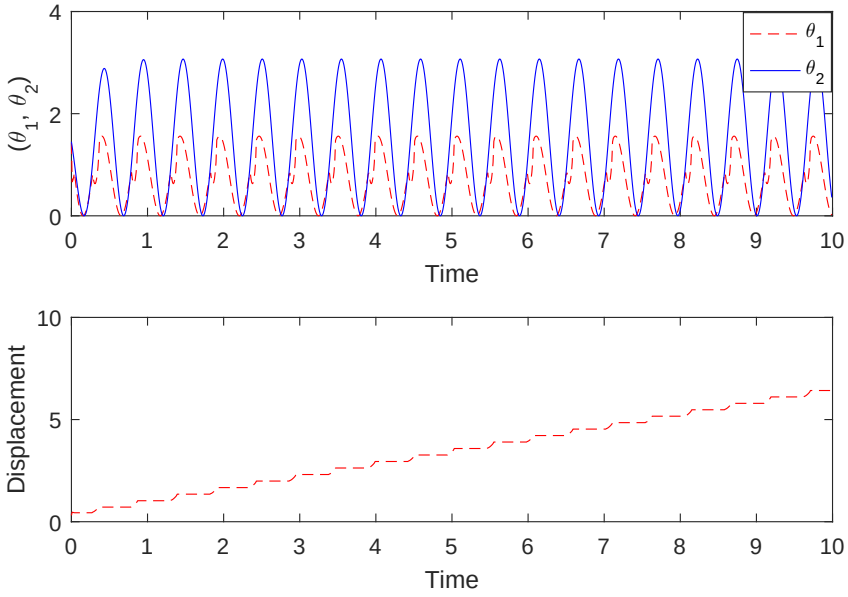


Figure 4.5: Outputs and displacement for unidirectional two CPGs corresponding to the same values in Figure 4.4

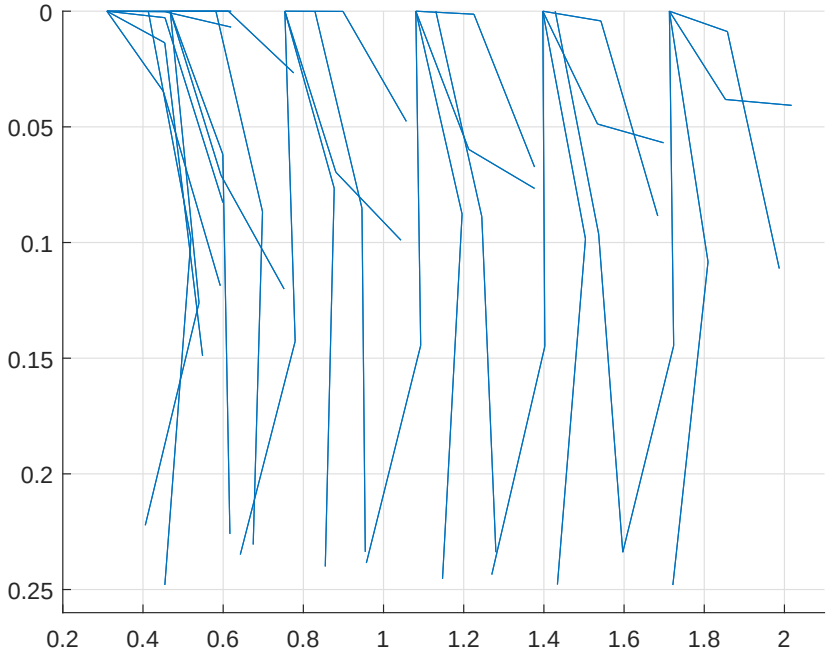

Figure 4.6: One leg animation for bidirectional two CPGs of the first type corresponding to the values $a_1 = 9.5946$, $v_1 = 1.9499$, $R_1 = 0.8009$, $w_{12} = 1.2422$, $\phi_{12} = 5.5546$, $a_2 = 48.1560$, $v_2 = 1.9717$, $R_2 = 1.2744$, $w_{21} = 1.9235$, and $\phi_{21} = 5.5546$.

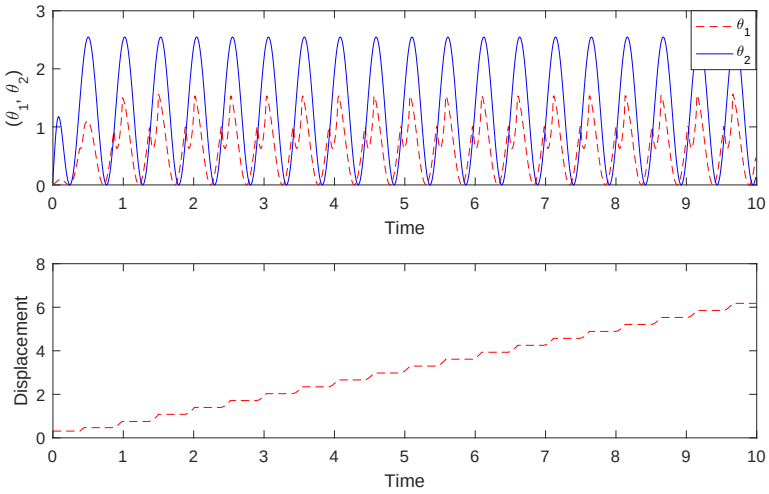


Figure 4.7: Outputs and displacement for bidirectional two CPGs of the first type corresponding to the same values in Figure 4.6

## 4.4 Optimization of the second type of CPGs

We use the same objective function $J$ and follow the same strategy. Different results are obtained. Figures 4.8 and 4.9 show the locomotion of one leg without constraints and the outputs of the CPGs. It is a clear that the angles of the hip and knee are randomly changing without constraints.

By applying constraints, the bidirectional two CPGs are optimized and the results are given in Figures 4.10, 4.11 and 4.12. We take $C_1 = C_2 = 0.5$.

Figures 4.13 and 4.14 show the one leg animation and the outputs of the CPGs. It is clear that there is a large variance between steps despite having optimized the objective function in two cases, $C_1C_2 \neq 0$ and $C_2 = 0$. However, by using the stability conditions, especially the results that derive from the bidirectional two CPGs when $\mu < 0$ and $E\mu\gamma < \omega^2$, the optimization is performed just for 4 parameters instead of 10, and the results become much better as seen in Figures 4.15 and 4.16.

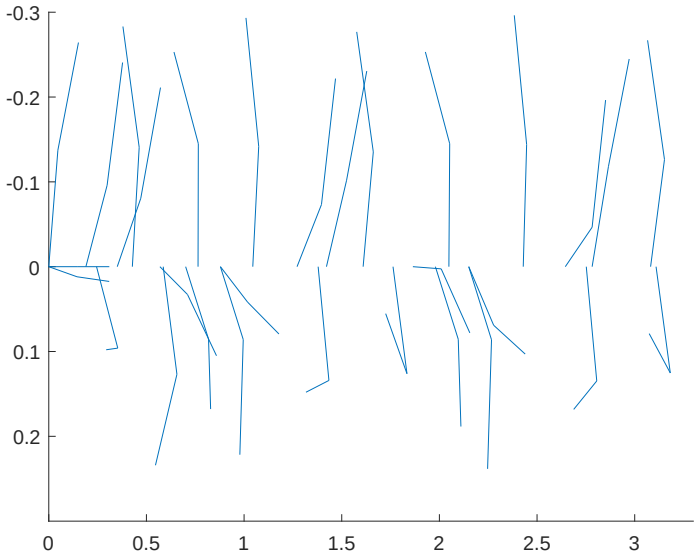


Figure 4.8: Simulation of walking gait without constraints for the uncoupled two CPGs corresponding to the values $\mu_1 = 2.3452$, $\gamma_1 = 44.2530$, $\omega_1 = 40.5129$, $\mu_2 = 5.9689$, $\gamma_2 = 1.7984$, and $\omega_2 = 39.9821$.

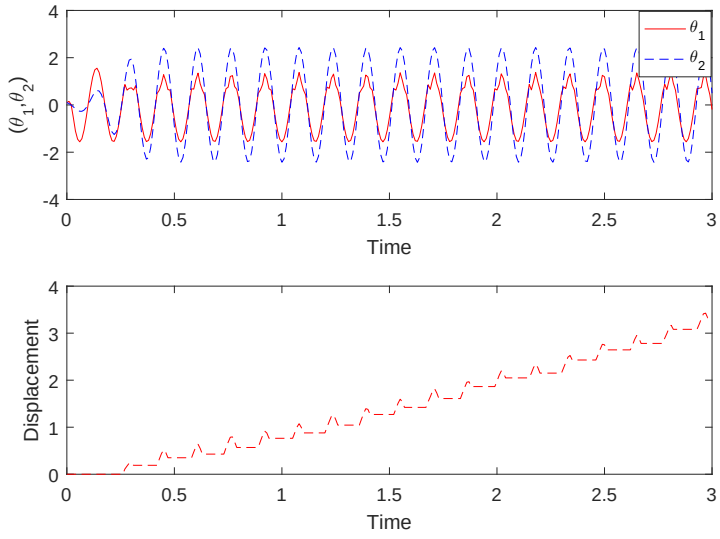


Figure 4.9: Outputs of the CPGs and displacement without constraints of the second type corresponding to the same values in Figure 4.8

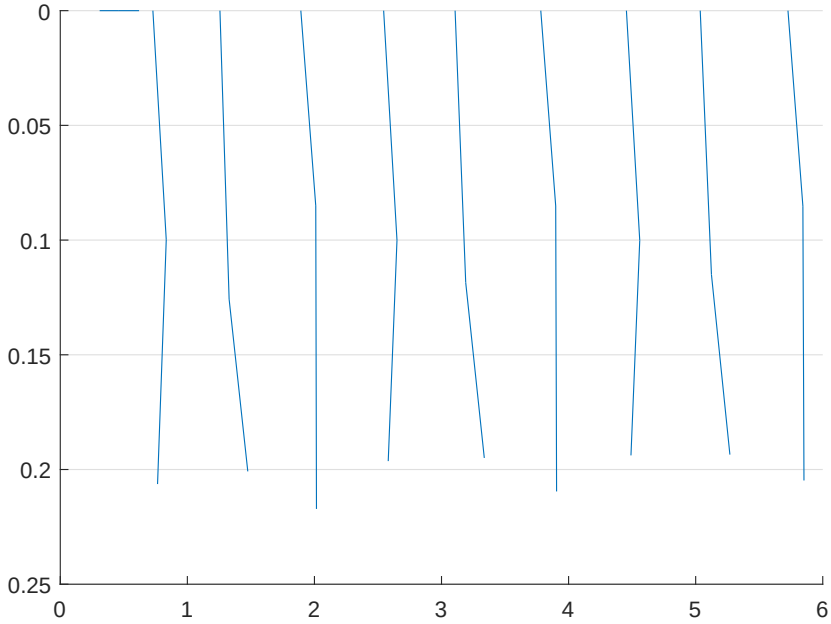


Figure 4.10: Simulation of walking gait with constraints corresponding to the values $\mu_1 = 1.5651$, $a_1 = 43.0613$, $b_1 = 32.1987$, $\omega_1 = 2.4237$, $E_1 = 3.1859$, $\mu_2 = 3.1653$, $a_2 = 50.3422$, $b_2 = 54.3037$, $\omega_2 = 0.1487$, and $E_2 = 2.8842$.

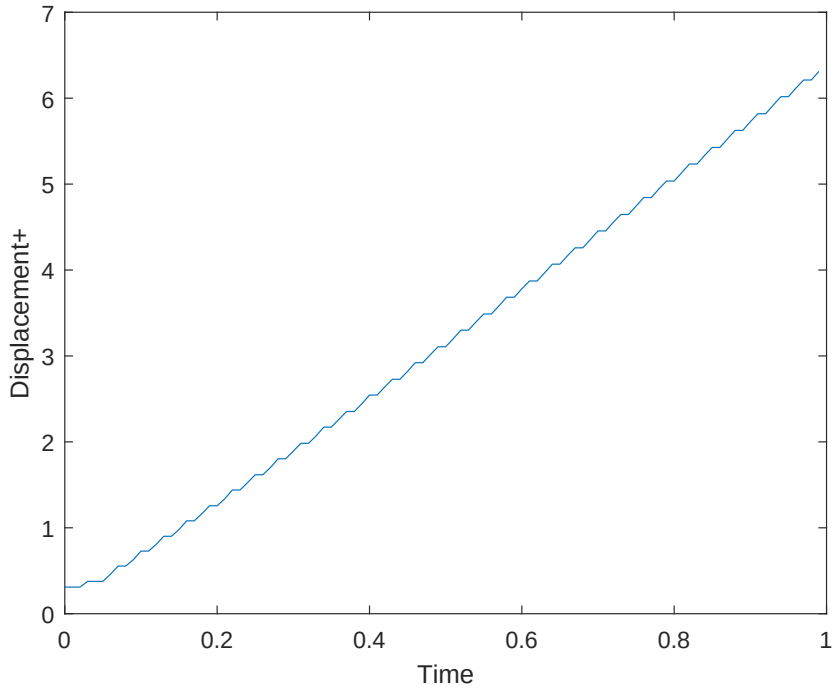


Figure 4.11: Displacement of one leg corresponding to the same values in Figure 4.10

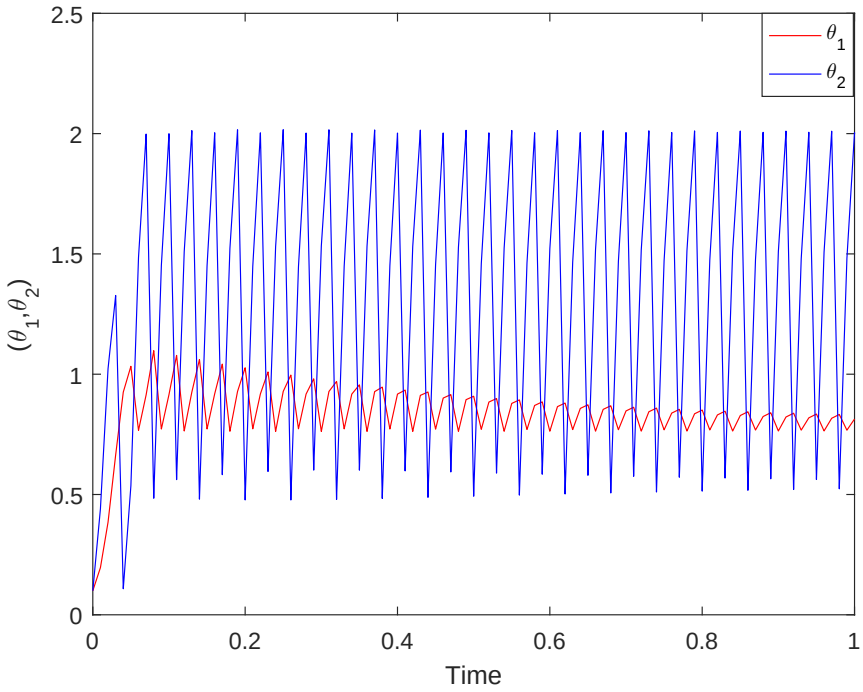


Figure 4.12: Outputs of the CPGs with constraints corresponding to the same values in Figure 4.10

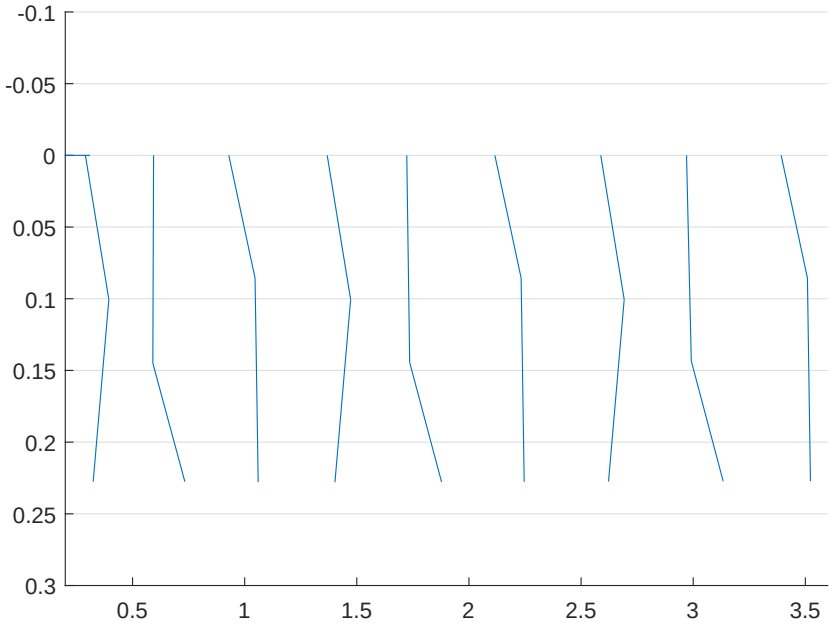


Figure 4.13: One leg animation when $C_1 = C_2 = 0.5$ corresponding to the values $\mu_1 = 0.8570$, $a_1 = 40.9730$, $b_1 = 31.5528$, $\omega_1 = 1.8821$, $E_1 = 1.9008$, $\mu_2 = 3.1640$, $a_2 = 50.4387$, $b_2 = 54.3306$, $\omega_2 = 0.1323$, and $E_2 = 3.3600$

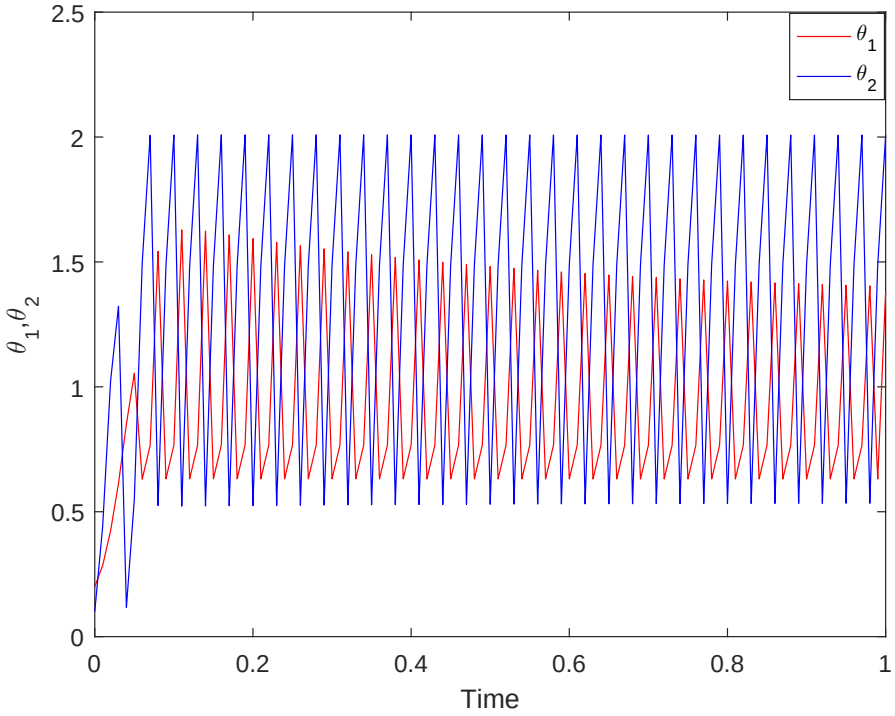


Figure 4.14: Outputs of the CPGs corresponding to the same values in Figure 4.13.

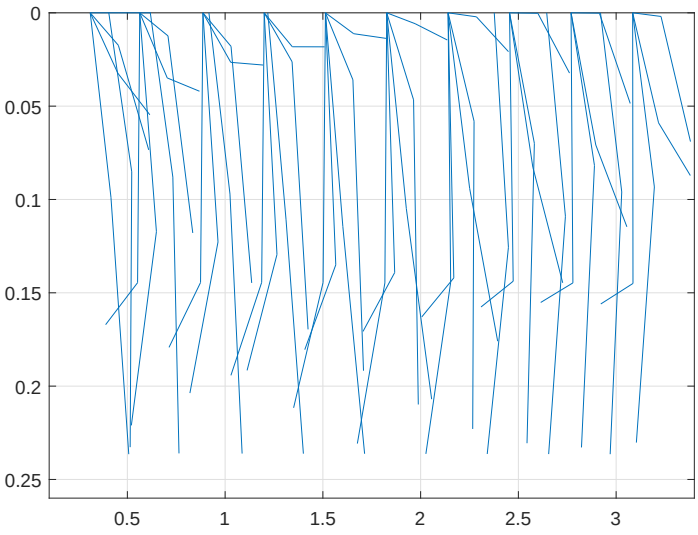


Figure 4.15: One leg animation when $C_1 = C_2 = 0.5$ corresponding to the values $\mu = -0.8389$, $\gamma = 9.7826$, $\omega = 3.4998$, and $E = 2.2789$.

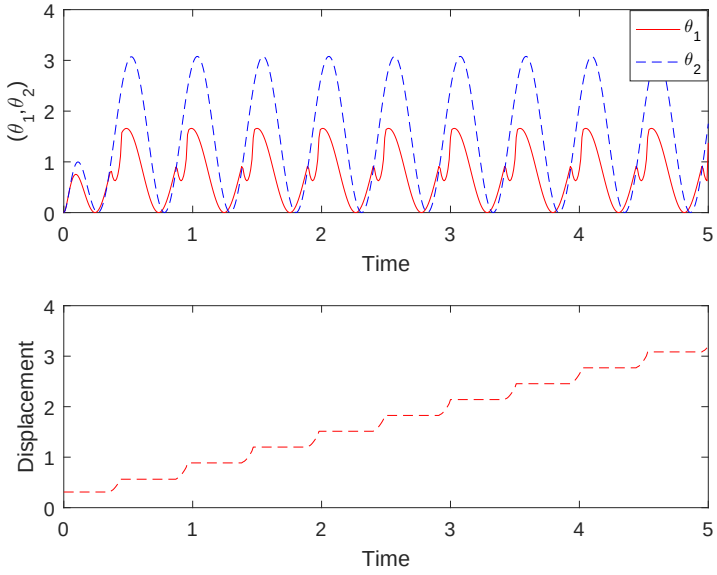


Figure 4.16: Outputs of bidirectional two CPGs and displacement corresponding to the same values in Figure 4.15

Tables 4.10, 4.11, 4.12, 4.13, 4.14 and 4.15 summarize the optimization of the second type and indicate that there is a large variance between steps during locomotion. It is also difficult to design phase coupling of two CPGs without disturbing the amplitude $\mu$ of both CPGs by adding couple weight $E$, which was just a constant and its sign decides whether these two oscillators are in phase or anti phase. In fact, we need to use sensory feedback for this type of CPGs to obtain better results.

Table 4.10: Uncoupled two CPGs of the second type when $C_1C_2 \neq 0$

| Solver | Parameter values | $J$ | $x_b$ |
|---|---|---|---|
| GA | 1.4458 49.6166 42.5420 0.0057 3.2989 48.9648 55.3396 0.1121 | −17781 | 70.7119 |
| GA | 1.4180 50.5328 42.3507 0.0045 3.2990 48.9647 55.3371 0.1059 | −17845 | 70.7159 |
| GA and PS | 1.4012 52.5781 39.9536 0.0030 3.2990 48.9611 55.3422 0.1095 | −17921 | 71.2255 |
| GA and FM | 1.3718 50.9654 41.6556 0.0027 3.2990 48.9765 55.3330 0.0685 | −17941 | 70.1690 |

Table 4.11: Uncoupled two CPGs of the second type when $C_2 = 0$

| Solver | Parameter values | $J$ | $x_b$ |
|---|---|---|---|
| GA | 1.6880 48.1652 46.0745 0.0149 3.2498 50.1045 55.4567 0.2563 | −34148 | 67.7661 |
| GA and PS | 1.6785 51.3340 46.0340 0.0147 3.2498 50.1059 55.4573 0.2444 | −34158 | 67.6113 |
| GA and FM | 1.3040 50.6130 42.1460 −0.0001 3.3010 48.9174 55.3674 0.0514 | −36115 | 71.9112 |

Table 4.12: Unidirectional two CPGs of the second type when $C_1C_2 \neq 0$

| Solver | Parameter values | $J$ | $x_b$ |
|---|---|---|---|
| GA | 1.9032 39.5103 44.0602 3.2913 3.1875 50.6699 53.8496 0.0118 3.4653 | −17368 | 69.5316 |
| GA and PS | 1.9147 39.6366 43.8043 3.2915 3.1875 50.6710 53.8492 0.0107 3.4809 | −17358 | 69.5098 |
| GA and FM | 1.9147 39.6366 43.8043 3.2915 3.1875 50.6710 53.8492 0.0107 3.4809 | −17358 | 69.5098 |

Table 4.13: Unidirectional two CPGs of the second type when $C_2 = 0$

| Solver | Parameter values | $J$ | $x_b$ |
|---|---|---|---|
| GA | 3.2839 20.9516 30.5813 1.5033 3.2462 50.0512 18.8460 −0.8808 1.7777 | −25959 | 51.2497 |
| GA and PS | 2.1824 22.1102 28.7280 1.8590 3.1394 51.1790 19.1222 −0.8278 1.9199 | −31799 | 63.7632 |
| GA and FM | 1.0140 52.4703 23.7631 3.1501 3.1757 51.1576 17.1403 −0.8808 4.9729 | −28275 | 55.9564 |

Table 4.14: Bidirectional two CPGs of the second type when $C_1C_2 \neq 0$

| Solver | Parameter values | $J$ | $x_b$ |
|---|---|---|---|
| GA | 0.8569 40.9743 31.5531 1.8824 1.9008 3.1640 50.4389 54.3306 0.1322 3.3600 | −17463 | 65.3686 |
| GA and PS | 0.8416 48.0750 28.2205 1.9042 2.2687 3.1675 50.3775 54.2680 0.2156 3.3600 | −17418 | 64.8242 |
| GA and FM | 0.8589 38.8062 31.2842 1.7514 1.7236 3.1640 50.4318 54.3302 0.1278 3.4051 | −17476 | 61.4358 |

Table 4.15: Bidirectional two CPGs of the second type when $C_2 = 0$

| Solver | Parameter values | $J$ | $x_b$ |
|---|---|---|---|
| GA | 1.5651 43.0613 32.1987 2.4237 3.1859 3.1653 50.3422 54.3037 0.1487 2.8842 | −34549 | 41.5323 |
| GA and PS | 0.8510 40.0128 31.5992 1.9080 1.9011 3.1640 50.4410 54.3305 0.1172 3.3600 | −34948 | 62.4536 |
| GA and FM | 0.8197 40.9826 32.6101 1.9221 1.9162 3.1641 50.4428 54.3251 0.1210 3.3530 | −34973 | 62.9298 |

## 4.5 Optimization of the third type of the CPGs

### 4.5.1 Uncoupled two CPGs of the third type

Similar optimizations are performed and the results are presented in Tables 4.16 and 4.17. Figures 4.17, 4.18 and 4.19 show one leg animation with the outputs of the uncoupled two CPGs and the displacement.

The optimization of the uncoupled two CPGs failed to produce suitable RPs for one leg with 2 DOFs because the fixed point is unstable.

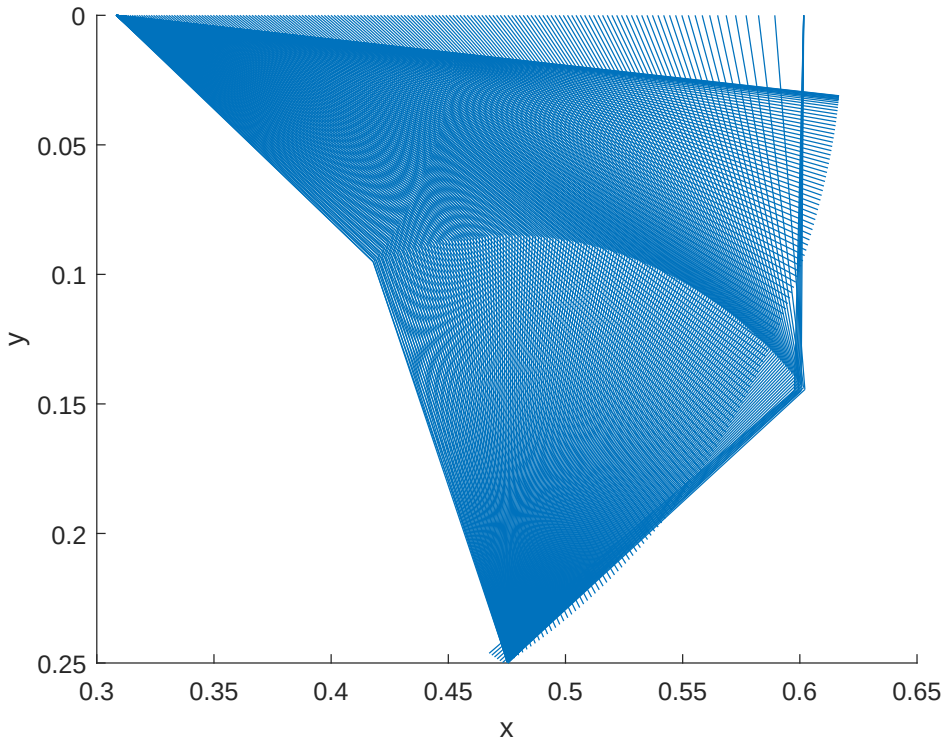


Figure 4.17: One leg animation of uncoupled two CPGs corresponding to the values $\tau_1 = 28.9834$, $\alpha_1 = 36.2518$, $E_1 = 4.5906$, $\tau_2 = 111.2763$, $\alpha_2 = 35.3121$ and $E_2 = 9.8696$

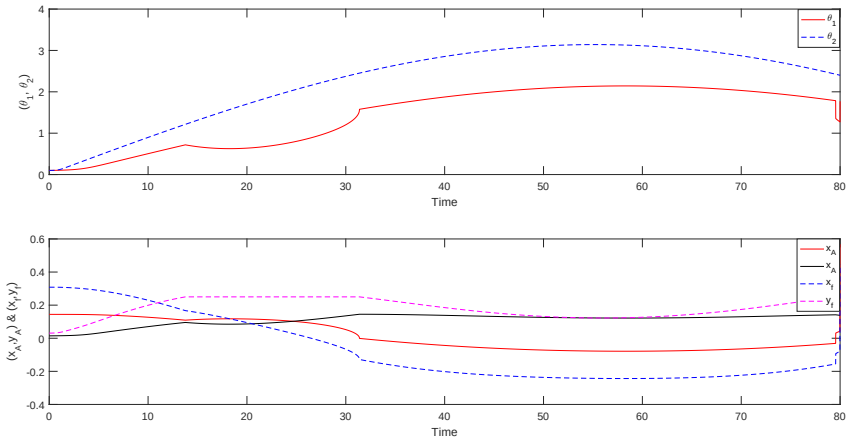


Figure 4.18: Outputs of uncoupled two CPGs corresponding to the same values as in Figure 4.17.

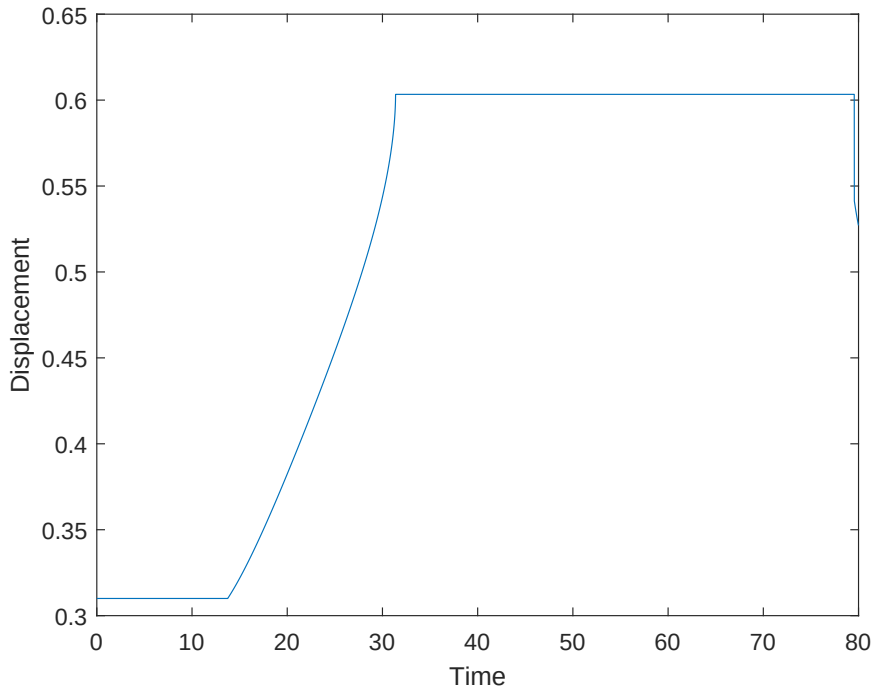


Figure 4.19: Displacement for uncoupled two CPGs corresponding to the same values as in Figure 4.17.

Table 4.16: Uncoupled two CPGs of the third type when $C_1C_2 \neq 0$

| Solver | Parameter values | $J$ | $x_b$ |
|---|---|---|---|
| GA | 28.9834 36.2518 4.5906 111.2763 35.3121 9.8696 | −2048.5 | 0.5271 |
| GA | 31.5979 36.3647 4.5536 110.8210 35.3333 9.8660 | −2050.4 | 0.5299 |
| GA with PS | 32.9827 36.6254 4.5648 110.8486 35.2849 9.8694 | −2052.7 | 0.5257 |
| GA with FM | 52.6429 61.4651 8.2096 18.6831 28.2615 6.9612 | −1998 | 0.6037 |

Table 4.17: Uncoupled two CPGs of the third type when $C_2 = 0$

| Solver | Parameter values | $J$ | $x_b$ |
|---|---|---|---|
| GA | 43.4261 79.7966 14.7043 96.3819 41.6429 9.8691 | −3916.3 | 0.5942 |
| GA | 44.4261 78.7966 14.2043 98.0069 41.7679 9.8691 | −3915.6 | 0.5940 |
| GA with PS | 46.6724 79.0434 14.4197 100.0917 41.0695 9.8547 | −3934 | 0.5951 |
| GA with FM | 54.3031 83.7118 11.7086 16.1890 33.7975 7.5507 | −3870 | 0.6038 |

### 4.5.2 Unidirectional two CPGs of the third type

According to Tables 4.16 and 4.17, increasing optimization time or extending the region renders the leg unable to move. Also, Tables 4.18 and 4.19 support the results given previously such that the CPGs are unable to produce RPs for one leg to move. Figures 4.20, 4.21 and 4.22 show the results of the optimization that were obtained by optimizing the unidirectional two CPGs.

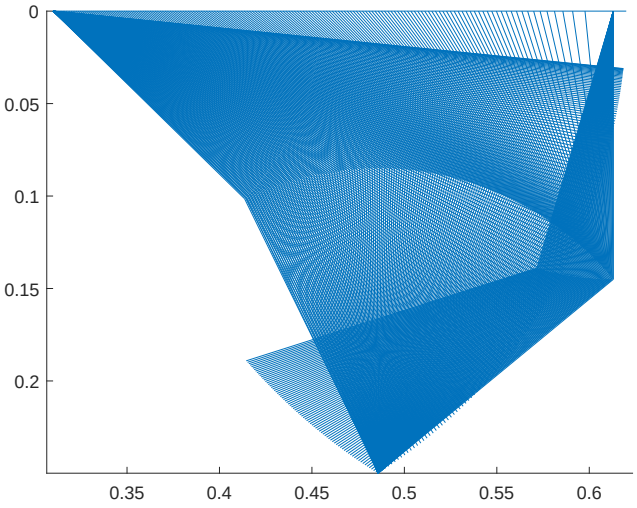


Figure 4.20: Animation of one leg for unidirectional two CPGs corresponding to the values $\tau_1 = 37.8704$, $\alpha_1 = 23.8309$, $E_1 = 2.2214$, $a_{12} = 39.5901$, $b_{12} = 20.4244$, $\tau_2 = 33.2256$, $\alpha_2 = 26.1536$ and $E_2 = 9.8616$

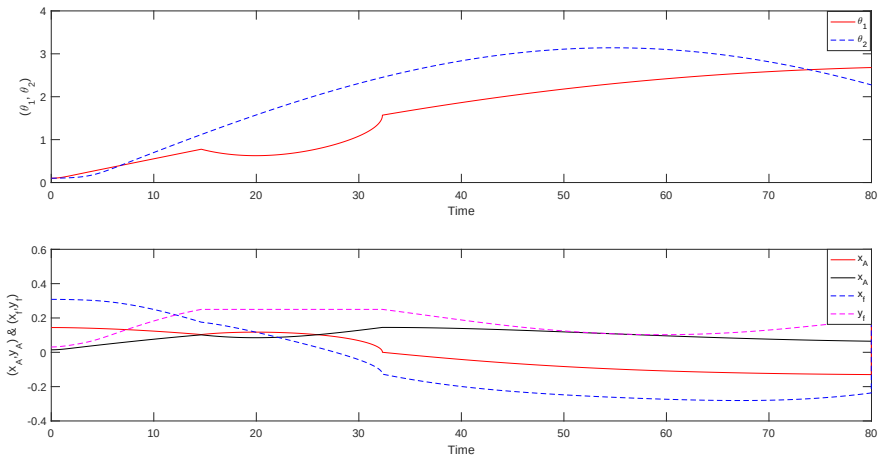


Figure 4.21: Outputs of unidirectional two CPGs corresponding to the same values in Figure 4.20

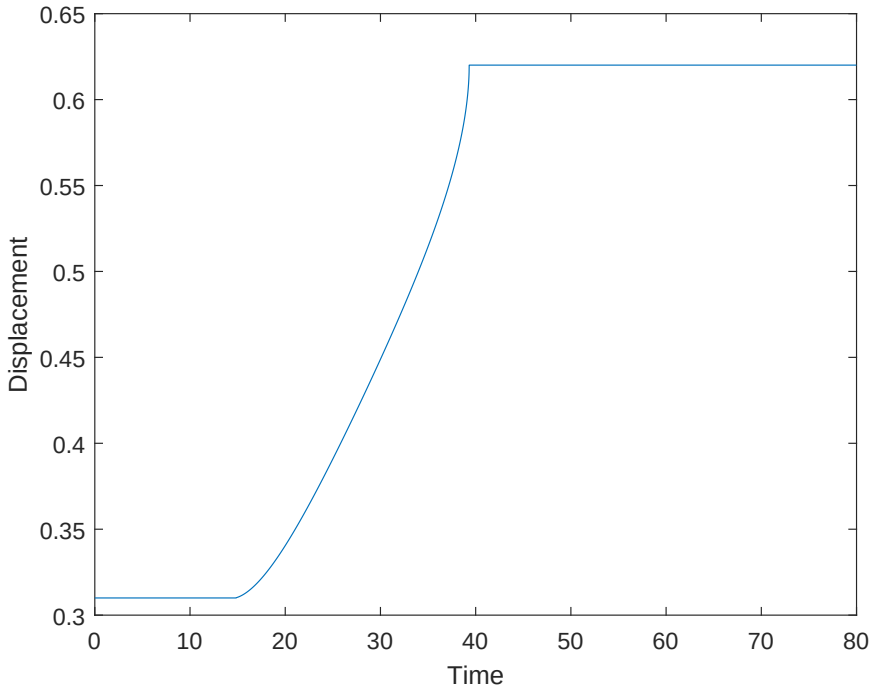


Figure 4.22: Displacement for unidirectional two CPGs corresponding to the same values in Figure 4.20.

Table 4.18: Unidirectional two CPGs of the third type when $C_1C_2 \neq 0$

| Solver | Parameter values | $J$ | $x_b$ |
|---|---|---|---|
| GA | 23.8309 37.8704 2.2214 39.5901 20.4244 26.1536 33.2256 9.8616 | −2367.3 | 0.6130 |
| GA | 57.1658 38.1815 2.1811 4.8573 24.7362 58.3004 47.0796 9.8694 | −2257.4 | 0.6150 |
| GA with Hyp | 57.7655 38.1815 2.1811 4.8534 24.9237 58.3017 47.0796 9.8694 | −2257.6 | 0.6151 |
| GA with Hyf | 59.5006 34.2580 2.2877 7.7744 30.2325 60.7280 39.4452 9.8668 | −2336.9 | 0.6141 |

Table 4.19: Unidirectional two CPGs of the third type when $C_2 = 0$

| Solver | Parameter values | $J$ | $x_b$ |
|---|---|---|---|
| GA | 19.1593 37.3610 2.4442 29.2822 23.7775 39.8811 31.5082 9.8595 | −4798.6 | 0.6103 |
| GA | 16.6046 12.9354 0.2630 29.7203 25.9645 41.3522 38.5263 9.8690 | −4722 | 0.6202 |
| GA with PS | 17.4443 12.7218 0.2635 32.9492 26.5549 59.7024 38.5626 9.8659 | −4741 | 0.6194 |
| GA with FM | 16.8698 14.1344 0.2599 30.8606 26.4618 43.3883 42.3464 9.8660 | −5259.9 | 0.6201 |

### 4.5.3 Bidirectional two CPGs of the third type

We first optimize the bidirectional two CPGs using the cost function $J$ and only the constraints $0 \leq \theta_1, \theta_2 \leq \pi$. Tables 4.20 and 4.21 summarize the results. Figures 4.23, 4.24 and 4.25 show the results when $C_1C_2 \neq 0$. Figures 4.26, 4.27 and 4.28 show the results when $C_2 = 0$. These figures present the animation of one leg, the outputs of the CPGs and displacement, respectively.

Table 4.20: Bidirectional two CPGs of the third type when $C_1C_2 \neq 0$.

| Solver | Parameter values | $J$ | $x_b$ | $\mu$ | $\beta_1$ | $\beta_2$ |
|---|---|---|---|---|---|---|
| GA | 0.9999 1.9982 0.5233 2.4831 1.6538 0.8678 2.2644 2.6215 2.4274 1.6276 | −877.5649 | 0.6204 | 0.4466 | 5.3960 | 0.4781 |
| GA | 1.0158 2.0092 0.5724 2.5768 1.6678 0.8976 2.2644 3.1261 2.4401 1.6481 | −1810.7 | 0.6209 | 0.4372 | 5.3595 | 0.3586 |
| GA with PS | 1.0517 1.2945 2.0737 1.3461 0.7428 2.1834 1.9535 3.3817 3.2864 3.2522 | −5078.9 | 2.1939 | 0.5460 | −0.1025 | 2.4519 |
| GA with FM | 1.0520 1.2952 2.0771 1.3466 0.7448 2.1885 1.9547 3.3832 3.2922 3.2542 | −5068.4 | 2.1966 | 0.5467 | −0.1031 | 2.4671 |

Table 4.21: Bidirectional two CPGs of the third type when $C_2 = 0$.

| Solver | Parameter values | $J$ | $x_b$ | $\mu$ | $\beta_1$ | $\beta_2$ |
|---|---|---|---|---|---|---|
| GA | 0.9961 1.0081 0.5403 2.3114<br>0.4843 0.9942 1.9538 2.3390<br>2.9803 2.6291 | −2411.2 | 0.6211 | 0.1848 | 8.7829 | 1.4235 |
| GA | 1.0033 1.0088 0.5403 2.3375<br>0.4844 0.9942 1.9539 2.3381<br>2.9809 2.6721 | −4904.6 | 0.6222 | 0.1858 | 9.0636 | 1.4250 |
| GA with PS | 0.9855 1.2981 2.0748 1.3475<br>0.7401 2.1861 1.9233 3.3868<br>3.3011 3.2758 | −10286 | 2.1852 | 0.5451 | −0.0948 | 2.5206 |
| GA with FM | 0.9940 1.3046 2.1067 1.3529<br>0.7216 2.2720 1.9025 3.4102<br>3.3188 3.3236 | −10332 | 2.2126 | 0.5342 | −0.0999 | 2.6629 |

In Tables 4.20 and 4.21, in contrast, the results are much better than the other cases despite the fact that we did not impose any conditions from the stability analysis during the optimization. These results indicate that, when the fixed points are stable, the bidirectional two CPGs are able to produce RPs. While the fixed points are unstable, the optimization of the bidirectional two CPGs are unable to produce RPS. The movement does not only depend entirely on the values of $\tau$ and $\alpha$, as shown in Tables 4.20 and 4.21, it also relies the stability of the fixed points, where the fixed points depend on the coupling weights $a_{ij}$ and $b_{ij}$.

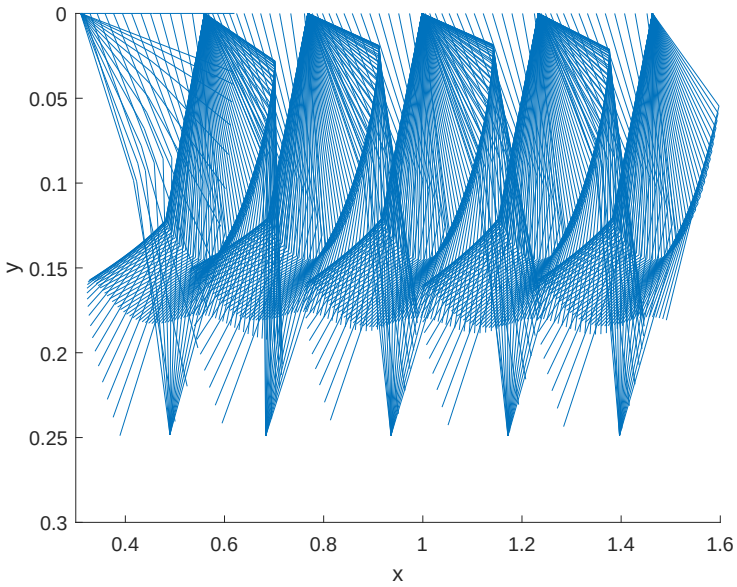


Figure 4.23: One leg animation for bidirectional two CPGs when $C_1C_2 \neq 0$ corresponding to the values $\alpha_1 = 1.0695$, $\tau_1 = 1.2666$, $E_1 = 2.1157$, $a_{12} = 1.3610$, $b_{12} = 0.7478$, $\alpha_2 = 2.2222$, $\tau_2 = 1.9279$, $E_2 = 3.4393$, $a_{21} = 3.2908$, $b_{21} = 3.2794$

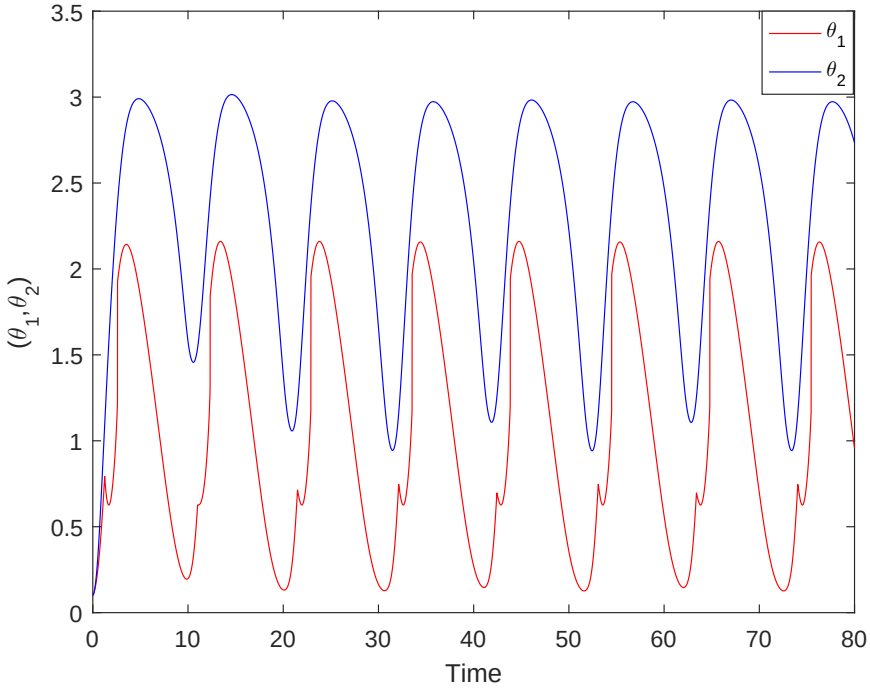


Figure 4.24: Outputs of bidirectional two CPGs when $C_1C_2 \neq 0$ corresponding to the same values in Figure 4.23.

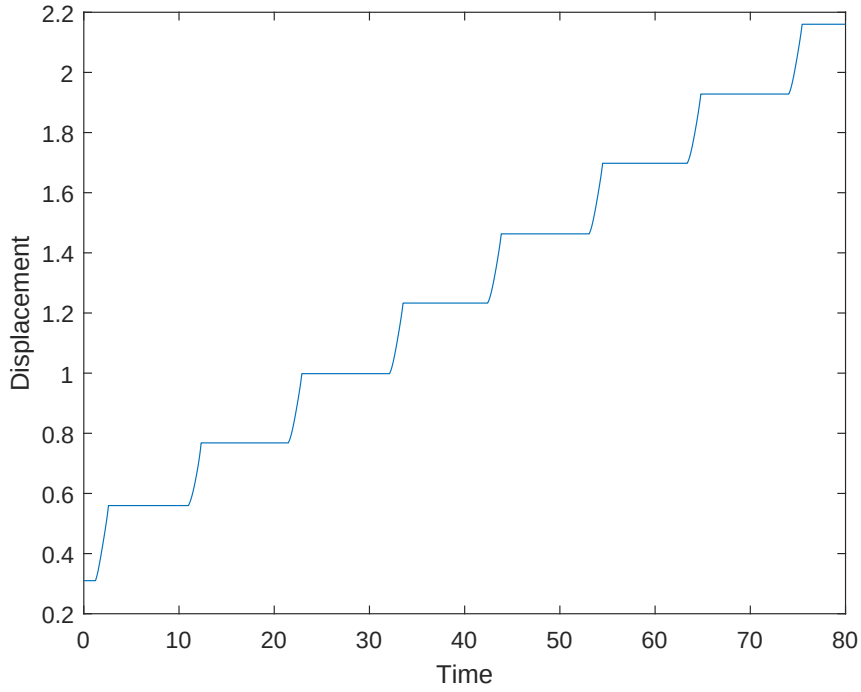


Figure 4.25: Displacement of one leg for bidirectional two CPGs when $C_1C_2 \neq 0$ corresponding to the same values in Figure 4.23.

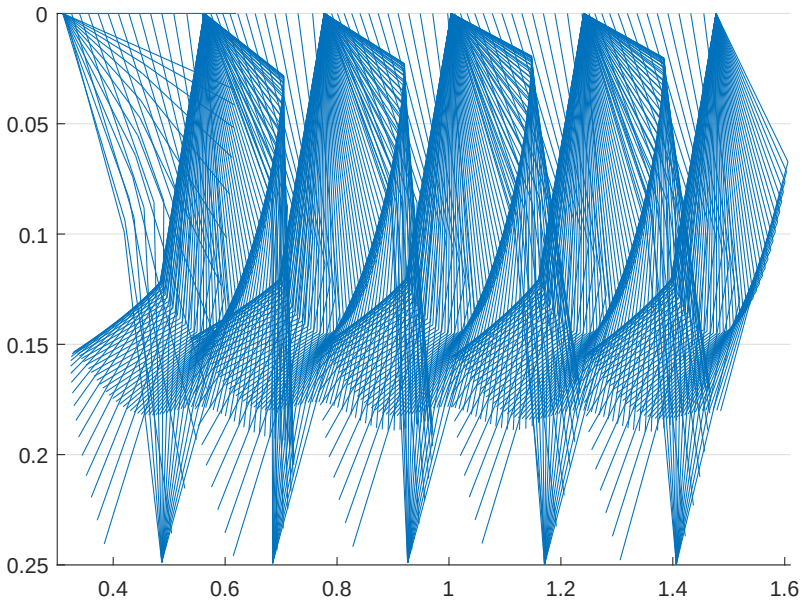


Figure 4.26: Animation of one leg using the outputs of the bidirectional two CPGs when $C_2 = 0$ corresponding to the values $\alpha_1 = 0.9855$, $\tau_1 = 1.2981$, $E_1 = 2.0748$, $a_12 = 1.3475$, $b_{12} = 0.7401$, $\alpha_2 = 2.1861$, $\tau_2 = 1.9234$, $E_2 = 3.3872$, $a_{21} = 3.3011$, and $b_{21} = 3.2758$.

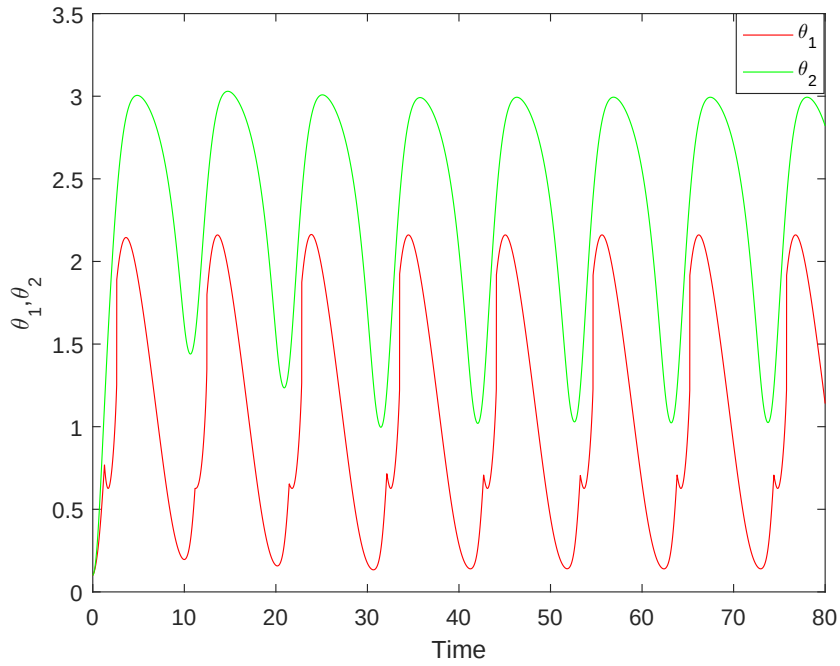


Figure 4.27: Outputs of bidirectional two CPGs when $C_2 = 0$ corresponding to the same values in Figure 4.26.

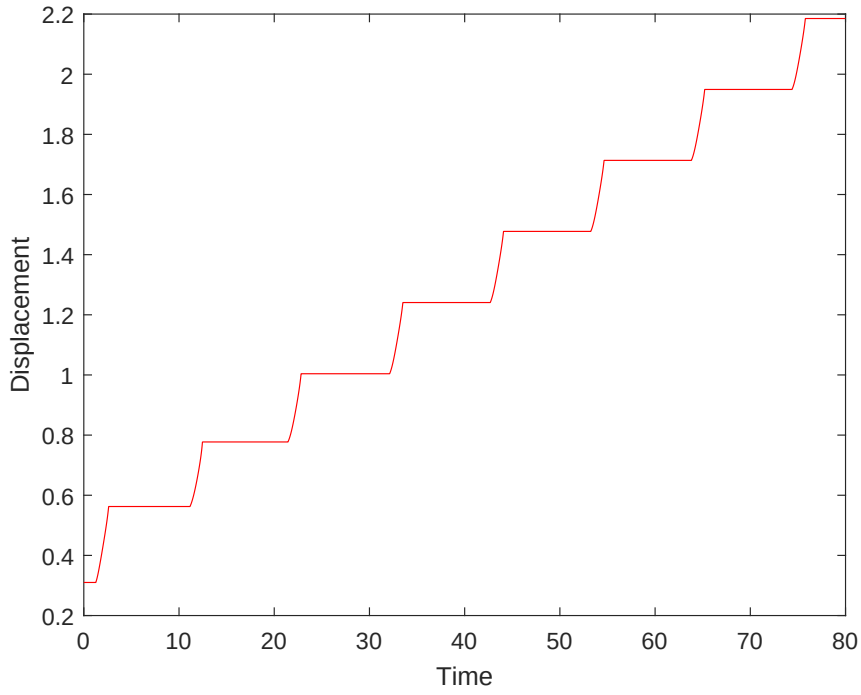


Figure 4.28: Displacement for bidirectional two CPGs when $C_2 = 0$ corresponding to the same values in Figure 4.26.

Experiments relying on the value of $\mu$, $\beta_1$ and $\beta_2$ show that an increase in the value of $\tau$ will decrease the displacement and velocity. An increase in the values of $\alpha$ will decrease the displacement and velocity when the fixed points are stable, as shown in Tables 4.20 and 4.21.

Moreover, when the angles are kept in the region $[0, 6\pi/7]$, to be more consistent with real life, the locomotion becomes better than the angles kept between $[0, \pi]$. To show that the bidirectional two CPGs are able to generate RPs only if the fixed points are stable, we will consider the following cases where we set

$$\beta_1 = \frac{\alpha(a_{12}^2 - E_1)}{\tau E_1}, \quad \beta_2 = \frac{\alpha(a_{21}^2 - E_2)}{\tau E_2} \quad \text{and} \quad \mu = \frac{b_{12}b_{21}}{a_{12}a_{21}}.$$

**Firstly:** Let $\mu = 1$. Take the mutation rate $M = 0.5$ and crossover fraction $C = 0.8$ :

1. $a_{12} = a_{21} = b_{12} = b_{21} = 1$. When $C_1C_2 \neq 0$ with the constraints $0 \leq \theta_1, \theta_2 \leq \frac{5\pi}{6}$, the CPGs are unable to generate the RPs for one leg because the fixed points are unstable.

2. $a_{12} = b_{21} = 1$ and $a_{21} = b_{12} = 2.5$. When $C_1C_2 \neq 0$, the CPGs are able to generate the RPs for one leg to move because the fixed points are stable. The results are shown in Figures 4.29 and 4.30.

3. If $a_{12} = b_{12} = 1$ and $a_{21} = b_{21} = 2.5$. Again, the fixed points are unstable and the results are summarized in Table 4.22.

Table 4.22: Bidirectional two CPGs of the third type when $\mu = 1$ and $C_1C_2 \neq 0$

| $M$ | $C$ | Parameter values | $\beta_1$ | $\beta_2$ | $\mu$ | $J$ | $x_b$ |
|---|---|---|---|---|---|---|---|
| 0.05 | 0.2 | 4.0000 4.0000 0.1000 1.0000 1.0000 0.1000 1.0000 1.0000 2.0000 | 8.9986 | 8.9999 | 1 | −1954.3 | 0.4760 |
| 0.5 | 0.2 | 2.5341 4.0000 3.9399 2.5000 2.5000 0.1169 1.0000 1.0000 2.0000 | 0.3714 | 4.7868 | 1 | −2011.7 | 0.5042 |
| 0.05 | 0.2 | 1.9081 3.9999 4.0000 2.5000 1.0000 0.1023 1.0000 2.5000 2.0000 | 0.2683 | 4.1840 | 1 | −2016.3 | 0.5054 |
| 0.05 | 0.2 | 1.3072 0.9332 0.8402 1.0000 2.5000 2.3580 2.5000 1.0000 1.5019 | 0.2664 | 2.3120 | 1 | −5493 | 1.9134 |
| 0.5 | 0.2 | When $a_{21} = b_{12} = 1$ and $a_{12} = b_{21} = 2.5$ | - | - | 1 | Not Feasible | - |

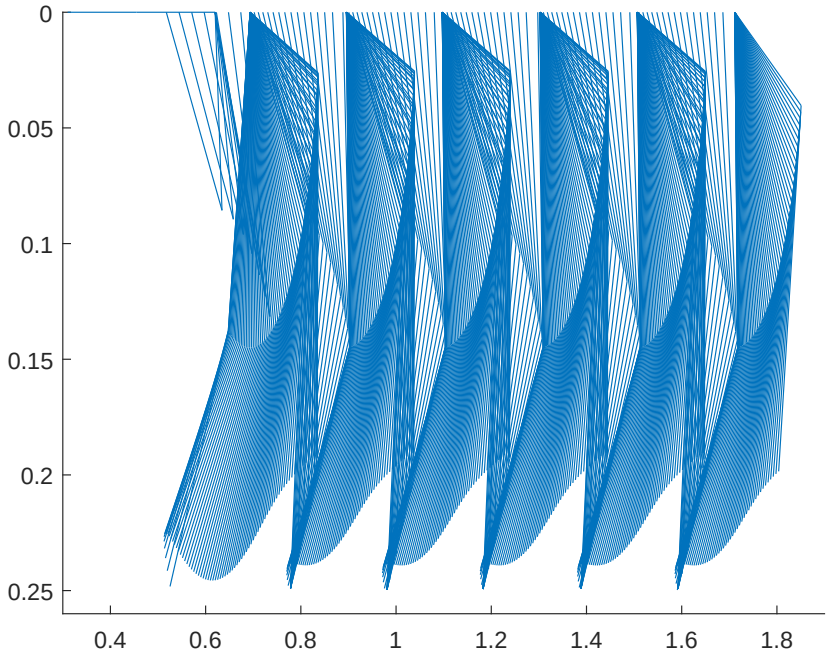


Figure 4.29: One leg animation when $\mu = 1$: This animation corresponds to the values $\alpha = 1.3072$, $\tau = 0.9332$, $E_1 = 0.8402$, $E_2 = 2.3580$ with $a_{12} = b_{21} = 1$, and $a_{21} = b_{12} = 2.5$.

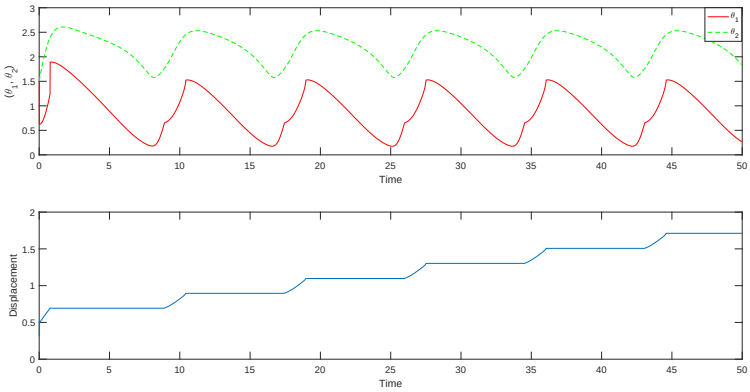


Figure 4.30: Outputs and displacement for bidirectional two CPGs corresponding to the same values in Figure 4.29

**Secondly:** Fix $\mu = 0$, and assume different cases for other parameters as follows:

1. $b_{21} = 0$, $a_{12}$, $b_{21}$ and $a_{21}$ are determined by the GA, and take $M = 0.5$ and $C = 0.8$. The CPGs are unable to generate RPs because $\beta_1 < 0$ and $\beta_2 > 0$ indicate that the fixed points are unstable.

2. $b_{21} = 0$, $a_{12}$, $b_{12}$ and $a_{21}$ are determined by optimizing two CPGs, and take $M = 0.5$ and $C = 0.2$. The CPGs are unable to generate RPs because $\beta_1 > 0$ and $\beta_2 > 0$ which means that the fixed points are unstable.

3. $b_{12} = 0$, $a_{12}$, $b_{12}$ and $a_{21}$ are determined by the optimizing bidirectional two CPGs, and take $M = 0.05$ and $C = 0.8$. The CPGs are able to generate RPs as shown in Figures 4.31, 4.32 and 4.33. In this case we have $\beta_1 > 0$ and $\beta_2 < 0$, i.e., the fixed points are stable. All these results are summarized in Table 4.23.

Table 4.23: Bidirectional two CPGs of the third type when $\mu = 0$ and $C_1C_2 \neq 0$

| $M$ | $C$ | Parameter values | IC | $\beta_1$ | $\beta_2$ | $\mu$ | $J$ | $x_b$ |
|---|---|---|---|---|---|---|---|---|
| 0.5 | 0.8 | 2.2597 1.3266 2.4060 2.9764 0.0000 3.7644 1.7859 1.4422 0.9627 | $V$ | 4.5689 | −0.2602 | 0 | −3675.7 | 1.4057 |
| 0.5 | 0.2 | 3.9857 2.0077 1.0000 3.0000 3.0000 3.0000 3.0000 0.0000 0.9561 | $V$ | 15.8818 | 3.9705 | 0 | −2804.1 | 0.7088 |
| 0.05 | 0.8 | 0.5318 4.0000 1.1789 1.0000 1.6750 0.3624 3.9977 0.7374 2.5000 0.0000 | $F$ | −0.0202 | 0.6778 | 0 | −2590.6 | 0.9219 |

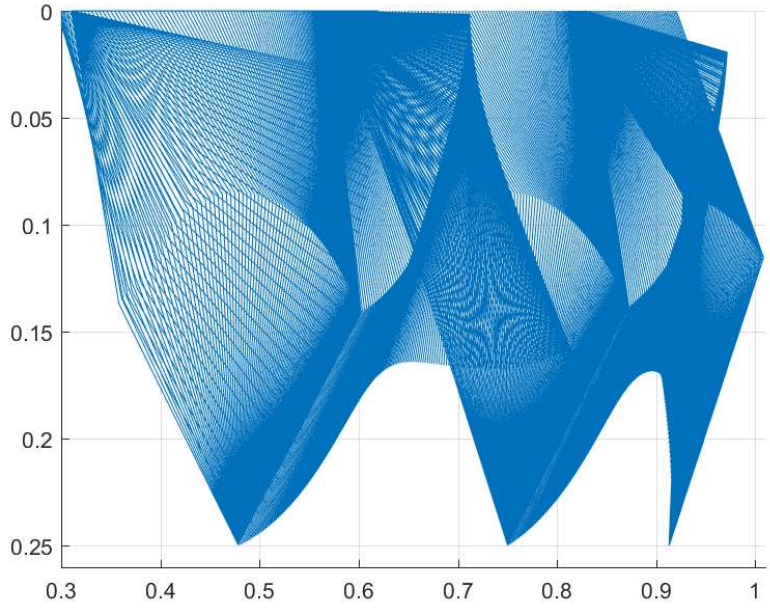


Figure 4.31: Animation of one leg when $\mu = 0$ corresponding to the values $\alpha_1 = 0.5318$, $\tau_1 = 4$, $E_1 = 1.1789$, $a_{12} = 1$, $b_{12} = 1.6750$, $\alpha_2 = 0.3624$, $\tau_2 = 3.9977$, $E_2 = 0.7374$, $a_{21} = 2.5$, and $b_{21} = 0$.

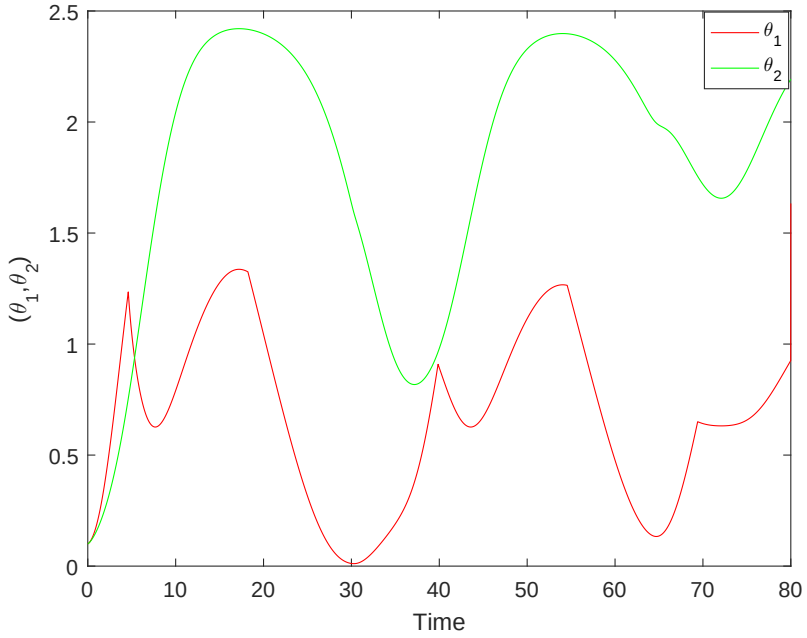


Figure 4.32: Outputs of bidirectional two CPGs when $\mu = 0$ corresponding to the same values in Figure 4.31.

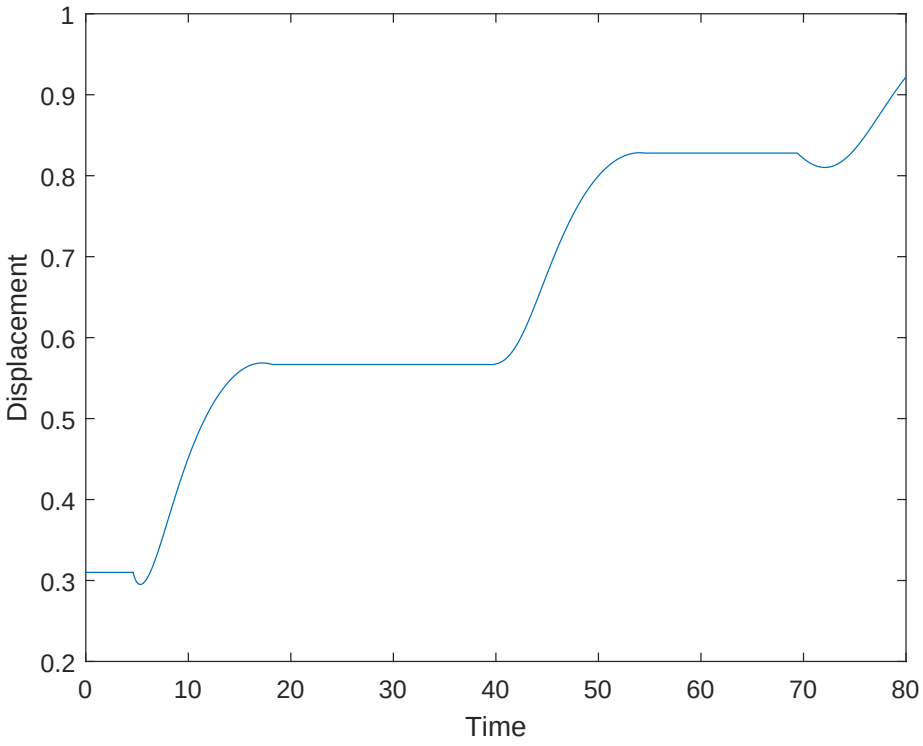


Figure 4.33: Displacement corresponding to the same values in Figure 4.31.

**Thirdly:** Let $\mu < 0$, and keep other parameters changeable. In this case, the fixed points are stable. The results are given in Figures 4.34 and 4.35 and summarized in Table 4.24.

Table 4.24: Bidirectional two CPGs of the third type when $\mu < 0$

| $M$ | $C$ | Parameter values | $\beta_1$ | $\beta_2$ | $\mu$ | $J$ | $x_b$ |
|---|---|---|---|---|---|---|---|
| 0.1 | 0.2 | 1.2692 0.1005 2.5165<br>1.3322 0.2271 2.4815<br>2.5000 −0.0029 | −3.7207 | 19.1729 | −0.00019 | −56538 | 28.3078 |
| 0.1 | 0.2 | 1.0408 0.1003 2.6896<br>1.3301 0.2833 2.0841<br>2.4385 −0.0005 | −3.5496 | 19.2211 | −0.00004 | −61480 | 30.7029 |
| 0.5 | 0.2 | 0.9480 0.1011 2.6940<br>1.3219 0.1477 2.0899<br>2.4394 −0.0001 0.6327 | −3.2950 | 17.3251 | $-0.24 \cdot 10^{-7}$ | −64903 | 32.2447 |

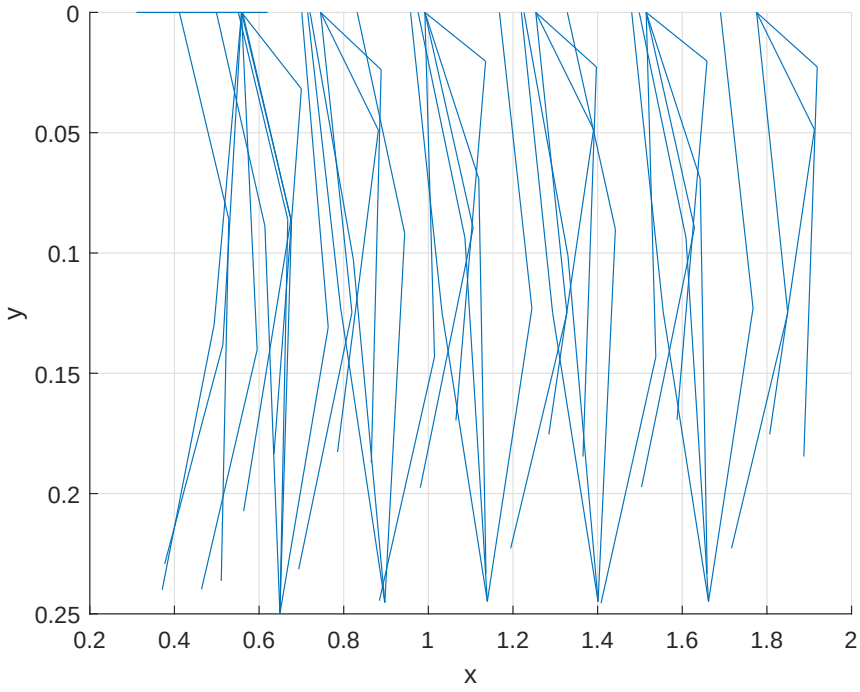


Figure 4.34: Animation of one leg when $\mu < 0$ corresponding to the values $\alpha = 0.9480$, $\tau = 0.1011$, $E_1 = 2.6940$, $a_{12} = 1.3219$, $b_{12} = 0.1477$, $E_2 = 2.0899$, $a_{21} = 2.4394$, and $b_{21} = -0.000005$.

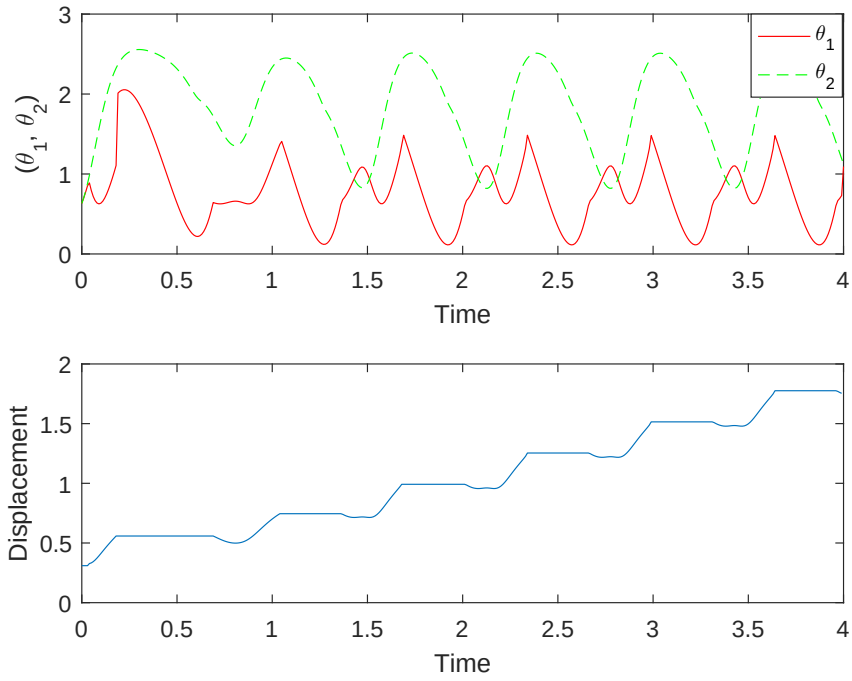


Figure 4.35: Outputs and displacement for bidirectional two CPGs when $C_1C_2 \neq 0$ and $\mu < 0$ corresponding to the same values in Figure 4.34.

**Fourthly:** Let $\mu = 0.4$, $a_{21} = 2.5$, $a_{12} = b_{12} = b_{21} = 1$, $M = 0.05$ and $C = 0.8$.. Since $0 < \mu < 1$, the stabilities of the fixed points depend on $\beta_1$ and $\beta_2$. With constraints $0 \leq \theta_1, \theta_2 \leq \frac{4\pi}{5}$, when the values of $\beta_1$ and $\beta_2$ are greater than zero, then the fixed points are stable, while the fixed points are unstable when $\beta_1 < 0$ and $\beta_2 > 0$. Although the CPGs generate RPs, the locomotion is not good. These results are shown in Tables 4.25 and 4.26. One of the cases in Table 4.26 is depicted in Figure 4.36.

Table 4.25: Bidirectional two CPGs of the third type when $0 < \mu < 1$ and $C_2 = 0$

| $M$ | $C$ | Values of parameters | $\beta_1$ | $\beta_2$ | $\mu$ | $J$ | $x_b$ |
|---|---|---|---|---|---|---|---|
| 0.05 | 0.2 | 0.3674 2.5030 0.8979 1.0000 1.0000<br>2.5996 3.5360 3.0088 2.5000 1.0000 | 0.0127 | 0.5286 | 0.4 | −6792.1 | 1.2511 |
| 0.5 | 0.2 | 0.4996 2.2103 1.0901 1.0000 1.0000<br>2.6068 3.4761 2.9436 2.5000 1.0000 | −0.0187 | 0.8423 | 0.4 | −7493.5 | 1.4399 |

Table 4.26: Bidirectional two CPGs of the third type when $0 < \mu < 1$ and $C_1C_2 \neq 0$

| $M$ | $C$ | Values of Parameters | $\beta_1$ | $\beta_2$ | $\mu$ | $J$ | $x_b$ |
|---|---|---|---|---|---|---|---|
| 0.05 | 0.2 | 0.2164 0.7505 1.3686<br>1.0000 1.0000 2.2733<br>1.7979 2.9456 2.8930<br>1.0000 | −0.0776 | 2.3282 | 0.3457 | −5153.2 | 2.1476 |
| 0.05 | 0.2 | 0.7279 0.1992 1.5080<br>1.0912 0.1590 0.8865<br>0.3586 1.4789 2.4560<br>3.5548 | −0.7691 | 7.6106 | 0.2109 | −34248 | 17.0133 |
| 0.05 | 0.8 | 3.2300 0.7645 0.7875<br>1.0000 1.0000 1.1214<br>1.0034 1.8443 2.5130<br>1.0000 | 1.1404 | 2.7090 | 0.3979 | −2275.4 | 0.5751 |
| 0.05 | 0.8 | 0.5318 4.0000 1.1789<br>1.0000 1.6750 0.3624<br>3.9977 0.7374 2.5000<br>$4.1200 \cdot 10^{-6}$ | −0.0202 | 0.6778 | $2.7634 \cdot 10^{-6}$ | −2590.6 | 0.9219 |
| 0.05 | 0.8 | 0.6714 0.2154 1.3861<br>1.0313 0.0938 0.7598<br>0.3653 1.3265 2.3583<br>3.4752 | −0.7256 | 6.6401 | 0.1341 | −31535 | 15.4452 |
| 0.5 | 0.2 | 0.3104 2.5870 0.8164<br>1.0000 1.0000 2.7421<br>3.6211 3.0713 2.5000<br>1.0000 | 0.0270 | 0.7837 | 0.4 | −3234.7 | 1.1584 |
| 0.5 | 0.2 | 0.1493 2.1906 0.5755<br>1.0000 1.0000 1.3358<br>2.9900 2.1192 2.5204<br>1.0000 | 0.0503 | 0.8924 | 0.3968 | −3617.3 | 1.2895 |
| 0.5 | 0.2 | 0.7517 0.2103 1.4679<br>1.0806 0.1562 0.8568<br>0.3630 1.4201 2.4345<br>3.5360 | −0.7309 | 7.4894 | 0.2100 | −32730 | 16.0738 |
| 0.5 | 0.8 | 1.4180 0.2427 1.2386<br>1.0000 1.0000 0.7285<br>0.3653 0.9347 2.5000<br>1.0000 | −1.1253 | 11.3403 | 0.4 | −11208 | 5.1882 |
| 0.5 | 0.8 | 0.1896 2.8647 0.5639<br>1.0000 1.0000 3.4767<br>3.0286 3.2580 2.4672<br>1.0000 | 0.0512 | 0.9969 | 0.4053 | −3371.4 | 1.2076 |
| 0.5 | 0.8 | 1.4181 0.2427 1.2386<br>1.0000 1.0001 0.7285<br>0.3653 0.9348 2.5002<br>1.0002 | −1.1256 | 11.3404 | 0.4001 | −11260 | 5.2203 |

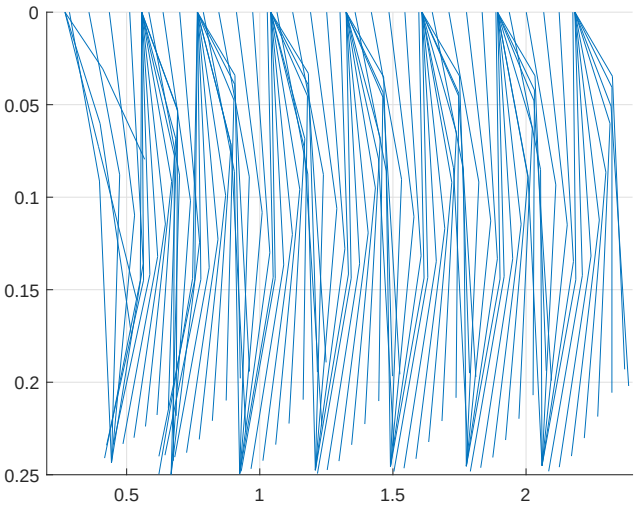


Figure 4.36: Animation of one leg when $\mu = 0.2109$ corresponding to the values $\alpha_1 = 0.7279$, $\tau_1 = 0.1992$, $E_1 = 1.5080$, $a_{12} = 1.0912$, $b_{12} = 0.1590$, $\alpha_2 = 0.8865$, $\tau_2 = 0.3586$, $E_2 = 1.4789$, $a_{21} = 2.4560$, and $b_{21} = 3.5548$.

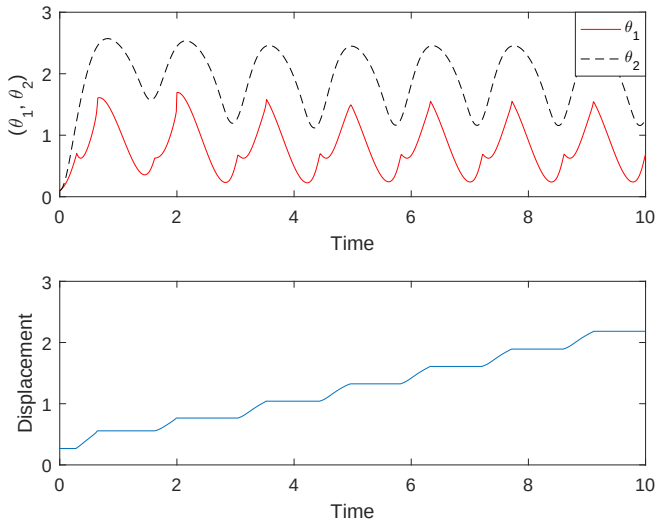


Figure 4.37: Outputs and displacement for bidirectional two CPGs when $C_1C_2 \neq 0$ and $\mu > 0$ corresponding to the same values in Figure 4.36.

# CHAPTER 5

# OUTPUTS OF THE CPGS VERSUS THE REAL DATA

In this part, the outputs of the CPGs will be compared with the real data that are obtained by one leg of human locomotion with two and three joints (as in Figure 5.1). In fact, as explained in the previous chapters, we have three types of CPGs and each type has three cases, that are namely uncoupled, unidirectional and bidirectional two CPGs. Among all cases, it will be seen that the bidirectional two CPGs of the third type produces the best results.

Presumably, collecting the real data is the shortest and most straightforward method to produce a CPG-induced acceleration motion trajectory for biped locomotion. In order to determine the kinematic attributes with the system behavior while walking, we first use the rubrics of biped kinematics on the sagittal plane to outline the simple kinematic precepts of robotic bipedal locomotion with two or three DOFs (see [84, 85] for more details). A comparison of the acceleration or forward motion trajectory gleaned from the real data with CPGs will be simultaneously drawn. Figure 5.1 illustrates how CPGs are used to produce rhythmic patterns for the hip, knee, and ankle angles via one leg of a human when the lower body is parallel to the ground. It is worth mentioning here that the results obtained are contingent upon the manner in which CPGs are analyzed. A closer look into the kinematics of the hip, knee, and ankle angles in the swing phase reveals the following basic kinematics equations: From the joint between hip and knee, we have

$$x_1 = x_d + L_1 \cos\theta_1 \quad \text{and} \quad y_1 = y_d + L_1 \sin\theta_1.$$

From the other two joints we get

$$x_2 = x_1 + L_2 \cos\theta_2, \quad y_2 = y_1 + L_2 \sin\theta_2, \quad x_3 = x_2 + L_3 \cos\theta_3 \quad \text{and} \quad y_3 = y_2 + L_3 \sin\theta_3,$$

where $x_d$ is the preceding displacement (i.e., the distance during locomotion) and $y_d$ stands for the positive direction of the hip height at each step. $L_1$, $L_2$ and $L_3$ represent three lengths: from the hip-joint to the knee-joint, from the knee-joint to the ankle-joint, and from the ankle-joint to the end of effector, respectively. The angles, $\theta_1$, $\theta_2$ and $\theta_3$, which represent the hip, knee, and ankle angles, respectively, will acquire their rhythmic patterns from the CPGs. With regard to $y_d$, it is assumed to be zero when the lower body is parallel to the ground.

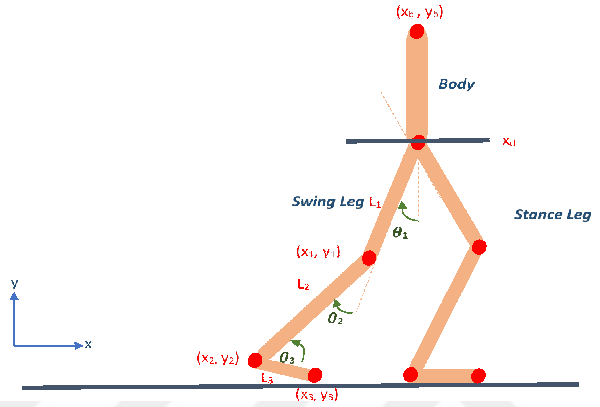


Figure 5.1: Planar biped model when the lower body is parallel to the ground

## 5.1 Collecting real data

Obtaining real data involves different objectives. One of the major objectives, for instance, is to learn whether the output of the CPGs may be endorsed. Another important and legitimate inquiry is whether manipulating CPGs would establish rhythmic patterns for the hip, knee, and ankle angles akin to those seen in nature. To collect the real data, we actually need a high-speed (2000 fps) Camera, as in the Figure 5.2. As the second step, we should define three joints, namely the hip, knee and ankle in one leg of a human. We put a special sign on each of them to release the place of the joints during locomotion, such as in Figure 5.3. The real data were obtained through video recordings at the laboratory of the Mechatronics Department at Atilim University, as described in Figure 5.3. In fact, in order to be able to analyze the video-recorded real data, the researchers used the Tema Motion software. The results of using the Tema Motion to establish real data for the hip and knee angles are shown in Figure 5.4.

Figure 5.2: PHOTRON FASTCAM MC2.1: High speed Camera

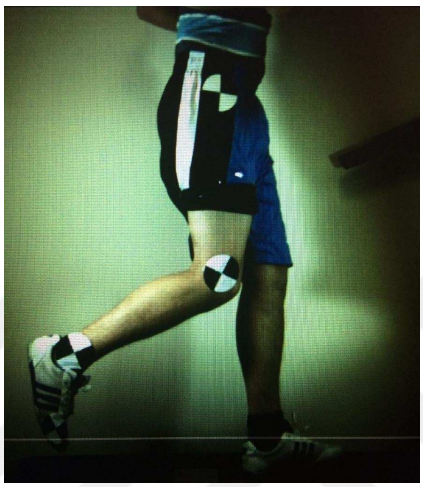

Figure 5.3: Video-recorded data

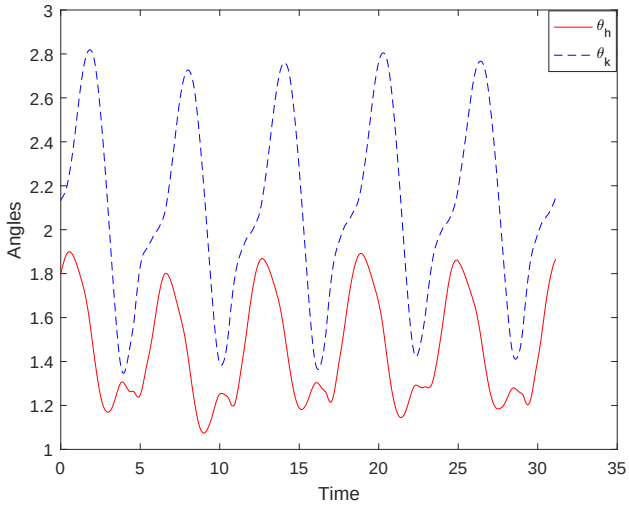


Figure 5.4: Angles of the hip and knee that are collected by real data.

## 5.2 Comparing the real data with bidirectional two CPGs of the third type.

In fact, we optimized all other cases and made comparisons with the real data. We find that, the closet one is that of the outputs of the bidirectional two CPGs of the third type which generate rhythmic patterns similar those collected from the real data. In order to generate rhythmic motions similar to those we see in natural human locomotion, we need to determine the optimal parameter sets by manipulating the GA. This study endeavors to utilize more than one cost function. The first objective function is:

$$J_1 = \sum_{k=1}^{n} \left( (\theta_1(k) - \theta_h(k))^2 + (\theta_2(k) - \theta_k(k))^2 \right), \tag{5.1}$$

where $\theta_1$ and $\theta_2$ are the outputs of the CPGs as defined before, $\theta_h$ and $\theta_k$ are the angles of the hip and knee of the real data respectively, and $n$ is the total number of step times. The conclusive goal here is to minimize any differences between the outputs of the CPGs and the real data for the angles of the hip and knee in the region captured by the stability analysis. To decrease the error, we set the initial conditions in the CPGs as variables determined by the GA optimization, in which the mutation rate and crossover fraction are predicted to be 0.05 and 0.2, respectively, as described in Figures 5.5, 5.6, 5.7 and 5.8.

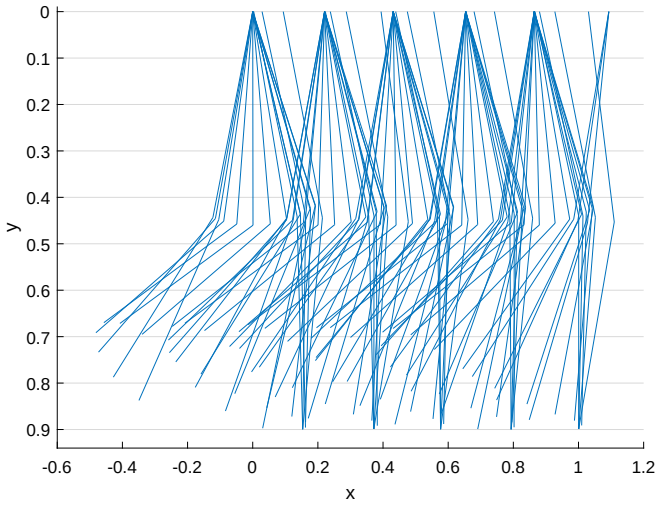


Figure 5.5: One leg animation for the CPGs corresponding to the values $\alpha = 0.0010$, $\tau = 0.9624$, $E_1 = 0.4721$, $a_{12} = 1.5071$, $b_{12} = 0.0288$, $E_2 = 1.3746$, $a_{21} = 2.1200$, $b_{21} = -0.0479$ and the initial conditions $x_1(0) = 1.8139$, $v_1(0) = 0.1369$, $x_2(0) = 2.1081$, $v_2(0) = 0.5569$.

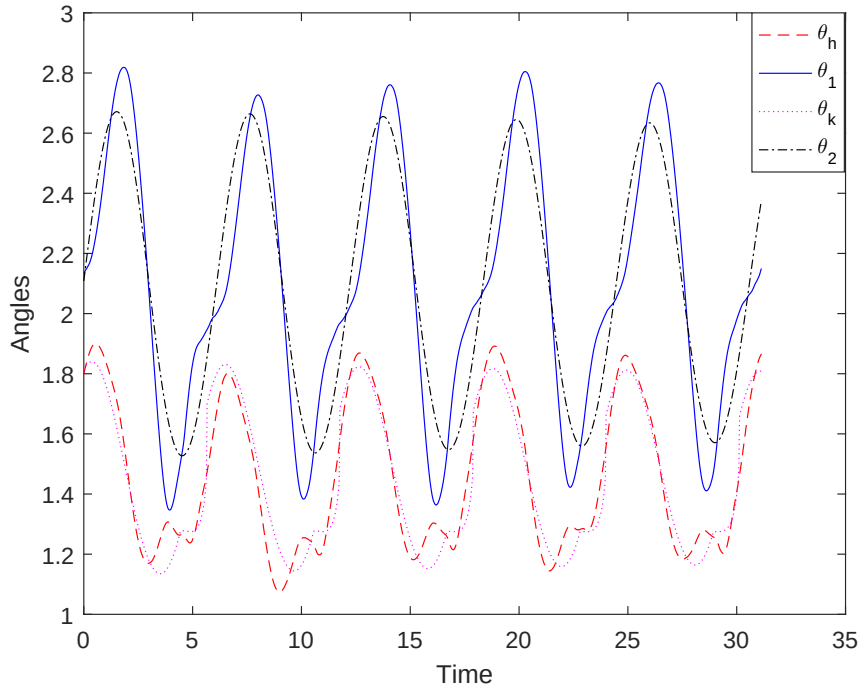


Figure 5.6: Outputs of the CPGs and real data: The outputs of the CPGs correspond to the same values in Figure 5.5

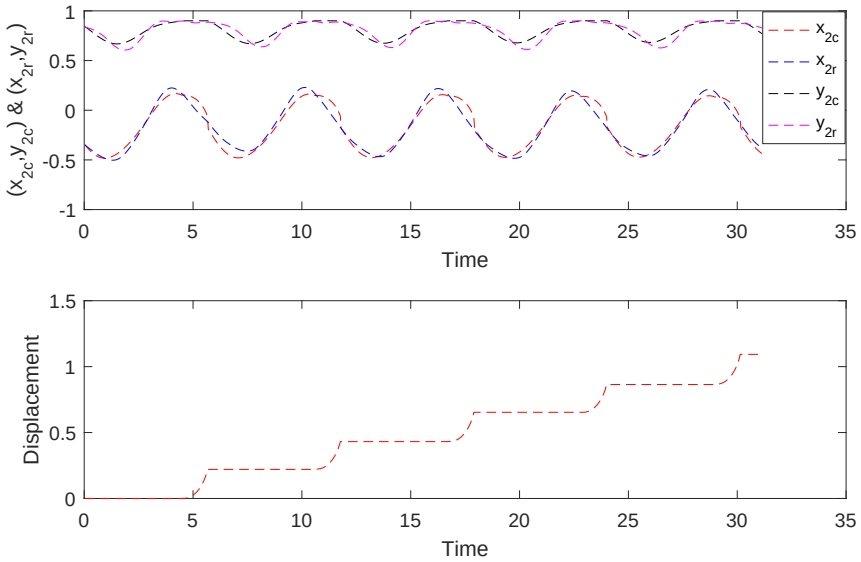


Figure 5.7: Coordinates of the knee joint and displacement against time

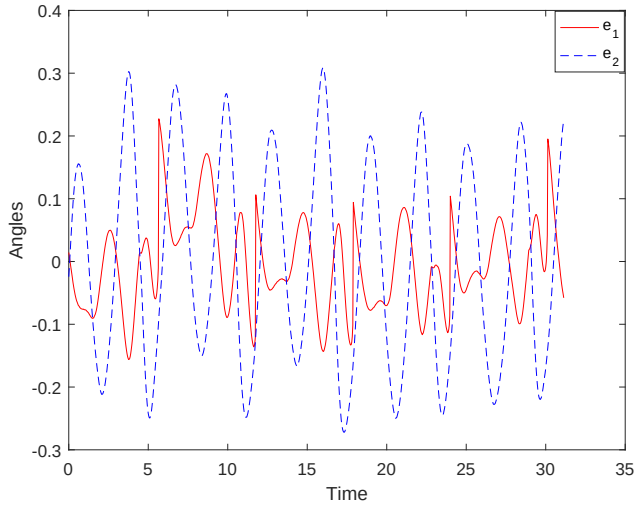


Figure 5.8: Errors between the outputs of the CPGs and the real data at each angle corresponding to the same values in Figure 5.5

$e_1$ and $e_2$ are the errors between each angle, respectively. Remarkably, concentrating on three joints with three DOFs of the ankle, knee, and hip angles, and using the same technique above, we succeeded in obtaining the real data for the three angles as shown in Figure 5.9.

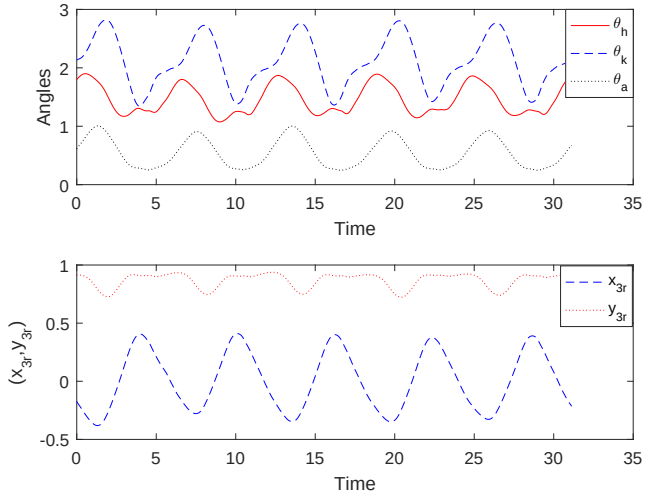


Figure 5.9: Angles of the hip, knee and ankle that are collected from the real data

The new objective function including the three angles is

$$J_2 = J_1 + \sum_{k=1}^{n} \left( (\theta_3(k) - \theta_a(k))^2 \right), \tag{5.2}$$

where $\theta_3$ is the output of the third CPG for the angle of the ankle and $\theta_a$ is the angle of the ankle obtained from the real data. For the last CPG different couplings may be used. In this study, for the ankle joint we use two CPGs coupled bidirectionally and we take only one output, followed by optimizing the objective function $J_2$. The results are shown in Figures 5.10, 5.11 and 5.12 below. Note that, the outputs of the CPGs are close to those coming from the real data, although, the hip joint being fixed.

The outputs correspond to the values $\alpha = 0.0024$, $\tau = 0.9601$, $E_1 = 0.1989$, $a_{12} = 1.4845$, $b_{12} = 0.0614$, $E_2 = 5.0000$, $a_{21} = 2.1210$, $b_{21} = -0.0586$ and the initial condition $x_1(0) = 1.8135$, $v_1(0) = 0.1390$, $x_2(0) = 2.1075$, $v_2(0) = 0.5540$ for the first two CPGs and $\alpha_1 = 0.3653$, $\tau_1 = 0.9623$, $E_3 = 1.2259$, $a_{34} = 0.6486$, $b_{34} = 0.0331$, $E_4 = 3.0105$, $a_{43} = 1.6668$, $b_{21} = -0.0054$ and the initial condition $x_3(0) = 0.6162$, $v_3(0) = 0.3347$, $x_4(0) = 0.4661$, $v_4(0) = 0.0174$ for the last two CPGs. where $e_1$, $e_2$ and $e_3$ are the errors between each angle respectively in Figure 5.12.

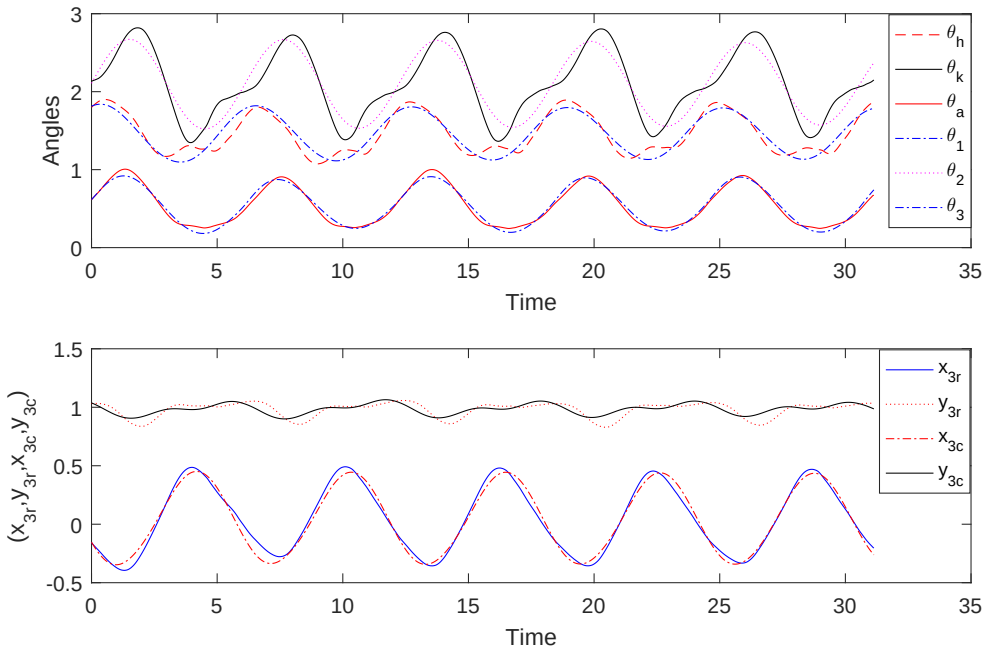


Figure 5.10: Outputs of the three CPGs and the real data

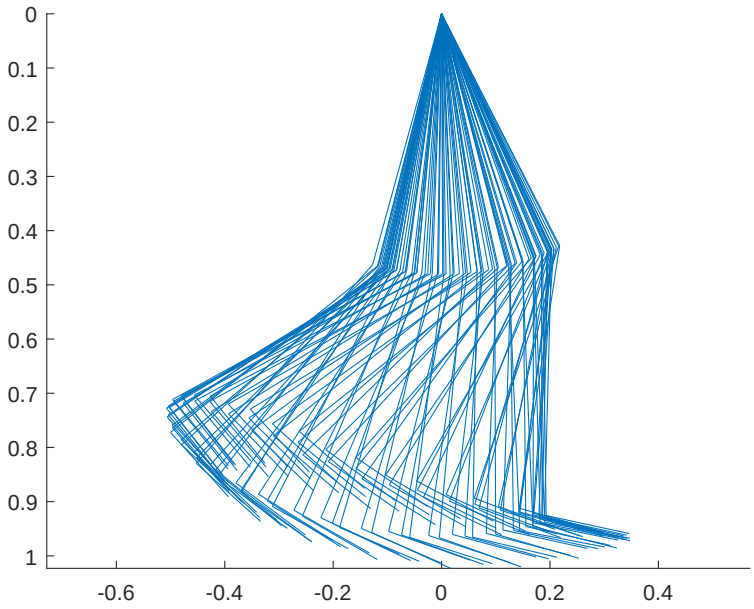


Figure 5.11: One leg animation with three DOFs in swing phase corresponding to the same values in Figure 5.10.

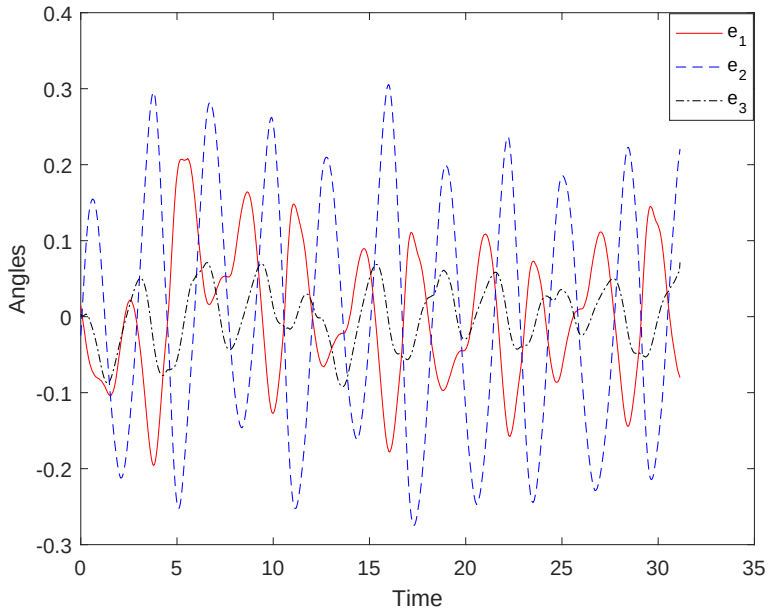


Figure 5.12: Errors between the outputs of the CPGs and the real data at each angle corresponding to the same values in Figure 5.10.

In order to reduce the error between the real data and the outputs of the bidirectional two CPGs in one leg with 2 DOFs, we should optimize the objective function below:

$$J_3 = J_1 + \sum_{k=1}^{n} \left( (x_{2c}(k) - x_{2r}(k))^2 + (y_{2c}(k) - y_{2r}(k))^2 \right), \tag{5.3}$$

where $(x_{1c}, y_{1c})$, $(x_{2c}, y_{2c})$, $(x_{1r}, y_{1r})$ and $(x_{2r}, y_{2r})$ are the coordinates that are generated from the outputs of the CPGs and real data during locomotion. The CPGs are able to generate the RPs similar to the outputs of the real data. The results of the optimization are shown in Figures 5.13, 5.14, 5.15 and 5.16.

The objective function $J_3$ indicates that the standard deviation or the error between the outputs of the bidirectional two CPGs and real data are decreased compared with the previous case for one leg with two DOFs. Despite the fact that the error still exists in this case, the outputs of the CPGs corresponds to the same values of the parameters, which applies our conditions of the stability of the bidirectional two CPGs.

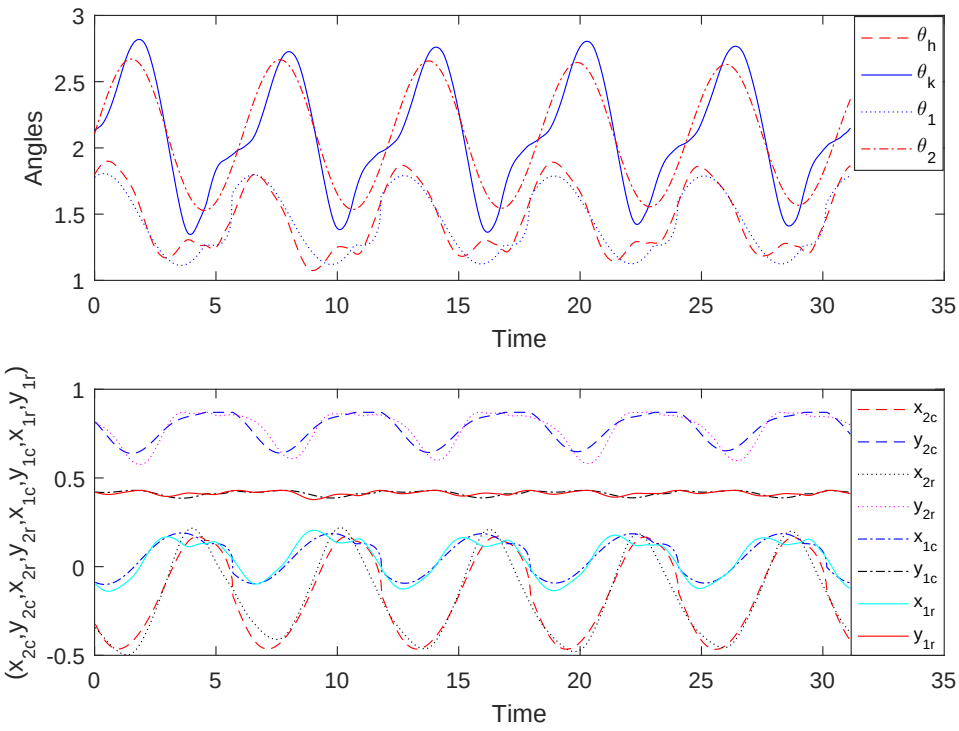


Figure 5.13: Angles of the hip and knee using the outputs of the CPGs and the real data: The outputs of CPGs correspond to the values $\alpha = 0.0012$, $\tau = 0.9617$, $E_1 = 0.2003$, $a_{12} = 1.4789$, $b_{12} = 0.0478$, $E_2 = 5.9966$, $a_{21} = 2.1212$, $b_{21} = -0.0512$ and the initial conditon $x_1(0) = 1.7785$, $v_1(0) = 0.1390$, $x_2(0) = 2.1075$, $v_2(0) = 0.5540$.

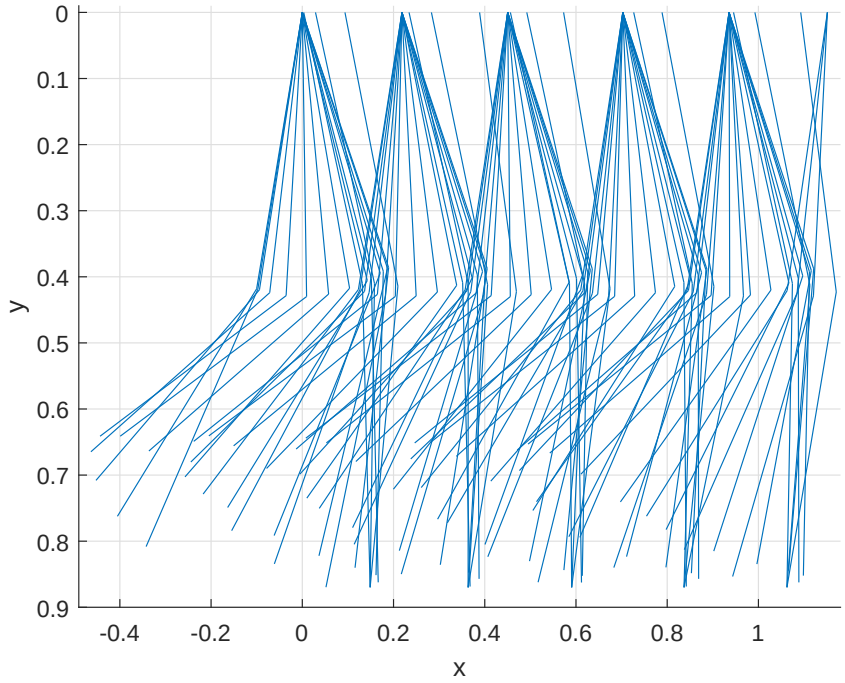


Figure 5.14: Animation of one leg with 2 DOFs corresponding to the same values in Figure 5.13.

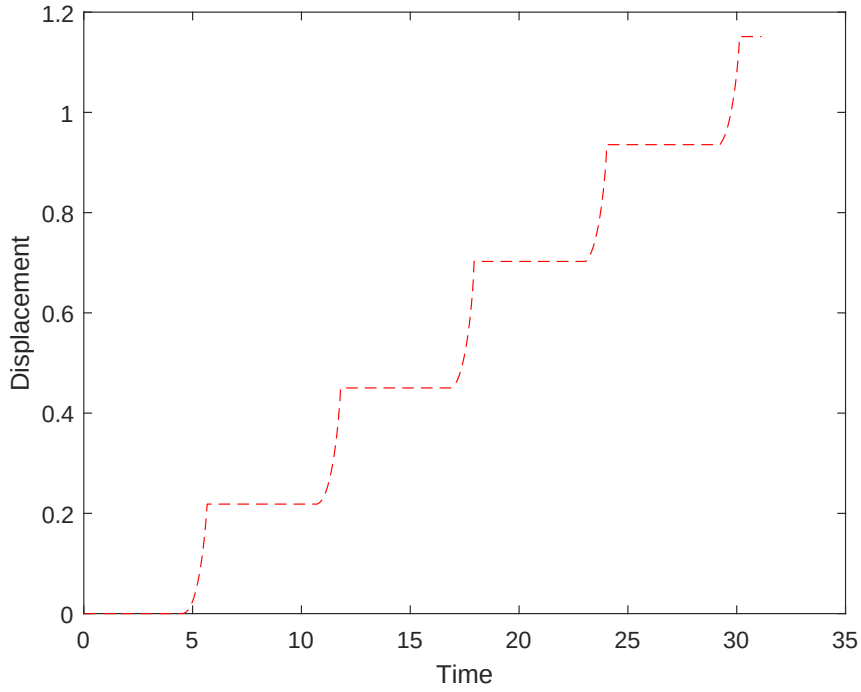


Figure 5.15: Displacement against time corresponding to the same values in Figure 5.13.

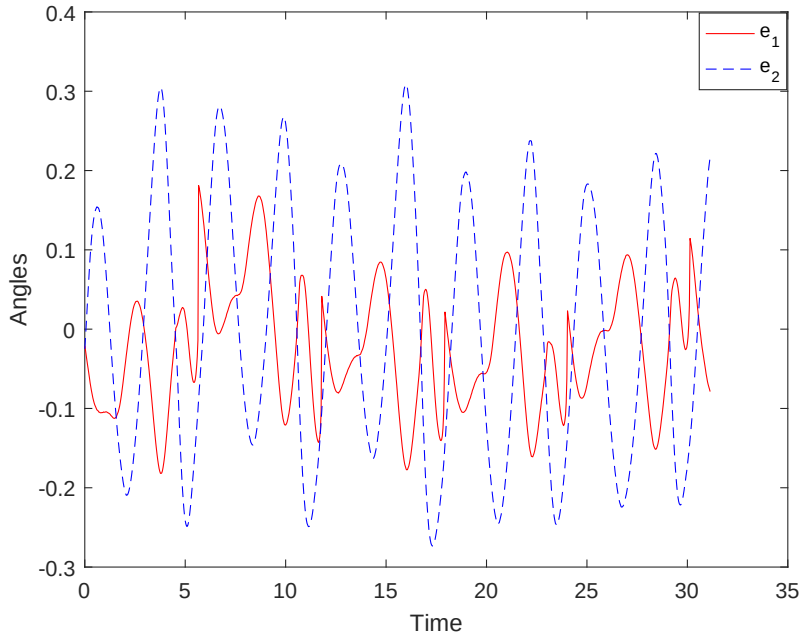


Figure 5.16: Errors between the outputs of the CPGs and the real data at each angle corresponding to the same values in Figure 5.13

However, to optimize the model with three joints, it is highly recommended that we use the objective function in (5.4) below:

$$J_4 = J_3 + \sum_{k=1}^{n} \left( (\theta_3(k) - \theta_a(k))^2 + (y_{3c}(k) - y_{3r}(k))^2 \right) \tag{5.4}$$

where $(x_{3c}, y_{3c})$ and $(x_{3r}, y_{3r})$ are the coordinates of the outputs from the CPGs and the real data during locomotion. The results of the optimization are shown in Figures 5.17, 5.18 and 5.19 which are the outputs of the CPGs with the real data, and the errors between the outputs of the CPGs and the real data, respectively. Unlike the other case-induced results, these results have improved greatly when using the bidirectional two CPGs. We here show that the third type of CPG of the bidirectional two CPGs case has generated rhythmic patterns that are closest to those derived from the real data by using the GA and pattern search solvers. We here show our hypothesis. Most importantly, this type of CPG has produced the best results compared to every other type of CPG thus far available.

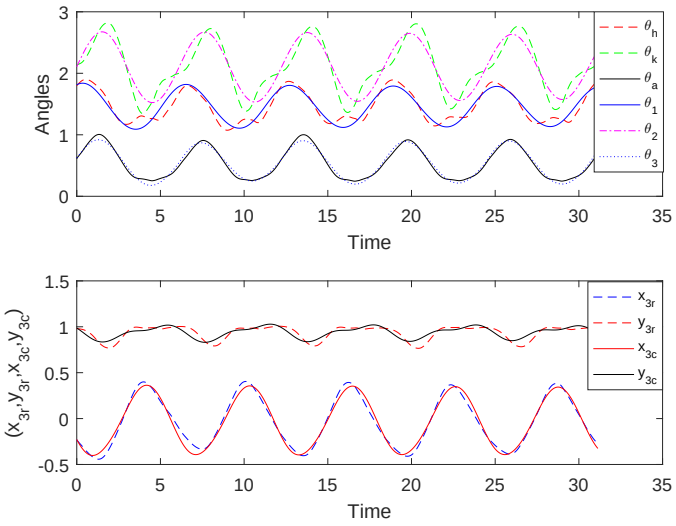


Figure 5.17: Angles of the hip, knee and ankle using the outputs of the CPGs and the real data: The outputs of the CPGs correspond to $\alpha = 0.0023$, $\tau = 0.9599$, $E_1 = 0.2020$, $a_{12} = 1.4808$, $b_{12} = 0.0582$, $E_2 = 4.9724$, $a_{21} = 2.1238$, $b_{21} = -0.0612$, $\alpha_1 = 0.3225$, $\tau_1 = 0.9623$, $E_3 = 1.9637$, $a_{34} = 0.6509$, $b_{34} = 0.0278$, $E_4 = 2.1947$, $a_{43} = 1.4209$, $b_{21} = -0.0010$ and the initial conditons $x_1(0) = 1.8135$, $v_1(0) = 0.1390$, $x_2(0) = 2.1075$, $v_2(0) = 0.5540$, $x_3(0) = 0.6258$, $v_3(0) = 0.3154$, $x_4(0) = 0.4318$, $v_4(0) = 0.0218$.

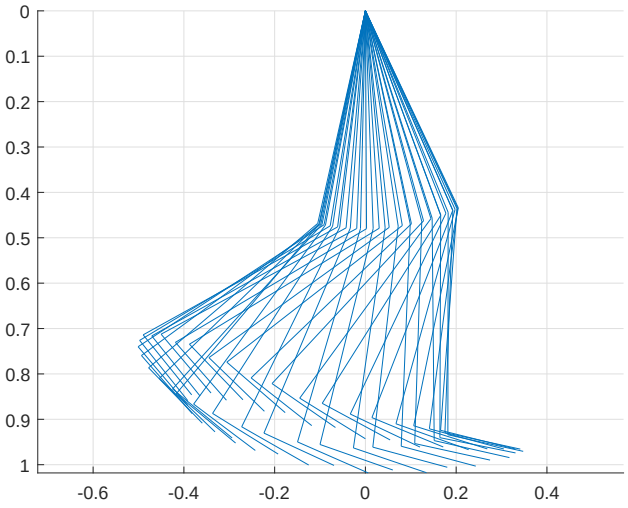

Figure 5.18: One leg with 3 DOFs animation in the swing phase corresponding to the same values in Figure 5.17.

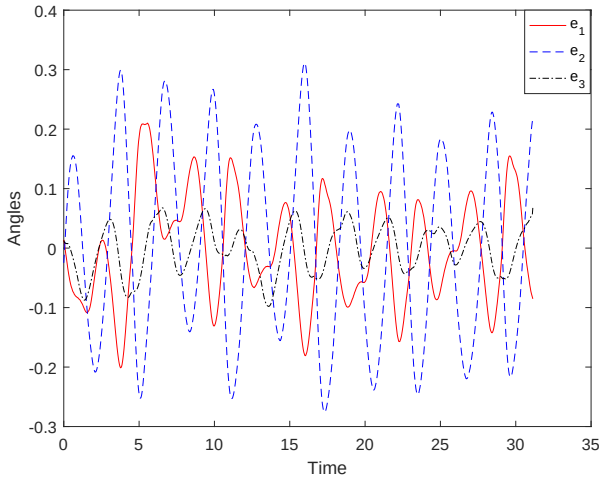


Figure 5.19: Errors between the outputs of the CPGs and the real data at each angle corresponding to the same values in Figure 5.17.

## 5.3 Effective Parameters in CPGs

In this part of the study, we attempted to optimize the parameters of the CPGs with the objective of determining the operational parameters in the bidirectional two CPGs. The results reveal that the most effective parameters are $\tau$ and $\alpha$, where the parameter $\tau$ stands for the number of oscillations. In order to verify the results, we repeated the optimization of human locomotion shown in Figures 5.5 and 5.6, and started changing the value of $\tau$. The results reveal two distinct patterns: the first unfolds an inverse pattern, where an increase in the value of $\tau$ results in a decrease in displacement and velocity. The second one, by contrast, reveals that a decrease in the value of $\tau$ produces an increase in displacement and velocity. Table 5.1 summarizes these results where the values of the fixed parameters are $\alpha = 0.0010$, $E_1 = 0.4721$, $a_{12} = 1.5071$, $b_{12} = 0.0288$, $E_2 = 1.3746$, $a_{21} = 2.1200$, and $b_{21} = -0.0479$:

Table 5.1: Effects of $\tau$ on $J_1$ and $x_b$ when the other parameters are fixed.

| $\tau$ | $J_1$ | $x_b$ |
|---|---|---|
| 0.9624 | 29.7447 | 1.0671 |
| 1.9624 | 430.0472 | 0.4366 |
| 2.9624 | 403.9559 | 0.2183 |
| 3.9624 | 466.4726 | 0.2156 |
| 0.5624 | 415.6542 | 1.6304 |
| 0.1624 | 359.8602 | 3.4021 |

In a similar fashion, an increase in the value of parameter $\alpha$ contributes to a decrease in the displacement and velocity. However, decreasing the value of $\alpha$ by a small amount results in an equal percentage increase in the displacement and velocity. These results are not inconsistent with the conclusions obtained from the stability section. Table 5.2 summarizes the results of increasing and decreasing the value of parameter $\alpha$, where the values of the fixed parameters are $\tau = 0.9624$, $E_1 = 0.4721$, $a_{12} = 1.5071$, $b_{12} = 0.0288$, $E_2 = 1.3746$, $a_{21} = 2.1200$, and $b_{21} = -0.0479$:

Table 5.2: Effects of $\alpha$ on $J_1$ and $x_b$ when the other parameters are fixed.

| $\alpha$ | $J_1$ | $x_b$ |
|---|---|---|
| 0.0020 | 34.0806 | 1.0502 |
| 0.0080 | 37.8369 | 1.0015 |
| 0.0180 | 49.4105 | 0.7352 |
| 0.0900 | 125.3871 | 0.1278 |
| 0.0005 | 33.9530 | 1.0756 |
| 0.0001 | 33.9977 | 1.0581 |

In view of the fact that we used the GA for optimization, the outputs of the CPGs were not identical to the real results obtained for the hip and knee; however, they were almost identical. This small difference may be attributable to the facts that the Genetic Algorithm only yielded the local minimum, the waist of the lower body in our model is parallel to the ground and the hip joint is fixed.

To show the effect of the coupling weights $a_{ij}$ and $b_{ij}$ we repeat the same experiment that is done in Tables 5.1 and 5.2, by running the optimization and using the cost function $J_1$, the results are shown by Tables 5.3, 5.4, 5.5, 5.6, 5.7 and 5.8. Table 5.3 presents the results of changing the couple weights $a_{12}$, $b_{12}$ and $\tau$. In this table the values of the fixed parameters are $\alpha = 0.0010$, $E_1 = 0.4721$, $E_2 = 1.3746$, $a_{21} = 2.1200$, and $b_{21} = -0.0479$. Note that, the errors between the real data and the outputs of the CPGs in Table 5.3 have decreased relative to Table 5.1.

Table 5.3: Values of $J_1$ and $x_b$ for different choices of $a_{12}$, $b_{12}$ and $\tau$

| $\tau$ | $a_{12}$ | $b_{12}$ | $J_1$ | $x_b$ |
|---|---|---|---|---|
| 0.9624 | 1.5071 | 0.0288 | 29.7447 | 1.0671 |
| 1.9624 | 1.5993 | −0.1322 | 402.7306 | −0.1514 |
| 2.9624 | 1.5889 | −0.1820 | 382.4701 | −0.1229 |
| 3.9624 | 1.5845 | −0.2920 | 441.6822 | −0.1467 |
| 0.5624 | 1.4999 | 0.0434 | 33.1957 | 1.0906 |
| 0.1624 | 1.5916 | 0.0086 | 318.3521 | 0.3164 |

These results are similar to the coupling weights $a_{21}$ and $b_{21}$ as seen in Table 5.4. In this table the values of the fixed parameters are $\alpha = 0.0010$, $E_1 = 0.4721$, $a_{12} = 1.5071$, $b_{12} = 0.0288$ and $E_2 = 1.3746$.

Table 5.4: Values of $J_1$ and $x_b$ for different choices of $a_{21}$, $b_{21}$ and $\tau$

| $\tau$ | $a_{21}$ | $b_{21}$ | $J_1$ | $x_b$ |
|---|---|---|---|---|
| 0.9624 | 2.1200 | −0.0479 | 29.7447 | 1.0671 |
| 1.9624 | 2.0087 | −0.2107 | 412.9008 | −0.1514 |
| 2.9624 | 1.9999 | −0.3484 | 385.4969 | 0.1865 |
| 3.9624 | 2.0474 | −0.4382 | 448.4796 | 0.1493 |
| 0.5624 | 2.0650 | −0.1311 | 388.3686 | 0.9846 |
| 0.1624 | 2.1228 | −0.1216 | 337.6760 | 0.8460 |

We follow the same steps by changing the value of $\tau$ and the four parameters $a_{12}$, $b_{12}$, $a_{21}$ and $b_{21}$ as in Table 5.5. In this table the values of the fixed parameters are $\alpha = 0.0010$, $E_1 = 0.4721$, and $E_2 = 1.3746$. Note that the results presented in Table 5.5 are much better than those in Tables 5.3 and 5.4.

Table 5.5: Values of $J_1$ and $x_b$ for different choices of $a_{12}$, $b_{12}$ $a_{21}$, $b_{21}$ and $\tau$

| $\tau$ | $a_{12}$ | $b_{12}$ | $a_{21}$ | $b_{21}$ | $J_1$ | $x_b$ |
|---|---|---|---|---|---|---|
| 0.9624 | 1.5071 | 0.0288 | 2.1200 | −0.0479 | 29.7447 | 1.0671 |
| 1.9624 | 1.4579 | −3.2676 | 2.1651 | 2.6068 | 68.6185 | 0.4021 |
| 2.9624 | 1.5900 | −1.7699 | 2.1651 | 2.6068 | 309.9797 | 0.02 |
| 3.9624 | 1.5731 | −3.1830 | 2.2245 | 3.8558 | 282.0600 | 0.0338 |
| 0.5624 | 1.6839 | 0.0275 | 2.0681 | −0.2714 | 334.0745 | −0.7771 |
| 0.1624 | 1.6210 | 0.0028 | 2.0515 | −0.0736 | 310.0280 | −0.6511 |

We repeat the same experiment by changing the value of $\alpha$ as seen in Table 5.6 and finding the optimal values of the coupling weights $a_{12}$ and $b_{12}$. where the values of the fixed parameters in this table are $\tau = 0.9624$, $E_1 = 0.4721$, $E_2 = 1.3746$, $a_{21} = 2.1200$, and $b_{21} = -0.0479$. Comparing Table 5.6 with Table 5.2, the results present in Table 5.6 are much better than in the Table 5.2, and the variance still decreases in this case.

Table 5.6: Values of $J_1$ and $x_b$ for different choices of $a_{12}$, $b_{12}$ and $\alpha$.

| $\alpha$ | $a_{12}$ | $b_{12}$ | $J_1$ | $x_b$ |
|---|---|---|---|---|
| 0.0020 | 1.4953 | 0.0463 | 32.9604 | 1.0966 |
| 0.0080 | 1.4720 | 0.0629 | 33.7362 | 1.0834 |
| 0.0180 | 1.4457 | 0.0894 | 40.6344 | 0.6922 |
| 0.0900 | 1.4270 | 0.2965 | 114.2399 | 0 |
| 0.0005 | 1.5023 | 0.0420 | 33.3595 | 1.0854 |
| 0.0001 | 1.5023 | 0.0420 | 33.9977 | 1.0581 |

When we do the same experiment as illustrated in Table 5.7, it is seen how the optimal values of the coupling weights $a_{21}$ and $b_{21}$ change as we change the value of $\alpha$. In this table the values of the fixed parameters are $\tau = 0.9624$, $E_1 = 0.4721$, $a_{12} = 1.5071$, $b_{12} = 0.0288$ and $E_2 = 1.3746$.

Table 5.7: Values of $J_1$ and $x_b$ for different choices of $a_{21}$, $b_{21}$ and $\alpha$.

| $\alpha$ | $a_{21}$ | $b_{21}$ | $J_1$ | $x_b$ |
|---|---|---|---|---|
| 0.0020 | 2.1176 | −0.0442 | 34.0415 | 1.0465 |
| 0.0080 | 2.1119 | −0.0415 | 37.6606 | 0.9852 |
| 0.0180 | 2.1031 | -0.0334 | 48.7535 | 0.8090 |
| 0.0900 | 2.0661 | 0.3425 | 113.8988 | 0.1641 |
| 0.0005 | 2.1192 | −0.0447 | 33.9311 | 1.0664 |
| 0.0001 | 2.1197 | −0.0448 | 33.9790 | 1.0745 |

By comparing Table 5.7 with Table 5.2, it is a clear that, the results present in Table 5.7 are better than Table 5.2. In spite of this, there are small differences between Table 5.7 and Table 5.6. However, both mention that the coupling weights influence the outputs of the CPGs when we change the value of $\alpha$.

We follow the same technique by changing the value of $\alpha$. We will optimize the bidirectional two CPGs in order to find the optimal values of parameters $a_{12}$, $b_{12}$, $a_{21}$ and $b_{21}$. These results are illustrated in Table 5.8. In this table the values of the fixed parameters are $\tau = 0.9624$, $E_1 = 0.4721$, and $E_2 = 1.3746$.

Table 5.8: Values of $J_1$ and $x_b$ for different choices of $a_{12}$, $b_{12}$ $a_{21}$, $b_{21}$ and $\alpha$

| $\alpha$ | $a_{12}$ | $b_{12}$ | $a_{21}$ | $b_{21}$ | $J_1$ | $x_b$ |
|---|---|---|---|---|---|---|
| 0.0020 | 1.4950 | 0.0474 | 2.1256 | −0.0398 | 32.8514 | 1.1122 |
| 0.0080 | 1.4729 | 0.0667 | 2.1262 | −0.0291 | 33.2497 | 1.0495 |
| 0.0180 | 1.4535 | 0.1074 | 2.1254 | −0.0019 | 38.2692 | 0.5752 |
| 0.0900 | 1.4719 | 0.4715 | 2.1231 | 0.2778 | 60.2143 | 0 |
| 0.0005 | 1.5019 | 0.0428 | 2.1251 | −0.0419 | 33.2938 | 1.1200 |
| 0.0001 | 1.5038 | 0.0415 | 2.1250 | −0.0425 | 33.4570 | 1.1157 |

In conclusion, the parameters of the coupling weights are important in order to balance the disturbance during optimization. Moreover, when the parameters $\alpha$ and $\tau \in (0, 3]$, the bidirectional two CPGs of the third type are definitely able to generate different RPs for one leg to move; these RPs generate different types of locomotion when the couple parameters $a_{ij}$ and $b_{ij} \in [-2, 3]$. It is certain that it is possible to generate the rhythmic patterns by optimizing the bidirectional two CPGs outside of the above regions.

# CHAPTER 6

# CONCLUSION

To sum up, the first type of CPGs, uncoupled, unidirectional and bidirectional two CPGs are used to generate rhythmic motion for one leg with two degrees of freedom. The study shows that when optimization is conducted in an unbounded region and used both GA and hybrid function, the results are impossible to be implemented physically. However, when we consider the stability analysis that is presented in Chapter 3 and optimize these type of CPGs in order to decrease the variation between steps, the results become much better than before for all cases. Such results can be implemented physically.

Otherwise, it is vital that we control the amplitude and the frequency to obtain better results. The study also reveals CPGs can control bipedal locomotion. When we compare the outputs of this type of the CPGs with the real data, we see a big variance between them, in other words, all cases of the first type of the CPGs are unable to produce RPs similar to those what we obtained by collection the real data.

For the second type of the CPGs, the study has pointed out that when the optimization is conducted in an unbounded region, there is also a big variance between each step, despite of, we optimized the objective function $J$ in two cases $C_1C_2 \neq 0$ and $C_2 = 0$. Because, it was too difficult to design phase coupling of two CPGs without disturbing the amplitude $\mu$ of both CPGs, by adding linear couple weight $E$ which was just a constant and its sign decides if these two oscillators are in phase or anti-phase, the results were too hard to implement in physical situation. However, utilizing genetic algorithms with the hybrid function and adapting the CPGs to robotic systems that perform one leg movement may yield positive results when the fixed point is stable

for the case of the bidirectional two CPGs. Indeed, by adding extra constraints related with the amplitude and the frequency, the results become much better and variance between each steps decrease.

Finally, for the third type of the CPGs, the uncoupled, unidirectional and bidirectional two CPGs are used to generate motion for one leg with two degrees of freedom. When the optimization was performed in the first two cases, the CPGs are unable to produce RPs. In contrast, by utilizing the bidirectional two CPGs, the results showed far greater improvement than the other cases. That is, the bidirectional coupling yielded the best performance level.

If $|\mu|$ and $\tau$ are sufficiently small, and the fixed points are stable, then both the velocity and displacement become greater. These results depend on the value of the parameters $\mu$, $\beta_1$ and $\beta_2$. The experiments show that a small adjustment in the parameter settings of the CPGs cause different results. The study also shows that an increase in the values of $\tau$ and $\alpha$ decreases the displacement and the velocity, whereas a decrease in their values increases the displacement and the velocity.

It is sure that, it is not only both parameters $\tau$ and $\alpha$ are important, but also the coupling weight $a_{ij}$ and $b_{ij}$ that are driven the system to two diverging phases, which lead to obtaining the conflicting perturbations. These perturbations are influenced by the energies $E_j$ of the bidirectional two CPGs. For instance, during the experiment, when the amplitude of the second CPG is very small, the coupling weight will be definitely week. We show that RPs depend on the coupling weights $a_{ij}$ and $b_{ij}$ and also both $\tau$ and $\alpha$. The parameters of the coupling weights are very important to balance the disturbance during the optimization, and also when $\alpha, \tau \in (0, 3]$, the bidirectional two CPGs are definitely able to produce different RPs for one leg. These different RPs will show different types of locomotion when the couple weights $a_{ij}$ and $b_{ij} \in [-2, 3]$. By applying these results for comparison between the outputs of this type of CPGs with the real data, it is indicated that the outputs of the bidirectional two CPGs produce RPs similar to those obtained from the real data.

This study indicates that not only do CPGs in the spinal cord of humans influence human locomotion, they also take over the locomotion without any provided sensory feedback. To the extent that bidirectional two CPGs are the most effective essentials

akin to real life-induced rhythmic patterns, it is reasonable for them to be considered pivotal features most conducive to locomotion. The results of the study warrant broader future applications of bidirectional two CPGs of the third type to account for a variety of upper limb locomotion. These results are important, then not only because of what they may contribute to the ongoing discussion of locomotion but also for the support that they give to bidirectional two CPGs as a critical aspect of locomotion. These results pave the way for further research into CPGs as potential controllers of upper limbs for different movements.

# REFERENCES


[1] Ijspeert, A. J. (2008). Central pattern generators for locomotion control in animals and robots: a review. Neural networks, 21(4), 642-653.

[2] Larsen, J. C. Central Pattern Generators in modern Science.

[3] Larsen, J. C. (2011). Locomotion through morphosis (Doctoral dissertation, Faculty of Science and Engineering, University of Southern Denmark).

[4] Sillar, K.T. (1996). The development of central pattern generators for vertebrate locomotion. Advances in Psychology, 115, 205-221.

[5] Delcomyn, F. (1980). Neural basis of rhythmic behavior in animals. science, 210(4469), 492-498.

[6] Billard, A., and Ijspeert, A. J. (2000). Biologically inspired neural controllers for motor control in a quadruped robot. In Neural Networks, 2000. IJCNN 2000, Proceedings of the IEEE-INNS-ENNS International Joint Conference on (Vol. 6, pp. 637-641). IEEE.

[7] Bucher, D., Haspel, G., Golowasch, J., and Nadim, F. (2000). Central pattern generators. eLS.

[8] Casasnovas, B., and Meyrand, P. (1995). Functional differentiation of adult neural circuits from a single embryonic network. Journal of Neuroscience, 15(8), 5703-5718.

[9] Van Vreeswijk, C., Abbott, L. and Ermentrout, G.B. (1994). When inhibition not excitation synchronizes neural firing. Journal of computational neuroscience, 1(4), 313-321.

[10] Williamson, M. M. (1999). Robot arm control exploiting natural dynamics (Doctoral dissertation, Massachusetts Institute of Technology).

[11] Arikan, K.B. and Irfanoglu, B. (2011). A Test Bench to Study Bioinspired Control for Robot Walking. Journal of Control Engineering and Applied Informatics, 13(2), 76-80.

[12] Abdalftah Elbori, Mehmet Turan and Kutluk Bilge Arıkan. Optimization of Central Patterns Generators. 2017. 12(5): p. 1164-1172.

[13] Kimura, H., Fukuoka, Y. and Cohen, A.H. (2007). Adaptive dynamic walking of a quadruped robot on natural ground based on biological concepts. The International Journal of Robotics Research, 26(5), 475-490.

[14] Wu, X., Teng, L., Chen, W., Ren, G., Jin, Y., and Li, G. (2013). CPGs with continuous adjustment of phase difference for locomotion control. International Journal of Advanced Robotic Systems, 10(6), 269.

[15] Ijspeert, A.J. and Cabelguen, J.M. (2006). Gait transition from swimming to walking: investigation of salamander locomotion control using nonlinear oscillators, In Adaptive Motion of Animals and Machines (pp. 177-188). Springer.

[16] Amrollah, E. and Henaff, P. (2010). On the role of sensory feedbacks in Rowat-Selverston CPG to improve robot legged locomotion. Frontiers in neurorobotics, 4, 113.

[17] Qijun, Z. J. T. M. C., and Chengju, L. I. U. (2011). Dynamic walking of AIBO with Hopf Oscillators. Chinese Journal of Mechanical Engineering, 24(4), 612-617.

[18] Nachstedt, T., Tetzlaff, C., and Manoonpong, P. (2017). Fast Dynamical Coupling Enhances Frequency Adaptation of Oscillators for Robotic Locomotion Control. Frontiers in neurorobotics, 11.

[19] Brown, T. G. (1911). The intrinsic factors in the act of progression in the mammal. Proceedings of the Royal Society of London. Series B, containing papers of a biological character, 84(572), 308-319.

[20] Cohen, A. H., and Wallén, P. (1980). The neuronal correlate of locomotion in fish. Experimental brain research, 41(1), 11-18.

[21] Grillner, S. (1985). Neural control of vertebrate locomotion-central mechanisms and reflex interaction with special reference to the cat Feedback and motor control in invertebrates and vertebrates (pp. 35-56): Springer.

[22] Ekeberg, Ö. (1993). A combined neuronal and mechanical model of fish swimming. Biological cybernetics, 69(5-6), 363-374.

[23] Delvolvé, I., Branchereau, P., Dubuc, R. and Cabelguen, J.-M. (1999). Fictive rhythmic motor patterns induced by NMDA in an in vitro brain stem-spinal cord preparation from an adult urodele. Journal of Neurophysiology, 82(2), 1074-1077.

[24] Grillner, S., Georgopoulos, A. and Jordan, L. (1997). Neurons, networks, and motor behavior: Citeseer.

[25] Kopell, N., Ermentrout, G. and Williams, T. (1991). On chains of oscillators forced at one end. SIAM Journal on Applied Mathematics, 51(5), 1397-1417.

[26] Matsuoka, K. (1987). Mechanisms of frequency and pattern control in the neural rhythm generators. Biological cybernetics, 56(5-6), 345-353.

[27] McClellan, A. D. and Jang, W. (1993). Mechanosensory inputs to the central pattern generators for locomotion in the lamprey spinal cord: resetting, entrainment, and computer modeling. Journal of Neurophysiology, 70(6), 2442-2454.

[28] Di Prisco, G. V., Walle, P. and Grillner, S. (1990). Synaptic effects of intraspinal stretch receptor neurons mediating movement-related feedback during locomotion. Brain research, 530(1), 161-166.

[29] Williams, T. L., Sigvardt, K. A., Kopell, N., Ermentrout, G. B. and Remler, M. P. (1990). Forcing of coupled nonlinear oscillators: studies of intersegmental coordination in the lamprey locomotor central pattern generator. Journal of Neurophysiology, 64(3), 862-871.

[30] Traven, H., Brodin, L., Lansner, A., Ekeberg, O., WallÃ©n, P. and Grillner, S. (1993). Computer simulations of NMDA and non-NMDA receptor-mediated synaptic drive: sensory and supraspinal modulation of neurons and small networks. Journal of Neurophysiology, 70(2), 695-709.

[31] Hellgren, J., Grillner, S. and Lansner, A. (1992). Computer simulation of the segmental neural network generating locomotion in lamprey by using populations of network interneurons. Biological cybernetics, 68(1), 1-13.

[32] Wadden, T., Hellgren, J., Lansner, A. and Grillner, S. (1997). Intersegmental coordination in the lamprey: simulations using a network model without segmental boundaries. Biological cybernetics, 76(1), 1-9.

[33] Cohen, A. H., Holmes, P. J. and Rand, R. H. (1982). The nature of the coupling between segmental oscillators of the lamprey spinal generator for locomotion: a mathematical model. Journal of mathematical biology, 13(3), 345-369.

[34] Collins, J. J. and Richmond, S. A. (1994). Hard-wired central pattern generators for quadrupedal locomotion. Biological cybernetics, 71(5), 375-385.

[35] Grillner, S., Wallen, P., Brodin, L. and Lansner, A. (1991). Neuronal network generating locomotor behavior in lamprey: circuitry, transmitters, membrane properties, and simulation. Annual review of neuroscience, 14(1), 169-199.

[36] Arena, P., (2000). The central pattern generator: A paradigm for artificial locomotion. Soft Computing, 4(4), 251-266.

[37] Lu, Z., et al. (2005). Serpentine locomotion of a snake-like robot controlled by cyclic inhibitory CPG model. In 2005 IEEE/RSJ International Conference on Intelligent Robots and Systems. IEEE.

[38] Okada, M., Tatani, K. and Nakamura, Y. (2002). Polynomial design of the nonlinear dynamics for the brain-like information processing of whole body motion. In Robotics and Automation Proceedings. ICRA'02. IEEE International Conference on IEEE.

[39] Arena, P. (2001). A mechatronic lamprey controlled by analog circuits. In Proceedings of the 9th IEEE mediterannean conference on control and automation

[40] Crespi, A. and Ijspeert, A.J. (2008). Online optimization of swimming and crawling in an amphibious snake robot. IEEE Transactions on Robotics, 24(1), 75-87

[41] Ijspeert, A.J. and Crespi, A. (2007). Online trajectory generation in an amphibious snake robot using a lamprey-like central pattern generator model. In Proceedings 2007 IEEE International Conference on Robotics and Automation. IEEE.

[42] Fukuoka, Y., Kimura, H. and Cohen, A.H. (2003). Adaptive dynamic walking of a quadruped robot on irregular terrain based on biological concepts. The International Journal of Robotics Research, 22(3-4), 187-202.

[43] Brambilla, G., J. Buchli and Ijspeert, A. J. (2006). Adaptive four legged locomotion control based on nonlinear dynamical systems. In International Conference on Simulation of Adaptive Behavior. Springer.

[44] Arena, P., et al., (2004). An adaptive, self-organizing dynamical system for hierarchical control of bio-inspired locomotion. IEEE Transactions on Systems, Man, and Cybernetics, Part B (Cybernetics), 34(4), 1823-1837

[45] Inagaki, S., Yuasa, H., and Arai, T. (2003). CPG model for autonomous decentralized multi-legged robot system-generation and transition of oscillation patterns and dynamics of oscillators. Robotics and Autonomous Systems, 44(3), 171-179.

[46] Inagaki, S., et al., (2006). Wave CPG model for autonomous decentralized multi-legged robot: Gait generation and walking speed control. Robotics and Autonomous Systems, 54(2), 118-126.

[47] Delcomyn, F. (1999). Walking robots and the central and peripheral control of locomotion in insects. Autonomous robots, 7(3), 259-270.

[48] Taga, G. (1998). A model of the neuro-musculo-skeletal system for anticipatory adjustment of human locomotion during obstacle avoidance. Biological Cybernetics, 78(1), 9-17.

[49] Taga, G.,Yamaguchi, Y. and Shimizu, H. (1991). Self-organized control of bipedal locomotion by neural oscillators in unpredictable environment. Biological cybernetics, 65(3), 147-159.

[50] Ishiguro, H., Ono, T., Imai, M., and Kanda, T. (2003). Development of an interactive humanoid robot (Robovie) -an interdisciplinary approach Robotics Research (pp. 179-191): Springer.

[51] Pinto, C. M., and Golubitsky, M. (2006). Central pattern generators for bipedal locomotion. Journal of mathematical biology, 53(3), 474-489.

[52] Wang, T., Chevallereau, C., and Tlalolini, D. (2014). Stable walking control of a 3D biped robot with foot rotation. Robotica, 32(4), 551-570.

[53] Inada, H., and Ishii, K. (2003). Behavior generation of bipedal robot using central pattern generator (CPG)(1st report: CPG parameters searching method by genetic algorithm). Paper presented at the Intelligent Robots and Systems, 2003.(IROS 2003). Proceedings. 2003 IEEE/RSJ International Conference on.

[54] Aoi, S. and Tsuchiya, K. (2005). Locomotion control of a biped robot using nonlinear oscillators. Autonomous robots, 19(3), 219-232.

[55] Endo, G., et al. (2005). Experimental studies of a neural oscillator for biped locomotion with QRIO. In Proceedings of the 2005 IEEE international conference on robotics and automation. IEEE.

[56] Righetti, L. and Ijspeert, A. J. (2006). Programmable central pattern generators: an application to biped locomotion control. Paper presented at the Proceedings 2006 IEEE International Conference on Robotics and Automation, 2006. ICRA 2006.

[57] Torres-Huitzil, C. and Girau, B. (2008). Implementation of central pattern generator in an FPGA-based embedded system. Paper presented at the International Conference on Artificial Neural Networks.

[58] Simoni, M. F. and DeWeerth, S. P. (2007). Sensory feedback in a half-center oscillator model. IEEE Transactions on Biomedical Engineering, 54(2), 193-204.

[59] Lewis, M. A., Tenore, F. and Etienne-Cummings, R. (2005). CPG design using inhibitory networks. Paper presented at the Proceedings of the 2005 IEEE international conference on robotics and automation.

[60] Nakada, K., Asai, T. and Amemiya, Y. (2003). An analog CMOS central pattern generator for interlimb coordination in quadruped locomotion. IEEE Transactions on Neural Networks, 14(5), 1356-1365.

[61] Ijspeert, A.J., et al., (2007). From swimming to walking with a salamander robot driven by a spinal cord model. Science, 315(5817), 1416-1420.

[62] Crespi, A. and Ijspeert, A.J. (2006). AmphiBot II: An amphibious snake robot that crawls and swims using a central pattern generator. In Proceedings of the 9th international conference on climbing and walking robots (CLAWAR 2006).

[63] Kimura, H., Akiyama, S. and Sakurama, K. (1999). Realization of dynamic walking and running of the quadruped using neural oscillator. Autonomous robots, 7(3), 247-258.

[64] Sproewitz, A., Moeckel, R., Maye, J. and Ijspeert, A. J. (2008). Learning to move in modular robots using central pattern generators and online optimization. The International Journal of Robotics Research, 27(3-4), 423-443.

[65] Parker, G. A., and Smith, J. M. (1990). Optimality theory in evolutionary biology. Nature, 348(6296), 27-33.

[66] Van den Kieboom, J. (2009). Biped locomotion and stability: A practical approach.

[67] Degallier, S., et al. Movement generation using dynamical systems: a humanoid robot performing a drumming task. in Humanoid Robots, 2006 6th IEEE-RAS International Conference on. 2006. IEEE.

[68] Degallier, S., et al. A modular bio-inspired architecture for movement generation for the infant-like robot iCub. in Biomedical Robotics and Biomechatronics, 2008. BioRob 2008. 2nd IEEE RAS and EMBS International Conference on. 2008. IEEE.

[69] Degallier, S. and A. Ijspeert, Modeling discrete and rhythmic movements through motor primitives: a review. Biological cybernetics, 2010. 103(4): p. 319-338.

[70] Degallier, S., et al., Toward simple control for complex, autonomous robotic applications: combining discrete and rhythmic motor primitives. Autonomous Robots, 2011. 31(2): p. 155-181.

[71] Marbach, D. (2004). Evolution and Online Optimization of Central Pattern Generators for Modular Robot Locomotion. Unpublished Master Thesis, Swiss Federal Institute of Technology Lausanne.

[72] Verhulst, F., Nonlinear differential equations and dynamical systems. 1996.

[73] van der Heijden, G., Hopf bifurcation. 2004, Routledge.

[74] Lynch, S., Dynamical systems with applications using MATLAB. 2004: Springer.

[75] Kelley, C. T. (1999). Iterative methods for optimization: SIAM.

[76] Grefenstette, J. J. (1986). Optimization of control parameters for genetic algorithms. IEEE Transactions on Systems, Man, and Cybernetics, 16(1), 122-128.

[77] KlÃmek, P., and KovÃ¡rÃk, M. (2014). Genetic Algorithms as a Tool of Production Process Control. Journal of Systems Integration, 5(3), 57.

[78] Roeva, O., Fidanova, S., and Paprzycki, M. (2013). Influence of the population size on the genetic algorithm performance in case of cultivation process modelling. Paper presented at the Computer Science and Information Systems (FedCSIS), 2013 Federated Conference on.

[79] Zhang, Q., Ogren, R. M., and Kong, S.-C. (2016). A comparative study of biodiesel engine performance optimization using enhanced hybrid PSO-GA and basic GA. Applied Energy, 165, 676-684.

[80] Sahnehsaraei, M. A., Mahmoodabadi, M. J., Taherkhorsandi, M., Castillo-Villar, K. K., and Yazdi, S. M. (2015). A hybrid global optimization algorithm: particle swarm optimization in association with a genetic algorithm Complex System Modelling and Control Through Intelligent Soft Computations (pp. 45-86): Springer.

[81] Back, T., and Schwefel, H.-P. (1993). An overview of evolutionary algorithms for parameter optimization. Evolutionary computation, 1(1), 1-23.

[82] Alexander, R.M. (1996). Optima for animals. Princeton University Press.

[83] Nolfi, S. and Floreano, D. (2000). Evolutionary robotics: The biology, intelligence, and technology of self-organizing machines. MIT press.

[84] Golden, J., Gait synthesis for the SD-2 biped robot to climb stairs. International Journal of Robotics and Automation, 1990. 5(4): p. 149-159.

[85] Kajita, S. and K. Tani. Study of dynamic biped locomotion on rugged terrain-theory and basic experiment. in Advanced Robotics, 1991.'Robots in Unstructured Environments', 91 ICAR., Fifth International Conference on. 1991. IEEE

# VITA

## PERSONAL INFORMATION

| | |
|---|---|
| Surname, Name: | Elbori, Abdalftah |
| Nationality: | Libya (LY) |
| Date and Place of Birth: | 23 May, 1981, Tarhuna |
| e-mail: | abdalftah81@yahoo.com |

## EDUCATION

| Degree | Institution | Year of Graduation |
|---|---|---|
| MSc | Heriot Watt University, Mathematics | 2007 |
| BSc | Elmergeb University, Mathematics | 2002 |
| High School | 7 April | 1997 |

## WORK EXPERIENCE

| Year | Place | Enrollment |
|---|---|---|
| 2008-2010 | Azzaytuna University, Mathematics | Instructor |
| 2013-Present | MODES Department | PhD Student |

## FOREIGN LANGUAGES

Arabic (fluent), English (fluent), Turkish (basic)

## PUBLICATIONS

- Abdalftah Elbori, Mehmet Turan, and Kutluk Bilge Arikan, *Optimization of Central Patterns Generators*. 2017. 12(5): p. 1164-1172. Journal of Engineering and Applied Sciences - Medwell Journals.

- Abdalftah Elbori, Mehmet Turan, and Kutluk Bilge Arikan, *Evaluation and Optimization of Nonlinear Central Pattern Generators for Robotic Locomotion*. Submitted to Journal of Control Engineering and Applied Informatics.
- Abdalftah Elbori and Ltfei Abdalsmd, Simulation of Simple Pendulum. International Journal of Engineering Science Invention, 2017. 6(2319 - 6734): p. 33-38.
- Abdalftah Elbori and Ltfei Abdalsmd, Simulation of Double Pendulum. Journal of Software Engineering and Simulation, 2017. 3(2321-3795): p. 1-13.

**CONFERENCE PRESENTATIONS**

- Abdalftah Elbori, Mehmet Turan, and Kutluk Bilge Arikan, *Optimization of Central Patterns Generators. 2017*Academic Fora Conference 17 January- Istanbul -Turkey
- Abdalftah Elbori, Mehmet Turan, and Kutluk Bilge Arikan *Optimization of Central Pattern Generators for Defining Human Locomotion. July 7th, EpsMsO 2017-Athens Greece*
- Abdalftah Elbori, Mehmet Turan, and Kutluk Bilge Arikan, *Estimating Gait Patterns of One Leg by Using Central Pattern Generators. 2017* International Conference on Control, Automation, Robotics and Vision Engineering (ICCARVE) Istanbul, Turkey 22nd December, 2017